Applied Energy

A Three-level Framework for Strategic Participation of Aggregated Electric Vehicle-owning Households in Local Electricity and Thermal Energy Markets

--Manuscript Draft--

Manuscript Number:	APEN-D-22-00417R3
Article Type:	Research Paper
Keywords:	electric vehicles; Thermal energy market; Strategic scheduling; Three-level optimization; Wholesale Electricity Market; local electricity market
Corresponding Author:	Sajad Najafi Ravadanegh, PhD Azarbaijan Shahid Madani University Tabriz, IRAN, ISLAMIC REPUBLIC OF
First Author:	Saeed Zeynali
Order of Authors:	Saeed Zeynali
	Nima Nasiri
	Sajad Najafi Ravadanegh, PhD
	Mousa Marzband
Abstract:	The impact of electric vehicles (EV) charging strategy will not be limited to power systems as integrated electricity, natural gas and thermal energy systems have become increasingly interconnected. We introduce a three-level framework for the aggregated electric vehicle-owning households (AEVH) to strategically participate in local electricity and thermal energy markets as a price-maker, while considering the strategic behavior of the integrated energy service provider (IESP) in thw wholesale electricity market (WEM) also as a price-maker. The AEVH operator forms the first level, while IESP and WEM operators are integrated at the second and third levels, respectively. To solve the three-level problem, the second and third levels are modified as a single-level problem through the Karush-Kuhn-Tucker (KKT) conditions, then the equilibrium point of the resulting single-level problem and the first level is achieved through two-step iterative method. At the first level, the arrival/departure time and daily travelled miles of EV fleets are modelled via stochastic scenarios, while renewable energy production at the second level is dealt with by information gap decision theory (IGDT). Ultimately, different case studies verify that AEVHs can deploy their thermal flexibility together with the smart charging strategy of the EVs
Suggested Reviewers:	Mohammadreza Jannati, PhD Azarbaijan Shahid Madani University Faculty of Engineering m.r.jannati@gmail.com
	Gevorge Gharepatian Amirkabir University of Technology Department of Electrical Engineering grptian@aut.ac.ir
	Mohammad Shahidepour IIT: Illinois Institute of Technology ms@iit.edu
	Amin Khodaei DU: University of Denver Amin.Khodaei@du.edu

Response to reviewer comments on the paper

A Three-level Framework for Strategic Participation of Aggregated Electric Vehicle-owning Households in Local Electricity and Thermal Energy Markets

As the team of authors, we would like to express our sincere gratitude to the respected editor and the honorable reviewers for giving us a third chance to revise our manuscript, while providing essential comments that will improve the quality of our work. We have done our best to address all concerns in the second round of revision and catch up with high standards in the prestigious journal of Applied Energy.

Our detailed answers are as follows.

Please note that the reviewer questions are in red while our answers are in black. Additions to the original paper appear in blue.

Editor-in-chief

The reviewers/editors have commented on your above paper. They indicated that it is not acceptable for publication in its present form. However, if you feel that you can suitably address the reviewers' comments (included below or the attachments in your account), I invite you to revise and resubmit your manuscript.

Reply: We sincerely thank the respected editor-in-chief for giving us a chance to revise our manuscript. We did our best to address the raised concerns in the third round of revision.

Reviewer #2

The authors carefully considered the comments of the review and thoroughly defended the positions taken in the manuscript. Contrary to these positions, the global energy landscape is continuously evolving. Power plants that are in operation today and operated by service providers, can be replaced by alternatives following technological advances in energy production and economic tools. These aspects can be reflected in the manuscript by addressing the following points:

Reply: We would like to thank the honorable reviewer for the valuable comments. We honestly believe that these insightful remarks had a great impact on improving our paper.

Comment R2.1

The authors indicate the schematic depiction of the energy service provider. Indeed the services currently provided by e.g. a company, are required in the system. But there is no limitation to the management of these services. The required services, and hence the role of the energy service provider, can be taken, for example, by members of an energy community. This can be indeed more difficult in large scale power/storage units such as CHP and hydroelectric stations due to the required capital, however is already happening in smaller scale distributed stations, including solar and wind power units.

Reply: We sincerely agree with the honorable reviewer that todays' power plants can be replaced by alternatives. As it was discussed in (*10.1016/j.renene.2021.01.078*), in the future energy systems, there will be energy communities that produce a percentage of their own energy. However, for following reason the energy service provider will be very important in the evolving power systems of the future:

1- Most energy communities cannot produce all of their demand and they need to have contracts with reliable energy service providers that can provide them energy at the shortage and even buy the surplus energy production of the energy communities.

2- Independent entities (companies, governments, ordinary citizen) can have the ownership of wind/ solar production farms in the future energy systems and as long as their price are competitive, they can sell their energy to these communities and be energy service provider. Therefore, the energy service provider always be present.

3- Small scale households prefer to buy energy from local energy systems, and energy service providers can participate in wholesale energy market and sell that energy in retail for the energy communities. So energy service providers do not always need to have large power plants. In fact, large energy generation companies (wind/solar farms, power plants) sell their energy to large scale buyers in wholesale market. The energy service providers buy the energy from wholesale energy market and sell it for retail consumers. For example, a large-scale producer is not interested in selling 1 kwh energy to a small consumer and prefers to sell large quantities (in MWh scale). Similarly, small-scale households cannot participate in the wholesale energy market and the energy service provider can be the link between large producers and small communities.

4- As the energy systems evolve, there will always be large scale producers. For example, the fossil fueled power plants will be replaced by large wind farms, and energy service providers will be needed to distribute this energy. Certainly, not all communities are able to afford energy production facilities considering the high capital cost, and they might be interested in buying from energy service providers that offer reasonable price.

5- Even when these communities produce part of their energy, they are unlikely to be able to produce natural gas, as it would be very expensive to invest in natural gas pipelines and drilling infrastructure.

We sincerely agree with the honorable reviewer that in the future, there will be energy communities that do not need energy service providers. However, for the above-mentioned reasons, the energy service providers will always be needed and they will co-exist with such energy communities.

Does the proposed three-level system apply in this case?

Reply: The short answer is yes. The AEVH can sell (produce) and purchase (consume) energy. So in fact, this study is similar to the energy community model proposed by the honorable reviewer. We have only applied a slightly different terminology based on the focus of the study.

Comment R2.2

There is no doubt that several published works utilize said bus systems. In addition, the bus systems are indeed a result of several years of research that cannot be compared to the effort of a single work. The proposed model and its algorithmic operation, however, relies on these systems. Would the model work if these systems are removed?

Reply: We would like to thank the honorable reviewer for this comment. In fact, the model would work and provide theoretically better results if these systems are removed. However, the results won't be reliable at all since removing these systems makes the model extremely simple and unrealistic. For instance, if we removed the power system model, the only power system equation would be (production=consumption), while as you can see in this study the power system has many equations and constraints. Ignoring the power system model has the following drawbacks:

1- The voltage of the power lines can drop or increase dramatically. For instance, the residential consumers should have the voltage value of 200-240 Volts. However, if the power system model was ignored, this value won't be considered and voltage can drop below 200 or be higher than 240, both these cases can harm the household appliances severely.
2- The power transmission capacity of the transmission lines are limited. Ignoring the power line nominal rates can harm the electricity distribution systems drastically and inflict damage on the power grids and power lines.
3- Energy transmission by the power system imposes power losses, these energy losses should be modelled to minimize the wasted energy.

4- The transformers of the power grid can overheat and even explode if their capacity is not considered in the models.

Similarly, when the natural gas network model is ignored, the pressure of the natural gas can drop for some consumers, while other consumers might have too much gas pressure. Moreover, the natural gas flow limits of the natural gas network should be considered as pipelines can only carry a limited amount of gas. In theory, it is possible to ignore natural gas network model and get better results. However, these outcomes won't be reliable in the real-world conditions and the energy system models are ignored in such studies. For instance, a damage to the natural gas pipelines will be catastrophic disaster. Furthermore, the thermal network models are important to deliver thermal energy to consumers and consider the thermodynamic characteristics of the thermal energy distribution system. Overall, it is certainly possible to ignore network models in theoretical studies, but including the models makes the outcomes more reliable and realistic.

For this reason, the main structure supported by relevant references and a fundamental but compact description of the bus systems is required to aid the reader of the manuscript. This structure and description was included in all five exemplary studies provided by the authors.

Reply: We sincerely agree with the honorable reviewer that the main data of the utilized networks should be summarized for the readers. We tried to address this essential comment in the revision by including the related references and tables similar to aforementioned studies.

In the revision, this comment was addressed in the first paragraph of section four by the following additions:

"Moreover, the structural data of the systems are summarized in Appendix C"

In the revision, this comment was also addressed in by including the data in Appendix C as follows:

"In this study, the IESP consists of an IEEE-33 bus ADS, a 20-node NGN, and an 8-node DHS that is supplied by 3 CHPs, 2 NGUs, 3 PVAs and 3 WTs. The data on these networks can be observed in [11, 33, 34]. Furthermore, the WEM is made up of a standard 6-node TN and its structural data is available in [11]. Overall, the summery of the main parameters are included in Table C.4 to Table C.7."

Table C.4: Data and information on DGs

	$\overline{P}_k^{DG}$	$\underline{P}_k^{DG}$	R_k^{up}	R_k^{DN}	T_k^{U}	T_k^{D}	C_k^{DG}
CHP1	---	---	4.5	4.5	2	2	---
CHP2	---	---	4.5	4.5	1	1	---
CHP3	---	---	0.8	0.8	1	1	---
NGU1	7	0.75	1.8	1.8	1	1	87
NGU2	7	0.75	0.5	0.5	1	1	92

Table C.5: Data and information on EVFs

BC_f	$ECPM_f$	η_f	EB_f	Cr_f	a_0
400 ($/KWh)	0.3 (m/KWh)	0.95	30 (KWh)	10 (KW/h)	0.000524

Table C.6: Data and information on district heating network

C_p	R	$Cair_{\vartheta,e}$	$n^{ho}_{\vartheta,e}$
1(MWh/kg.◦C)	18 (◦C/MWh)	1.1578e-6 (MWh\(kg.c))	6000

Table C.7: Data and information on active distribution system

$\overline{V_i^{DS}}$	$\underline{V_i^{DS}}$	$\overline{I_{i,j}^{DS}}$	$\overline{P_l^{IL}}$	η_{EB}	$\overline{P_{t,\vartheta,q}^{EB}}$
1.1 (P.U)	0.9 (P.U)	1.2 (A)	3 (MW)	1	10 (MW)

Comment R2.3

Indeed a three-level model is a novel contribution in the literature. The previous contribution of the authors in bi-level systems utilized similar datasets, as detailed in references [21] and [32]. https://doi.org/10.1016/j.apenergy.2021.117432

https://doi.org/10.1016/j.energy.2021.121398

Addition of a level in the previous bi-level model, offers a small increment of progress in the relevant literature. For this reason, a robust demonstration of how the proposed model succeeds into solving the problem at hand is required. The utilized optimization methods are indeed elegant ways of simplifying a multi-level problem to single level. The authors provided their description in appendices, but the advantages in cost are not clearly shown.

Reply: We would like to express our sincere gratitude to the honorable reviewer for acknowledging our contribution. In fact, we realized that there are many studies on the participation of energy systems in wholesale electricity market and many other studies have modelled the energy trade of the local consumers with the energy systems, which are bi-level models. However, to the best of our knowledge all three of these players had not been integrated in the same problem, which was the main motivation behind this study to address this issue by a three-level structure and propose a solving strategy for this model.

Overall cost estimates of the case studies are tabulated, but the cost advantages due to price shifting should be displayed together with power and energy generation profiles, fig. 10-13.

Reply: We would like to thank the honorable reviewer for this remarkable comment. In fact, drawing these figures can be very effective in the results section. We tried to address this valuable comment in the revision.

In the revision, this comment was addressed by including following parts at page 26

In order to provide a deeper insight about the cost values of Table 2, the hourly cost value is comparatively illustrated with total generation of each case study in Fig. 14, while Fig. 14 shows the hourly total generation and MCP in each case. As can be observed, **CS1** results in the highest operational cost value since in this case the EVFs are charged without a smart strategy, and it leads to highest total Genco production since peak demand is imported from the WEM. Thanks to the smart charging strategy of **CS2**, the demand is shifted from peak hours (15-19) to valley hour (1-7), while this shift is even more apparent in **CS3** as the thermal flexibilities open the electrical capacity of the CHP units. Overall, **CS2** provides 9.19% lower cost compared to CS1, and **CS3** provides 9.42% lower cost compared **CS1**. Based on the MCP outcomes of Fig. 15, it is noted that smart charging strategy and thermal load flexibilities in **CS2** and **CS3** can lead to 2.10 % lower WEM price in regard to **CS1**.

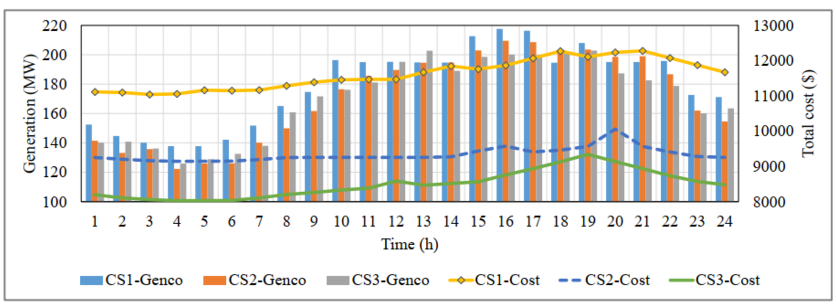

Figure 14: The MCP of the local electricity market (IEEE-33 bus)

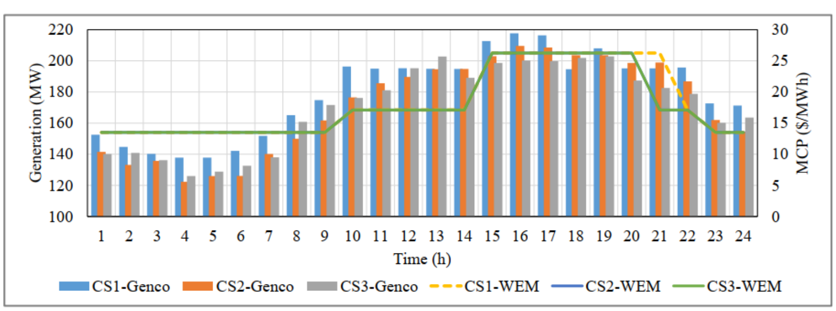

Figure 15: The MCP of the local electricity market (IEEE-33 bus)

- **The strategic participation of AEVH in local electricity and thermal energy markets as a price-maker is presented.**
- **The strategic behavior of the integrated energy service provider (IESP) in wholesale electricity market (WEM) as a price-maker is considered.**
- **A three-level framework for the aggregated electric vehicle-owning households is proposed.**
- **The second and third levels is modeled as a single-level problem through KKT condition.**

Acknowledgements

Funding: This research did not receive any specific grant from funding agencies in the public, commercial, or not-for-profit sectors.

A Three-level Framework for Strategic Participation of Aggregated Electric Vehicle-owning Households in Local Electricity and Thermal Energy Markets

Saeed Zeynali[a], Nima Nasiri[a], Sajad Najafi Ravadanegh[a], Mousa Marzband[b,c]

[a] *Resilient Smart Grids Research Lab, Electrical Engineering Department, Azarbaijan Shahid Madani University, Tabriz, Iran*
[b] *Northumbria University, Electrical Power and Control Systems Research Group, Ellison Place NE1 8ST, Newcastle upon Tyne, United Kingdom*
[c] *Center of Research Excellence in Renewable Energy and Power Systems, King Abdulaziz University, Jeddah 21589 Saudi Arabia*

Abstract

The impact of electric vehicles (EV) charging strategy will not be limited to power systems as integrated electricity, natural gas and thermal energy systems have become increasingly interconnected. We introduce a three-level framework for the aggregated electric vehicle-owning households (AEVH) to strategically participate in local electricity and thermal energy markets as a price-maker, while considering the strategic behavior of the integrated energy service provider (IESP) in thw wholesale electricity market (WEM) also as a price-maker. The AEVH operator forms the first level, while IESP and WEM operators are integrated at the second and third levels, respectively. To solve the three-level problem, the second and third levels are modified as a single-level problem through the Karush-Kuhn-Tucker (KKT) conditions, then the equilibrium point of the resulting single-level problem and the first level is achieved through two-step iterative method. At the first level, the arrival/departure time and daily travelled miles of EV fleets are modelled via stochastic scenarios, while renewable energy production at the second level is dealt with by information gap decision theory (IGDT). Ultimately, different case studies verify that AEVHs can deploy their thermal flexibility together with the smart charging strategy of the EVs

Email address: `s.najafi@azaruniv.ac.ir Corresponding author` (Sajad Najafi Ravadanegh)

to influence the local electricity, thermal energy and even WEM prices. Using the proposed three-level optimization framework reaches the best point of equilibrium between different market players. The outcomes prove the effectiveness of the proposed model. Based on the results, the AEVH can deploy the proposed model to diminish the WEM price by 2.1%, while the local electricity price was dropped by 18.85%. Furthermore, the thermal energy price was reduced by 5.82%, which illustrates that EVs can influence the thermal energy market through the combined heat and power units.

Keywords: Electric vehicles; Thermal energy market; Strategic scheduling; Three-level optimization; Wholesale electricity market; Local electricity market

---

Nomenclature

Indices	
s, t, k, r	Indices of scenario, time, DGs, wind turbine
l, ϑ, e	Indices of pipeline, node, demand in DHS
q, f	Indices of DHS source and EV fleets
pv, c, R	Indices of PVA, ILs and FOR in CHP units
n, w, lg, c	Indices of NGN nods, NGN producer, active pipeline, non-active pipeline
d, dg	Indices of ADS and, NGN loads
g, b, b', i	Indices of Genco, TN bus's, ADS buses
A_n^m, CHP	Set of m equipment's located at ADS and TN bus's or NGN nodes n and CHP
Tr	Set of interconnected buses in the TN.
A_i^f	Set of EV parking lots at node i of ADS
NGU	Set of non-gas fired units
TA_f,TD_f	Set of arrival/departure times
	Parameters
$SOC_{f,s}^{end}$	Highest possible SOC at departure time
SOC_f^{des}	Desired SOC at departure time

$\overline{SOC}_f$, $\underline{SOC}_f$	max/min SOC of EV fleets (%)
$ms_{t,l}$,$mr_{t,l}$	Water mass flow of supply/return DHS pipeline (kg/h)
$m^{de}_{t,\vartheta,e}$,$m^{sr}_{t,\vartheta,q}$	Water mass flow of demand/source at DHS nodes (kg/h)
$n^{ho}_{\vartheta,e}$	Number of households at DHS nodes
$Cair_{\vartheta,e}$	Average thermal capacity of AEVHs (MWh/°C)
π_s	Probability of scenario s
EB_f,η_f	EV fleets' battery capacity/efficiency (MWh)
$SOC^{In}_{f,s}$	SOC at arrival time (%)
$DT_{f,s}$	Travelled miles by EV fleets (mile)
EM_f	Energy consumption per mile (MWh/mile)
Cr_f	EV feets' nominal charge rate (MW)
C_p	Thermal capacity of water (MWh/kg.°C)
R	Thermal resistance of households (°C/MWh)
T^{out}_t	Outdoor temperature (°C)
$\underline{T}^{in}_{\vartheta,e}$,$\overline{T}^{in}_{\vartheta,e}$	Min/Max indoor temperature (°C)
$\underline{P}^{DG}_k$,$\overline{P}^{GD}_k$	Min/Max DG output (MWh)
P^R,ϕ^R	Thermal/electrical FOR of CHPs (MW)
η_{EB},$\overline{P}^{EB}_{t,\vartheta,q}$	Efficiency & max power of EB
γ_p,γ_H	Electrical/Thermal fuel ratio of CHP (%)
T^{Ue}_k,T^{De}_k	Min on, off time of DGs (h).
C^{SU}_k,C^{SD}_k	Start-up/shutdown cost of NGU ($/MWh)
R^{UP}_k	DGs' ramp rate (MWh)
$\overline{P}^{WT}_{r,t}$,$\overline{P}^{PV}_{pv,t}$	Maximum wind/solar production (MW)
Z^{DS}_{ij},R^{DS}_{ij}	Impedance/resistance of ADS feeders (ohm).
$\overline{I}^{DS}_{ij}$	Maximum current of ADS feeders (A).
$\underline{V}^{DS}_i$,$\overline{V}^{DS}_i$	Min/Max ADS node voltage (Kv)
$\underline{\nu_w}$,$\overline{\nu_w}$	Min/Max gas well production (kcf)
$\underline{Pr_n}$,$\overline{Pr_n}$	Min/Max NGN nodal pressure (bar)
$\overline{T}^{DHS}_l$,$\underline{T}^{DHS}_l$	Max/Min DHS pipe temp (°C)

$\overline{T_{\vartheta}^{DHS}}, \underline{T_{\vartheta}^{DHS}}$	Max/Min DHS node temperature (°C)
λ_l, L_l	Thermal conductivity & length of DHS pipeline (m)
$P_{f,s,t}^{L}$	Electrical AEVH demand (MW)
$K_{n,m}^{f}$	NGN pipeline coefficient
C^{PV}, C^{WT}	Cost of PV/WT production ($/MWh)
C_{w}^{gas}, C_{u}^{IL}	Gas well cost ($/kcf)/interruptible loads ($/MWh)
$\bar{P}_{t}^{RES}$	Expected RES production in IGDT (MW)
σ	Risk aversion controller in IGDT.
OF_{b}^{IP}	Optimal value of IESP objective ($)
$C_{g}^{G}, B_{b,b'}$	Genco cost ($/MWh)/ TN suseptance (1/ohm)
$P_{g,t}^{GMax}$	Maximum Genco production (MW)
	Variables
OF^{AH}	AEVHs' objective function
$dg_{f,s,t}$	Battery erosion of EV fleets ($)
$\lambda_{t,i}^{LM}, \lambda_{t,\vartheta}^{TM}$	MCP of LEM & TEM ($/MWh)
$P_{t,i}^{EH}$	AEVHs' Electrical energy purchase (MW)
$H_{t,\vartheta,e}^{ho}$	Thermal energy delivered to AEVHs (MWh)
$SOC_{f,s,t}$	State of charge of EV fleets (%)
$\sigma_{f,s,t}$	EV fleets' cycle depth (%)
$\psi_{f,s,t}$	Cycle depth degradation function
$MD_{f,s,t}$	Marginal battery degradation ($/MWh)
$P_{f,s,t}^{+}, P_{f,s,t}^{-}$	EV fleets' charge/discharge rate (MW)
$T_{t,\vartheta,e}^{in}$	Indoor temperature of AEVHs (°C)
$P_{k,t}^{DG}, H_{k,t}^{DG}$	DGs' electrical/thermal output (MW)
α_{t}^{R}	FOR coefficient of CHP (%)
$SU_{k,t}, SD_{k,t}$	Start-up/Shutdown cost of NGU ($)
$SU_{k,t}^{CHP}$, $SD_{k,t}^{CHP}$	Start-up/Shutdown fuel for CHP (kcf)
$G_{k,t}^{CHP}$	CHPs' natural gas consumption (kcf)
$I_{ij,t}^{DS}, V_{i,t}^{DS}$	Current/voltage of ADS (A), (kV)
$P_{ij,t}^{Loss}$	Power loss in ADS (MW)

$v_{w,t}$ $Pr_{n,t}$	Gas well production (kcf)/ node pressure (bar)
$f^{in}_{n,m,t}$, $f^{out}_{m,n,t}$	Inlet/Outlet flow of NGN pipe (KCF)
$f_{n,m,t}$	Average pipe flow of NGN (KCF)
$T^{ps,out}_{t.l}$, $T^{pr,out}_{t,l}$	End temp of supply/ return DHS pipe (°C)
$T^{ps,in}_{t.l}$,$T^{pr,in}_{t,l}$	Beginning temp of supply/return DHS pipe (°C)
$T^{ms}_{t,\vartheta}$,$T^{mr}_{t,\vartheta}$	Nodal temp of supply/return pipes in DHS (°C)
$H^{loss}_{t,l}$	Thermal energy loss in DHS (MWh)
$H^{sor}_{t,\vartheta,q}$	Thermal energy production in DHS (MWh)
$\lambda^{WEM}_{b,t}$	MCP of WEM ($/MWh)
P^{IESP}_{t}	Power purchased from WEM by IESP (MW)
$P^{IL}_{u,t}$	Interruptible loads (MW)
$P^{EB}_{t,\vartheta,q}$	EB power consumption
P^{RES}_{t},α	RES production (MW)/IGDT radios
$P^{G}_{g,t}$,$P^{D}_{b,t}$	Genco generation & TN demand (MWh)
$\delta_{b,t}$	TN bus voltage angle (°)
μ, ν, ζ	Inequality dual variables in the TN
λ	Equality dual variables in the TN

Binary variables

$u^{+}_{f,s,t}$,$u^{-}_{f,s,t}$	EV fleets' charge/discharge state
$I_{k,t}$	Commitment state of DGs
$y_{k,t}$,$z_{k,t}$	Start-up / Shutdown state of DGs

Abbreviations

AEVH	Aggregated electric vehicle-owning households
IESP	Integrated energy service provider
WEM	Wholesale electricity market
LEM,TEM	Local electricity market, Thermal energy market
ADS,DHS	Active distribution system,District heating system
NGN,MCP	Natural gas network, Market clearing price
RES,NGU	Renewable energy source, Non-gas-fired unit

Genco	Generation company
PHA	Photovoltaic array
IL,EB	Interruptible load, Electrical boiler

1. Introduction

The unprecedented boom in the electric vehicle (EV) sales testifies their economic viability and sustainability. For instance, the UK has pledged to enact legislation to prohibit the sales of fossil fuel-based vehicles by 2030 and only permit EVs by 2035. The co-occurrence of this trend with the proliferation of the high-efficiency combined heat and power units (CHP) is going to introduce new challenges since they entangle the thermal and electrical energy production [1], as well as influencing the natural gas demand [2]. Therefore, the CHPs create an interdependent energy market consisting of the active distribution system (ADS), natural gas network (NGN) and district heating systems (DHS), which is operated under the command of the integrated energy service provider (IESP) [3]. Considering the high penetration of EVs, their charging patterns will have a substantial impact on these markets. The reason is that smart charging strategies of the electric vehicles can increase the thermal and electrical flexibility of the CHP units, which will improve the thermal demand satisfaction in DHS, and reduce the pipeline congestion in NGN. The EVs can participate in energy markets individually as price-takers. However, it is known that a price-maker framework can induce greater profit by influencing market price [4]. Therefore, it is highly probable that EV-owning households would form a coalition to utilize their charging/discharging flexibilities together with their thermal demand flexibility to participate in local electricity and thermal energy markets as the price-makers. In other words, the aggregated EV-owning households (AEVHs) can influence the market-clearing price (MCP) in the thermal energy market (TEM) and local electricity market (LEM) to enhance their collective benefit. The IESP, as the local market operator, procures part of this energy from local distributed generation (DG) units and gas wells. At the same time, it also participates in the wholesale electricity market (WEM) as a price-maker that can submit offers/bids to purchase/sell electrical energy [5]. Accordingly, IESP is a price-maker in WEM, while AEVH operator is a price-maker in LEM and TEM (operated by the IESP), which makes the IESP an intermediary retailer between the WEM and AEVHs.

All these market formations have their individual objectives. For instance, the wholesale electricity market operator (WEMO) clears the WEM to maximize the public welfare, while the IESP's prime objective is to minimize the operational costs of ADS, DHS and NGN as well as the cost of participating in WEM. On the other hand, the AEVHs' objective is to minimize the cost of participating in LEM and TEM, using their flexibilities in thermal demand and EV-scheduling. To solve such a problem, a three-level framework should be devised that considers the AEVHs at the first level, the IESP at the second level and WEMO at the third level. Such a tool would be essential for market players to evaluate AEVHs as a thermal and electrical price-maker that can also pose a significant impact on WEM price through IESP.

Most of the small-scale consumers do not have enough power to participate in energy markets as a price-influencer. In this concern, some of the recent studies have unraveled the importance of demand response aggregators. Particularly, the EV-aggregators [6] have gained a great deal of attention on account of their flexibilities and green features. The altering direction method of multipliers (ADMM) has been proposed in [7] to investigate robust interaction between the EV-aggregator and the distribution company (Disco). Asrari *et al.* [8] evaluated the possibility of using the aggregated EVs to reduce distributed locational marginal price (DLMP), which showed that it is possible with proper congestion management. The authors in [9] inspected EVs as price-takers in LEM intending to diminish DLMP. In a more sophisticated study [10], the DLMP of the LEM was reduced through a bi-level optimization framework that considered EV-aggregators and Disco at upper and lower levels, respectively. These studies illustrate the impact that EVs can impose on Discos at the local level, while Disco's behavior at the wholesale market is also essential. In this regard, [11] proposed a bi-level framework to investigates Disco's strategic behavior at day-head and reserve markets, while information gap decision theory (IGDT) is adopted by [12] to investigate a similar problem. A risk-based Disco optimization has been investigated in [13], wherein the presence of microgirds was addressed at the lower level of the bi-level problem.

As can be observed, all of these studies have focused on a single type of energy, i.e., electricity. Nevertheless, co-generation technologies, such as CHP units, have created an interconnected energy market. Therefore, there has been increasing interest in this area. The authors in [14] proposed a stochastic bi-level approach to investigate strategic participation of a multi-energy system in WEM and real-time integrated markets. The authors in [15] proposed a hierarchical energy scheduling approach for the integrated energy systems, using Stackelberg game approach. The study modelled the energy service provider as a leader, while the households were defined as followers to minimize their cost. A decentralized optimization framework was proposed by [16] to minimize the cost and emissions of an integrated energy system via the multi-objective optimization framework. In [17], a model predictive energy management strategy was proposed for EV-charging stations and thermal energy supply of community buildings. The study used a moving-horizon stochastic programming approach to deal with the RES production uncertainties. The economic-environmental operation of a multi-energy system was addressed in [18], wherein the study aimed to maximize the benefits of the multi-energy operator and minimize the operational emissions at the same time. A non-dominated sorting genetic algorithm was investigated in [19] for the optimal emission-constrained operation of multi-energy systems. The main contribution of this study was to include thermo-hydraulic characteristic of the integrated electrical and thermal energy systems. The bi-level scheduling of multi-energy systems is scrutinized in [20], considering pool market, forward contracts and rival players.

Despite all the authentic novelties, the following shortcomings (**SH**) can be identified in these studies:

SH 1: In some studies [10–14, 17, 18, 20], the impacts of integrating EVs have been evaluated at local energy systems. However, EVs can also have a significant influence at WEM level.

SH 2: The current literature have not investigated the EVs as thermal price-makers that can be feasible through CHP units.

SH 3: The studies [11–13] have focused on a single type of energy (electricity)

SH 4: The IESP has not been studied as a price-maker in WEM.

To address the existing gaps, this study puts forward a three-level framework to model AEVHs as price-makers in LEM and TEM that is operated by IESP, which in turn is also a price-maker in WEM. At the first level, the AEVHs' objective is to minimize the cost of participating in TEM and LEM, using their thermal flexibility and smartly schedulable EVs. The IESP (second level) intends to minimize the operational cost and the cost of participating in WEM by submitting the best offer/bid. Eventually, at the third level, the WEMO clears the market to maximize public welfare. A hybridized KKT conditions and two-step iterative method is used to solve the three-level problem. Moreover, EVs' arrival/departure times are modelled through stochastic scenarios, while the IGDT framework is used to address the uncertainties of renewable energy sources (RES) at the second level. Table 1 provides the main traits of the previous publications and this study. Overall, the major contributions of this study can be summarized as follows:

i A three-level hybrid SP-IGDT framework is proposed to model AEVHs as price-makers in LEM and TEM, while considering IESP as a price-maker at WEM. (Addresses **SH1** and **SH2**)

ii The influence of strategic EV scheduling at local electricity, thermal markets as well as WEM is scrutinized. (Addresses **SH2** and **SH3**)

iii A novel method of integrating KKT conditions with the two-step iterative approach is proposed to solve the three-level optimization problem. (Addresses **SH3** and **SH4**)

2. problem description

In this study, the AEVHs partake in LEM and TEM as price-setter players, while considering that IESP is also a price-setter in WEM. For this purpose, a three-level optimization framework is established, where the AEVHs form the first level of the problem, while IESP and WEM are second and third level problems, respectively.

Table 1: Comparative evaluations between this study and previous publications

Ref	Uncertainty	Markets			Multi-level solving method	Flexible technologies	
		WEM	LEM	TEM		EV	Thermal demand
[6]	SP	✓	×	×	WoLF	✓	×
[7]	RO	✓	✓	×	Two-step	✓	×
[8]	-	×	✓	×	-	✓	×
[9]	SP	×	✓	×	-	✓	×
[10]	RO	×	✓	×	KKT	✓	×
[11]	SP	✓	✓	×	KKT	×	×
[12]	IGDT	✓	✓	×	KKT	×	×
[13]	SP	✓	✓	×	KKT	×	×
[14]	SP	✓	×	✓	KKT	×	✓
[15]	SP	×	✓	✓	Stackelberg	×	×
[16]	-	×	✓	✓	-	×	✓
[17]	SP	×	×	✓	-	✓	✓
[18]	-	×	×	×	-	✓	✓
[19]	-	×	✓	✓	-	×	✓
[20]	SP	✓	×	✓	KKT	×	✓
This study	**SP-IGDT**	**✔**	**✔**	**✔**	**Hybrid KKT & Two-step**	**✔**	**✔**

In other words, IESP is a follower to AEVHs, and WEM is a follower to IESP. The AEVHs operator sends its energy requirements to IESP operator. Subsequently, the IESP self-schedules the DGs, NGN, ADS and DHS. Afterwards, partakes in WEM and clears TEM and LEM to announce MCP of retail electrical and thermal energy. Simultaneously, the WEM operator receives the offers/bids from IESP, and clears the WEM to announce the MCP of the WEM. The IESP is an intermediary retailer that links AEVHS to WEM. The EV-related uncertain data, such as vehicles arrival/departure time and daily travelled miles are handled by stochastic scenarios, while uncertain climatic data such as solar and wind power is dealt with via risk-averse IGDT framework. The solving procedure, which is established in the next sections, ensures the best equilibrium for these various levels. The overall interactive relationship between these three levels, their corresponding objectives and decision variables, can be observed in Fig. 1.

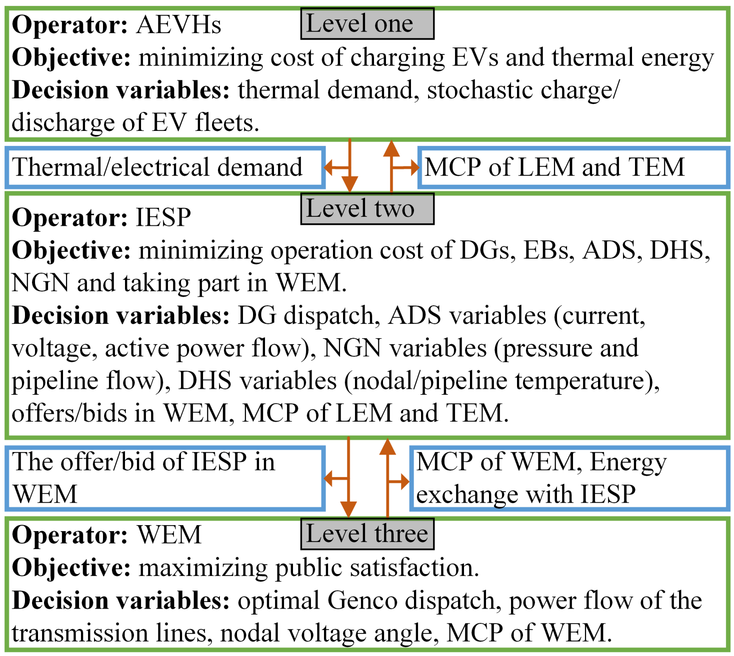

Figure 1: The interactive relationship of various levels of the problem

3. Formulation & Algorithm

3.1. Aggregated electric-vehicle-owning households (First level)

In this study, the EVs are clustered into fleets with distinct behavioral patterns via K-means clustering as presented in [21], and they are assumed to be present at the residential parking lots (equipped with level II chargers) from arrival to departure intervals. The objective function of the AEVHs (first level) is defined by Eq. (1), wherein the first term is the battery degradation cost of the EV fleets, while the second and the last terms represent the cost of participating in the local electricity and thermal energy markets. The decision variables of this level include thermal energy demand and stochastic charge/discharge of EV fleets. The SOC for each fleet is computed via Eqs. (2)-(3), while initial and final (at departure) SOC are declared in Eqs. (4)-(5). Eqs. (6)-(8) are conventional storage equations, and cycle depth is calculated by Eq. (9). Furthermore, the battery degradation cost is imposed in Eqs. (10)-(12), which is linearized and proved in [22]. Eventually, the flexible thermal demand of the households is established in Eq. (13), while Eq. (14) defines the expected electrical demand of the AEVHs.

$$\min OF^{AH} = \sum_t \begin{pmatrix} \sum_s \sum_f \pi_s.dg_{f,s,t} + \\ \sum_{i \in A_i^{EH}} \lambda_{t,i}^{LM} P_{t,i}^{EH} + \\ \sum_\vartheta \lambda_{t,\vartheta}^{TM} H_{t,\vartheta,e}^{ho} \end{pmatrix} \tag{1}$$

$$\begin{aligned} SOC_{f,s,t} &= SOC_{f,s,t-1} + \left(\eta_f.P^+_{f,s,t}/EB_f\right) \\ &- \left(P^-_{f,s,t}/EB_f.\eta_f\right) \forall f,s,t \neq TA_f \end{aligned} \tag{2}$$

$$\begin{aligned} SOC_{f,s,t} &= SOC^{In}_{f,s} + \left(\eta_f.P^+_{f,s,t}/EB_f\right) \\ &- \left(P^-_{f,s,t}/EB_f.\eta_f\right) \forall f,s,t = TA_f \end{aligned} \tag{3}$$

$$SOC^{In}_{f,s} = \max \begin{pmatrix} \underline{SOC_f}, 1- \\ (DT_{f,s} \times EM_f/EB_f) \end{pmatrix} \forall f,s \tag{4}$$

$$SOC_{f,s,t} = \min\left(SOC^{end}_{f,s}, SOC^{des}_f\right) \forall f,s,t = TD_f \tag{5}$$

$$\underline{SOC_f} \leqslant SOC_{f,s,t} \leqslant \overline{SOC_f} \forall f,s,t \tag{6}$$

$$P^+_{f,s,t} \leqslant Cr_f.uc_{f,s,t}, P^-_{f,s,t} \leqslant Cr_f.u^-_{f,s,t} \forall f,s,t \tag{7}$$

$$u^+_{f,s,t} + u^-_{f,s,t} = 1 \forall f,s,t \tag{8}$$

$$\sigma_{f,s,t} = \sigma_{f,s,t-1} - (P^-_{f,s,t}/EB_f.\eta_f) \forall f,s,t \tag{9}$$

$$\psi_{f,s,t}\left(\sigma_{f,s,t}\right) = a_0.(\sigma_{f,s,t})^{2.03} \forall f,s,t \tag{10}$$

$$MD_{f,s,t} = 2.03 a_0 (BC_f/EB_f.\eta_f) {\sigma_{f,s,t}}^{1.03} \forall f,s,t \tag{11}$$

$$dg_{f,s,t} = P^-_{f,s,t}.MD_{f,s,t} \forall f,s,t \tag{12}$$

$$\begin{aligned} &T^{in}_{t,\vartheta,e} = T^{in}_{t-1,\vartheta,e} e^{-1/((R/n^{ho}_{\vartheta,e}).Cair_{\vartheta,e})} \\ &+(H^{ho}_{t,\vartheta,e}.R/n^{ho}_{\vartheta,e} + T^{out}_t).(1 - e^{-1/((R/n^{ho}_{\vartheta,e}).Cair_{\vartheta,e})}) \\ &, \underline{T^{in}_{\vartheta,e}} \leqslant T^{in}_{t,\vartheta,e} \leqslant \overline{T^{in}_{\vartheta,e}} \forall t, \forall \vartheta, \forall e \end{aligned} \tag{13}$$

$$P_{t,i}^{EH} = \sum_{s} \pi_s (P_{f,s,t}^{+} - PD_{f,s,t}^{-} + P_{f,s,t}^{L}) \forall s, t, f \in A_i^f \tag{14}$$

3.2. Integrated energy service provider (second level)

3.2.1. Units' commitment

The commitment status of units is imposed by Eq. (15), while Eqs. (16)-(18) restrict CHPs' thermal/electrical generation within feasible operation region. The NGUs' start-up/shutdown cost is declared in Eq. (19), while Eq. (20) defines the CHPs' gas consumption at start-up/shutdown, and Eq. (21) is the CHPs' overall gas consumption. The ramp rate restrictions are enforced in Eqs. (22)-(23), and minimum on/off time limits are defined in Eqs. (24)-(30). Eventually, solar/wind generation bounds are imposed by Eq. (31) [23].

$$\underline{P_k^{DG}} I_{k,t} \leqslant P_{k,t}^{DG} \leqslant \overline{P_k^{GD}} I_{k,t} \forall t, k \in \{NGU\} \tag{15}$$

$$P_{k,t}^{DG} = \sum_{R=1} \alpha_t^R P^R, H_{k,t}^{DG} = \sum_{R=1} \alpha_t^R \phi^R \forall t, k \in CHP \tag{16}$$

$$\sum_{R=1} \alpha_t^R = I_{k,t}, 0 \leqslant \alpha_t^R \leqslant 1 \forall t, k \in CHP \tag{17}$$

$$Q_{k,t}^{CHP} = \gamma_p P_{k,t}^{DG} + \gamma_H H_{k,t}^{DG} \forall t, k \in CHP \tag{18}$$

$$SU_{k,t} \geqslant C_k^{SU} y_{k,t}, SD_{k,t} \geqslant C_k^{SD} z_{k,t} \forall t, k \in NGU \tag{19}$$

$$\begin{aligned} & SU_{k,t}^{CHP} \geqslant C_k^{CHP} y_{k,t}, SD_{k,t}^{CHP} \geqslant C_k^{CHP} z_{k,t} \\ & \forall t, k \in CHP \end{aligned} \tag{20}$$

$$G_{k,t}^{CHP} = Q_{k,t}^{CHP} + SU_{k,t}^{CHP} + SD_{k,t}^{CHP} \forall k \in \{CHP\}, \forall t \tag{21}$$

$$P_{k,t}^{DG} - P_{k,t-1}^{DG} \leqslant (1 - y_{k,t}) R_k^{UP} + y_{i,t} \underline{P_k^{DG}} \forall t, k \tag{22}$$

$$P_{k,t-1}^{DG} - P_{k,t}^{DG} \leqslant (1 - z_{k,t}) R_k^{UP} + z_{i,t} \underline{P_k^{DG}} \forall t, k \tag{23}$$

$$T_k^{Ue} = \min\left\{T, T_k^{U0}\right\}, T_k^{De} = \min\left\{T, T_k^{D0}\right\} \forall k \tag{24}$$

$$\sum_{t=1}^{T_k^{Ue}} I_{k,t} = T_k^{Ue}, \sum_{t=1}^{T_k^{De}} I_{k,t} = 0 \forall k \tag{25}$$

$$\sum_{t=r}^{t+T_k^{Ue}-1} I_{k,r} \geqslant T_k^{U} y_{k,t} \forall k, \forall t = \begin{bmatrix} T_k^{Ue} + 1, \cdots, \\ T - T_k^{U} + 1 \end{bmatrix} \tag{26}$$

$$\sum_{t=r}^{T} (I_{k,r} - y_{k,t}) \geqslant 0 \forall k, \forall t = \left[T - T_k^{U} + 2, \cdots, T\right] \tag{27}$$

$$\sum_{t=r}^{t+T_k^{D}-1} (1 - I_{k,r}) \geqslant T_k^{D} z_{k,t} \forall k, \forall t = \begin{bmatrix} T_k^{De} + 1, \cdots, \\ T - T_k^{D} + 1 \end{bmatrix} \tag{28}$$

$$\sum_{t=r}^{T}(1-I_{k,r}-z_{k,t})\geqslant 0\forall k,\forall t=\begin{bmatrix} T-T_k^D \\ +2,\cdots,T \end{bmatrix} \tag{29}$$

$$y_{k,t}-z_{k,t}=I_{k,t-1}-I_{k,t},y_{k,t}+z_{k,t}\leqslant 1\forall t,k \tag{30}$$

$$0\leqslant P_{r,t}^{Wind}\leqslant \overline{P_{r,t}^{WT}},0\leqslant P_{pv,t}^{PV}\leqslant \overline{P_{pv,t}^{PV}}\forall t,w,v \tag{31}$$

3.2.2. Active distribution system

Here, the power flow equations are solved by the linearized framework presented in [13]. The feeders' power flow is defined in Eq. (32), and Eq. (33) is the power loss equation. The current value is computed by Eq. (34), and current/voltage bounds are enforced in Eq. (35). Finally, the nodal power equilibrium is established in Eq. (36) for the slack bus and in Eq. (37) for other buses. The MCP of the LEM is obtained from the dual value of Eq. (37), and it is specified by $\lambda_{t,i}^{LM}$.

$$P_{ij,t}^{flow}=\left(R_{ij}^{DS}/(Z_{ij}^{DS})^2\right).(V_{i,t}^{DS\_sqr}-V_{j,t}^{DS\_sqr})\forall ij,\forall t \tag{32}$$

$$P_{ij,t}^{Loss}=R_{ij}^{DS}I_{ij}^{DS\_sqr}\forall ij,\forall t \tag{33}$$

$$I_{ij,t}^{DS}=(V_{i,t}^{DS}-V_{j,t}^{DS})/Z_{ij}^{DS}\forall ij,\forall t \tag{34}$$

$$-\overline{I_{ij}^{DS}}\leqslant I_{ij,t}^{DS}\leqslant \overline{I_{ij}^{DS}},\underline{V_i^{DS}}\leqslant V_{i,t}^{DS}\leqslant \overline{V_i^{DS}}\forall ij,\forall t \tag{35}$$

$$\begin{aligned} &P_t^{IESP}+\sum_{r\in A_i^r}P_{r,t}^{Wind}+\sum_{v\in A_i^v}P_{v,t}^{PV}+\sum_{k\in A_i^k}P_{k,t}^{DG} \\ &+\sum_{l\in A_i^l}P_{l,t}^{IL}=\sum_{l\in A_i^l}P_{l,t}^{DSRL}+\sum_{d\in A_i^d}P_{d,t}^{DSNRL} \\ &+0.5(\sum_{j\in DS}P_{ij,t}^{Loss}+\sum_{j\in DS}P_{ij,t}^{flow})\forall i=1,\forall t \end{aligned} \tag{36}$$

$$\begin{aligned} &\sum_{r\in A_i^r}P_{r,t}^{Wind}+\sum_{v\in A_i^v}P_{v,t}^{PV}+\sum_{k\in A_i^k}P_{k,t}^{DG}\forall i\neq 1,\forall t \\ &+\sum_{l\in A_i^l}P_{l,t}^{IL}=\sum_{l\in A_i^l}P_{l,t}^{DSRL}+P_{t,i}^{EH}+\sum_{\vartheta\in B_i^\vartheta}P_{t,\vartheta,q}^{EB}:\lambda_{t,i}^{LM} \\ &+\sum_{d\in A_i^d}P_{d,t}^{DSNRL}+0.5(\sum_{j\in DS}P_{ij,t}^{Loss}+\sum_{j\in DS}P_{ij,t}^{flow}) \end{aligned} \tag{37}$$

3.2.3. Natural gas network

The natural gas wells' production and nodal pressure of the NGN are restricted in Eq. (38). Eqs. (39)-(40) describe the Weymouth natural gas flow equation in non-active and active (with compressor) pipelines. The method presented in [24] is deployed to address the nonlinearities of Weymouth equations. Eventually, the natural gas equilibrium is defined by Eq. (42).

$$\underline{v_w} \leqslant v_{w,t} \leqslant \overline{v_w}, \underline{Pr_n} \leqslant Pr_{n,t} \leqslant \overline{Pr_n} \forall n, w, t \tag{38}$$

$$f^2_{n,m,t} = K^f_{n,m}(Pr^2_{n,t} - Pr^2_{m,t}) \forall (n,m) \notin z, \forall t \tag{39}$$

$$f^2_{n,m,t} \geqslant K^f_{n,m}(Pr^2_{n,t} - Pr^2_{m,t}) \forall t \forall (n,m) \in z, \forall t \tag{40}$$

$$f_{n,m,t} = (f^{in}_{n,m,t} - f^{out}_{m,n,t})/2 \tag{41}$$

$$\sum_{sp \in A^{sp}_n} v_{sp,t} - \sum_{k \in A^k_n} G^{CHP}_{k,t} = \sum_{m \in z} (f^{in}_{n,m,t} - f^{out}_{m,n,t}) \quad \forall n, \forall t \tag{42}$$

3.2.4. *District heating system*

In this study, the hot water DHS model is deployed as presented in [25]. The thermal equilibrium of the nodes is established through the pipelines entering that node in Eqs. (43)-(44) for the supply/return pipe networks. The temperature at the beginning of the pipelines is defined by Eq. (45) as equal to the nodal temperature of the node that pipeline exists. The thermal demands are satisfied via Eq. (46), and Eq. (47) expresses the temperature at the end of pipelines. The thermal energy loss along the pipes is established in Eq. (48), while Eqs. (49)-(50) declare the EB constraints. Eq. (51) denotes the thermal energy dispatched from CHPs and electrical boilers (EB). Overall thermal energy equilibrium is satisfied by Eq. (52). Eventually, the temperature bounds of DHS are declared in Eq. (53). The MCP of TEM is obtained from the dual value of Eq. (46), and it is specified by $\lambda^{TM}_{t,\vartheta}$.

$$\sum_{l \in s^-_\vartheta} (T^{ps,out}_{t,l} . ms_{t,l}) = T^{ms}_{t,\vartheta} \sum_{l \in s^-_\vartheta} ms_l \forall t, \vartheta \tag{43}$$

$$\sum_{l \in s^+_\vartheta} (T^{pr,out}_{t,l} . mr_{t,l}) = T^{mr}_{t,\vartheta} \sum_{l \in s^+_\vartheta} mr_l \forall t, \vartheta \tag{44}$$

$$\begin{cases} T^{ps,in}_{t,\vartheta} = T^{ms}_{t,l}, \quad l \in S^+_\vartheta \\ T^{pr,in}_{t,\vartheta} = T^{mr}_{t,l}, \quad l \in S^-_\vartheta \end{cases} \forall t, l \tag{45}$$

$$H^{ho}_{t,\vartheta,e} = C_p m^{de}_{t,\vartheta,e}(T^{ms}_{t,\vartheta,e} - T^{mr}_{t,\vartheta,e}) \forall t, \vartheta, e{:}\lambda^{TM}_{t,\vartheta} \tag{46}$$

$$\begin{matrix} T^{ps,out}_{t.l} = (T^{ps,in}_{t,l} - T^{out}_t) e^{-(\lambda_l L_l / C_p ms_l)} + T^{out}_t \\ T^{pr,out}_{t,l} = (T^{pr,in}_{t,l} - T^{out}_t) e^{-(\lambda_l L_l / C_p ms_l)} + T^{out}_t \end{matrix} \quad \forall t, l \tag{47}$$

$$H^{loss}_{t,l} = C_p m^{de}_{t,l}(T^{in}_{t,l} - T^{out}_{t,l}) \forall t, l \tag{48}$$

$$H^{sor}_{t,\vartheta,q} = \eta_{EB} P^{EB}_{t,\vartheta,q} q \in \{EB\} \tag{49}$$

$$0 \leqslant P^{EB}_{t,\vartheta,q} \leqslant \overline{P^{EB}_{t,\vartheta,q}} \tag{50}$$

$$H^{sor}_{t,\vartheta,q} = C_p m^{sr}_{t,\vartheta,q}(T^{in}_{t,\vartheta,q} - T^{out}_{t,\vartheta,q})\forall t, \vartheta, q_{\in\{CHP,EB\}} \tag{51}$$

$$\begin{aligned} &\sum_{\vartheta} \sum_{q\in\{CHP,EB\}} H^{sor}_{t,\vartheta,q} - \sum_{l\in S^+_\vartheta, S^-_\vartheta} H^{loss}_{t,l} \\ &- \sum_{\vartheta} \sum_{d} H^{ho}_{t,\vartheta,e} = 0 \end{aligned} \tag{52}$$

$$\begin{aligned} &\underline{T^{DHS}_{l}} \leqslant T^{ps,out}_{t.l}, T^{ps,in}_{t,l} \leqslant \overline{T^{DHS}_{l}}, \\ &\underline{T^{DHS}_{\vartheta}} \leqslant T^{ms}_{t.\vartheta}, T^{mr}_{t,\vartheta} \leqslant \overline{T^{DHS}_{\vartheta}} \forall t, \forall l \end{aligned} \tag{53}$$

3.2.5. IESP's Objective

The IESP's objective (second level) is established in Eq. (54), which consists of six terms, namely the cost of participating in WEM, wind turbine (WT) production, photovoltaic arrays (PHA) production, natural gas production, interruptible load (IL) shedding and non-gas-fired unit (NGU) operation. The decision variables of the IESP consist of DG dispatch power, ADS variables (current, voltage, active power flow), NGN variables (pressure and pipeline flow), DHS variables (nodal/pipeline temperature), offers/bids in WEM, MCP of LEM and MCP of TEM. Since IGDT framework is deployed to deal with uncertainties of renewable energy sources (RES), the main objective of the second level is redefined accordingly in Eq. (55), as the radius of uncertainty, while the accompanying constraints are expressed in Eqs. (56)-(59) [12].

$$OF^{IP} = \sum_{t} \left\{ \begin{array}{l} \lambda^{WEM}_{b,t} P^{IESP}_{t} + \sum_{r} C^{WT} P^{WT}_{r,t} \\ + \sum_{pv} C^{PV} P^{PV}_{pv,t} + \sum_{w} C^{gas}_{w} v_{w,t} \\ + \sum_{u} C^{IL}_{u} P^{IL}_{u,t} + \\ \sum_{k\in NGU} \left(\begin{array}{l} C^{DG}_{k} P^{DG}_{k,t} + \\ SU_{k,t} + SD_{k,t} \end{array} \right) \end{array} \right\} \tag{54}$$

$$\max\{\alpha\}, \alpha \geqslant 0 \tag{55}$$

$$u(\bar{P}^{RES}_{t}, \alpha) = \left\{ P^{RES}_{t} : \left| \frac{P^{RES}_{t} - \bar{P}^{RES}_{t}}{\bar{P}^{RES}_{t}} \right| \leqslant \alpha \right\} \tag{56}$$

$$OF^{IP}_{b} = \left\{ OF^{IP} : \min OF^{IP} \right\} \tag{57}$$

$$OF \leqslant OF_b(1+\sigma), 0 \leqslant \sigma \leqslant 1 \tag{58}$$

$$0 \leqslant P^{RES}_{t} \leqslant (1-\alpha)\bar{P}^{RES}_{t}, P^{RES}_{t} = P^{WT}_{r,t} + P^{PV}_{pv,t} \tag{59}$$

3.3. Wholesale electricity market (Third level)

The WEMO's objective (third level) is defined in Eq. (60). The terms of the equation include the production cost of Gencos and the profit/cost of selling/purchasing to/from IESP. The decision variable of the WEM are optimal Genco dispatch, power flow of the transmission lines, nodal voltage angle and MCP of WEM. Eq. (61) satisfies the energy equilibrium constraint of TN, while the capacity and ramp rate constraints are defined in Eqs. (62)-(66). The transaction with IESP is limited by Eq. (67). Ultimately, the power flow rate of the feeders and voltage angle limits of TN are restricted via Eqs. (68)-(69). The MCP of WEM is obtained from the dual value of the Eq. (61), it specified by $\lambda_{b,t}^{WEM}$.

$$\min\left\{\sum_{t}\sum_{g} C_g^G P_{g,t}^G - \sum_{t}\sum_{g} C_t^{IESP} P_t^{IESP}\right\} \tag{60}$$

$$\begin{aligned}&\sum_{g\in A_n^g} P_{g,t}^G - P_t^{IESP} - P_{b,t}^D = \sum_{b'\in Tr} B_{b,b'}(\delta_{b,t} - \delta_{b',t})\\&: \lambda_{b,t}^{WEM} \forall b, t\end{aligned} \tag{61}$$

$$0 \leqslant P_{g,t}^G \leqslant P_{g,t}^{GMax} : \underline{\mu_{g,t}^G}, \overline{\mu_{g,t}^G} \forall g, \forall t \tag{62}$$

$$P_{g,t}^G - P_{g,t-1}^G \leqslant RU_g : \mu_{g,t}^1 \forall g, t > 1 \tag{63}$$

$$P_{g,t}^G - P_{g,ini}^G \leqslant RU_g : \mu_{g,t}^2 \forall g, t = 1 \tag{64}$$

$$P_{g,t-1}^G - P_{g,t}^G \leqslant RD_g : \mu_{g,t}^3 \forall g, t > 1 \tag{65}$$

$$P_{g,ini}^G - P_{g,t}^G \leqslant RD_g : \mu_{g,t}^4 \forall g, t = 1 \tag{66}$$

$$\underline{P_t^{IESP}} \leqslant P_t^{IESP} \leqslant \overline{P_t^{IESP}} : \underline{\mu_t^{IESP}}, \overline{\mu_t^{IESP}} \forall t \tag{67}$$

$$\begin{aligned}&-\overline{C_{b,b'}} \leqslant B_{b,b'}(\delta_{b,t} - \delta_{b',t}) \leqslant \overline{C_{b,b'}}\\&: \underline{\nu_{b,b',t}}, \overline{\nu_{b,b',t}} \forall b, b', t\end{aligned} \tag{68}$$

$$-\pi \leqslant \delta_{b,t} \leqslant \pi : \underline{\xi_{b,t}}, \overline{\xi_{b,t}} \forall b, t \tag{69}$$

3.4. Proposed algorithm

In the proposed model, the IESP consists of an ADS, an NGN and a DHS. Furthermore, it is obliged to satisfy the energy demands of the customers in different markets. To this end, IESP incorporates WTs, gas wells, PVAs, NGUs, ILs, EBs and CHP units. That said, it also participates in WEM to procure/sell electrical energy. To solve this bi-level problem, IESP submits offers/bids in WEM; then the WEMO clears the market to announce the MCP. Afterwards, the IESP reschedules itself and resubmits offers/bids accordingly. This process is continued until reaching the equilibrium state for both IESP and WEM. In this study, KKT conditions are deployed to modify the WEM problem as constraints in IESPs' problem [13]. In other words, the second and third levels are merged into a single problem through KKT conditions, and the nonlinear production terms were addressed through the theory of strong duality. More information on the KKT conditions of the problem and the theory of strong duality is included in Appendix A and Appendix B. Henceforth, the equilibrium state of AEVHs and this merged problem is achieved. In this regard, the two-step method is used as it is elaborated in [25]. Accordingly, the IESP clears these markets (according to ADS and DHS limitations) and declares the thermal/electrical MCP. This process is the so-called first step. At the second step, the AEVHs' operator schedules the thermal demand of the households as well as smart charging of the EVs and submits thermal/electrical demand in LEM and TEM. These two steps are repeated until the criterion in Eq. (70) is satisfied. The overall algorithm is established as follows:

$$\left(\mathrm{OF}^{\mathrm{AH}^*}(\mathrm{Step1}) - \mathrm{OF}^{\mathrm{AH}^*}(\mathrm{Step2})\right) / \mathrm{OF}^{\mathrm{AH}^*}(\mathrm{Step1}) \leqslant \varepsilon \tag{70}$$

Algorithm: Hybrid KKT & two-step method.

Initialization: Get the input parameters of the first, second and third level problems.

1. Solve the second and third level problems based on KKT condition and theory of strong duality using Eqs. (15)-(69).

2. Receive $\lambda^{LM*}_{t,i}, \lambda^{TM*}_{t,\vartheta}$

3. Step1: Solve the first level problem using Eqs. (1)-(14) and calculate the optimal value of total cost.

4. Update values of $P^{EH*}_{t,i}, H^{ho}_{t,\vartheta,e}{}^{*}$.

5. Step2: Solve the second and third level problems based on KKT condition and theory of strong duality using Eqs. (15)-(69).

6. Update values of $\lambda^{LM*}_{t,i}, \lambda^{TM*}_{t,\vartheta}$

7. Calculate the optimal value of OF^{AH} using Eq. (1).

8. If the stop criterion Eq. (70) is satisfied, terminate the algorithm, otherwise return to stage **3**

4. Case studies and results

In this study, AEVHs are modelled through 6000 aggregated households with 3000 EVs that are clustered into 5 fleets by K-means clustering [26]. The data on the thermal characteristics of the households is taken from [27], and EVs data is provided in [28] and national household travel survey (NHTS) [29]. The overall schematic of the systems, connections and locations is depicted in Fig. 2. Moreover, the structural data of the systems are summarized in Appendix C. The empirical probability distribution functions of NHTS data for EVs arrival/departure times are plotted in Fig. 3. The arrival/departure time data distribution of the clustered EV fleets is illustrated in Fig. 4 and the probability distribution of their daily travelled miles is depicted in Fig. 5. These empirical distributions are utilized to generate stochastic scenarios for EV fleets. Moreover, the mixed-integer linear problem

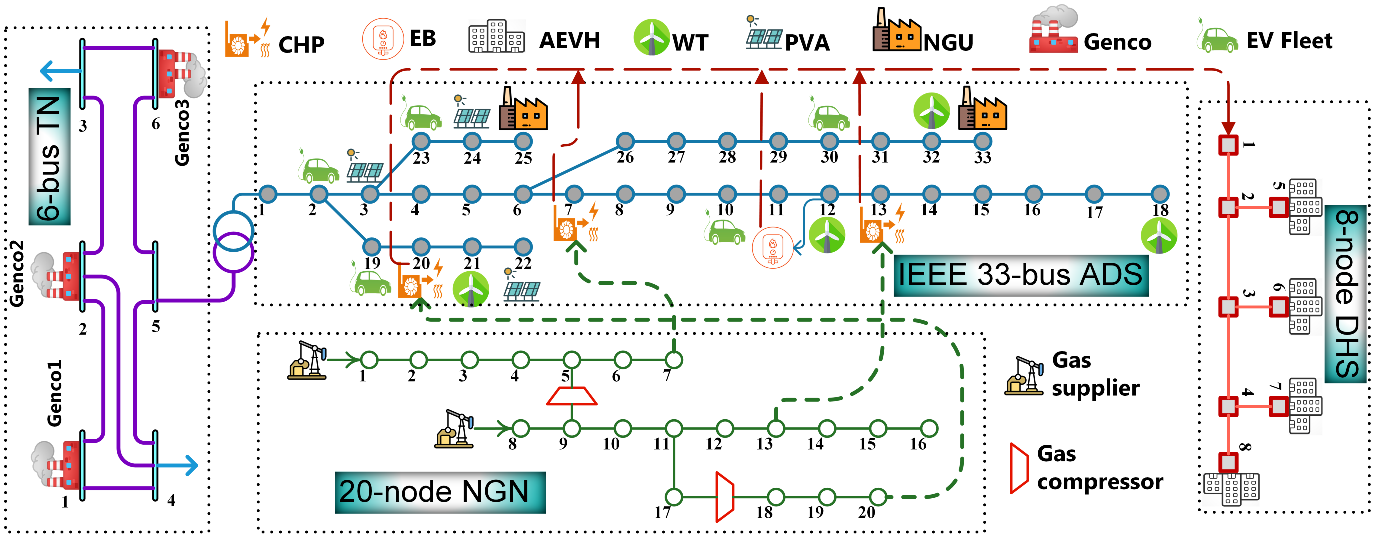

Figure 2: Overall schematic of the systems connections and locations

(MILP) was solved via the GUROBI solver. Eventually, the following case studies are designed to assess the proposed three-level framework.

- Case Study 1 (**CS1**): In this case, the thermal flexibility of the households is ignored (temperature fixed at 25°C), and EVs are charged uncoordinatedly as soon as they arrive.
- Case Study 2 (**CS2**): In this case, the thermal flexibility of the households is ignored (temperature fixed at 25°C), and EVs are charged smartly.
- Case Study 3 (**CS3**): In this case, the households are assumed to be thermally flexible (temperature interval of 18°C-25°C), and EVs are charged smartly.
- Case Study 4 (**CS4**): In this case, the IGDT approach is applied to RES in **CS3**.

It should be noted that in the smart charging method, the charge/discharge of the electric vehicles is a decision variable defined in the optimization process. Therefore, the electric vehicles charge/discharge schedule is obtained from solving the proposed formulation. However, when the charging scheduling is not smart (uncoordinated), the vehicles are charged without any control strategy.

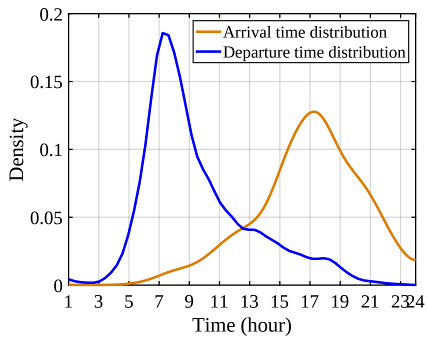

Figure 3: Arrival/departure time probability distribution of NHTS data

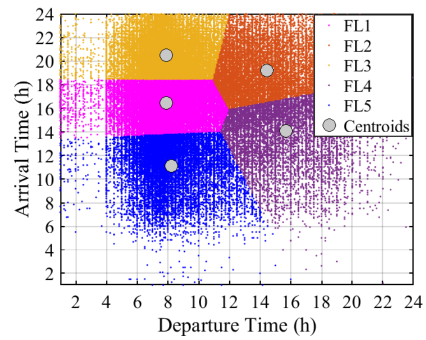

Figure 4: EV fleets' arrival/departure time distribution

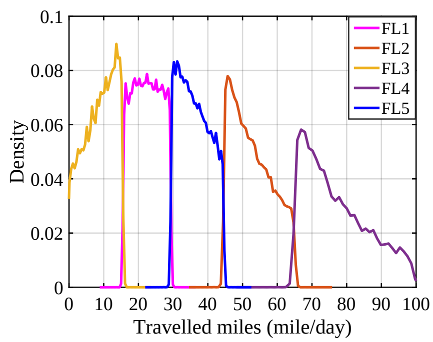

Figure 5: Probability distribution of EV fleets' daily travelled miles

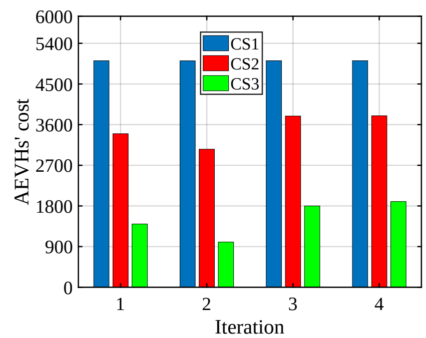

Figure 6: Convergence of the AEVHs' cost in two-step method.

The iterative convergence of the two-step method for different cases can be seen in Fig. 6. As can be seen, the AEVHs' cost is converged after three iterations in all cases. The expected SOC of EV fleets in different cases is demonstrated in Fig. 7. In **CS1**, the EV fleets are charged as soon as they arrive at the residential site. Therefore, EVs' SOC curve shows sharp slopes at hours 16-19. The reason is that according to Fig. 4, EV fleets' arrival time distribution is heavily concentrated around these times. However, hours 16-19 also coincide with the peak demand of IESP and WEM. In this regard, **CS2** enables the AEVHs' operator to shift demand to cheaper off-peak periods, which can be observed from the SOC of fleets in **CS2**, as EVs are mainly charged at hours 6-9, which is the departure time for most EVs. In **CS3**, this shift in demand is even more perceptible, as the thermal flexibility of

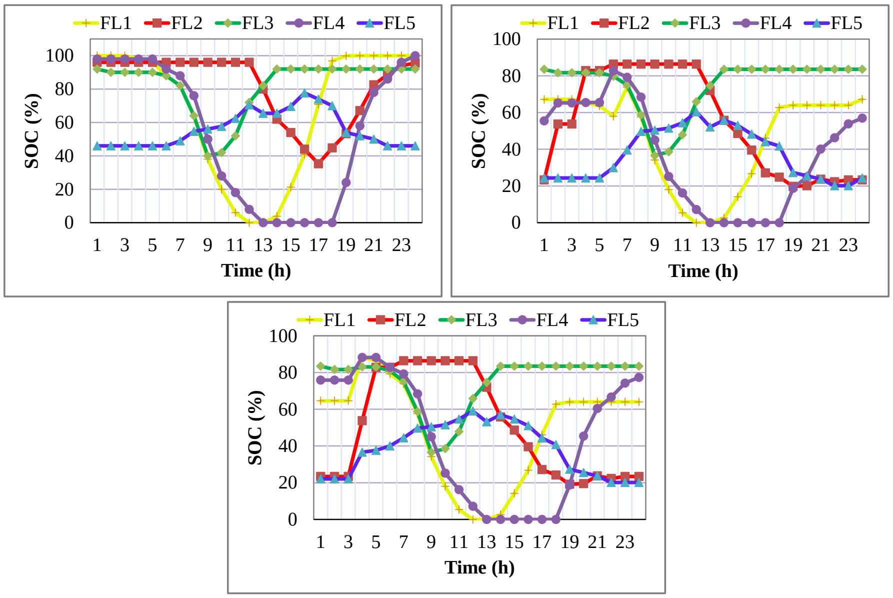

Figure 7: The SOC of EV fleets: a) **CS1** b) **CS2** c) **CS3**

AERHs improves the electrical capacity of the cheaper CHP units. The reason is that the electrical and thermal outputs of CHP units are inextricably interdependent.

The hourly dispatch scheduling of the IESP in three cases is illustrated by Fig. 8. Accordingly, in **CS1**, where there is no flexibility, the power imported from WEM is 0.45% less regarding **CS2** and 2.79% less regarding **CS3**. The reason is that in **CS2** and **CS3** more energy is imported during cheaper off-peak hours from WEM. As can be observed, **CS2** and **CS3** illustrate a sharp rise in the imported power from WEM during hours 1-5, which is the most inexpensive time interval for WEM price. Furthermore, the production of the expensive NGUs is declined by 25.40% and 32.25% in **CS2** and **CS3** compared to **CS1**. That said, the production of efficient CHP units is increased by 8.62% in **CS3** compared to **CS1**. Nevertheless, 0.06 MWh of the load is shed (with the cost of 500 $/MWh) in **CS1** to satisfy security bounds. Fig. 8 shows that there is a large demand profile for EVs at hours 15-18 in **CS1**, which is due to the uncontrolled charging strategy of the EVs in this case. Nonetheless, in **CS2**, this demand is spread over time periods 3-5 since the charging schedule is intelligent, and EVs are even discharged at time 21 to increase the profit.

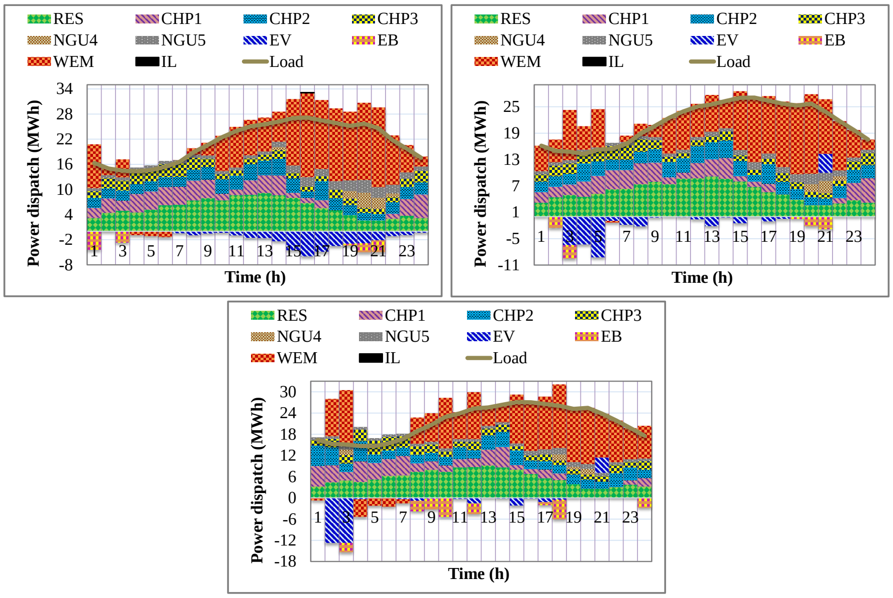

Figure 8: The power dispatch of units in ADS: a) **CS1** b) **CS2** c) **CS3**

These results also reflect on the MCP of the local electricity market. As it is illustrated in Fig. 9, **CS1** imposes the highest MCP cost. Overall, the MCP of the local electricity market in **CS2** is dropped by 2.42%, and in **CS3** by 11.87% in comparison to **CS1**. As can be seen, **CS2** and **CS3** have a slightly higher MCP at off-peak hours since they have shifted demand to these intervals.

Fig. 10 and Fig. 11 demonstrate the power dispatching of Genco1-3. In **CS1**, when EVs are charged uncoordinatedly, the IESP is forced to import energy at more expensive peak hours. Therefore, in **CS2**, the output power of the Genco1 (cheapest unit) has increased by 0.081%, and by 0.51% in **CS3**. Genco1 shows a slight rise in production during hours 1-6 for **CS2** and **CS3** since the smart charging improves the output of this cheap unit. On the other hand, Genco2 (the most expensive unit) shows a decline of 7.77% in **CS2** and 26.65% in **CS3** during peak hours of 16-19. The impact of this reduction can also be observed in the MCP of WEM in Fig. 12. For example, in **CS3** it is 2.10% less than that of the **CS1**. Furthermore, the thermal energy dispatch of IESP and the average temperature of the AEVHs are demonstrated by Fig. 13. Overall, in **CS3**, the thermal energy dispatch has decreased by 11.73%.

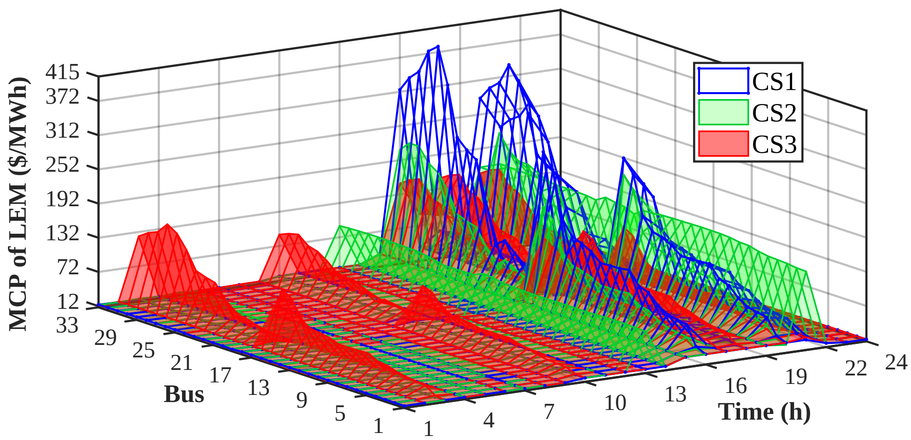

Figure 9: The MCP of the local electricity market (IEEE-33 bus)

However, the dispatch of EB in **CS3** has increased dramatically, as increased thermal flexibility enables the IESP to convert cheaper energy provided by RES to thermal energy. In this regard, the EB energy shows a significant rise during hours 8-10, where the electrical demand is low and RES production is not used. For the same reason, the temperature has risen at hours 8-10 to take maximum advantage of the available RES production. As can be seen from AEVHs' temperature curve in **CS3**, the temperature of the households is increased up to 24 C during off-peak periods to store energy in households, which is released back during peak hours, thereby enhancing thermal flexibility. The MCP of the TEM is illustrated in Fig. 12. Compared to **CS1**, the MCP of the TEM is 5.82% less in **CS3**, which illustrates how AEVHs can function as a thermal energy price-maker. Although the MCP of TEM is 16.01% more in **CS2**, this increment is compensated by a greater reduction in MCP of the LEM (in Fig. 9). The reason for this reduction is that the thermal and electrical outputs of the CHP units connect these two markets.

These findings can also be construed from cost values in different cases, as they are summarized in Table 2. As it was mentioned, in **CS3** and **CS2** higher quantity of electricity is procured at cheaper hours of WEM since EVs and thermal flexibilities shift the demand to cheaper periods. Moreover, the expensive NGUs show a great reduction in **CS3** and **CS2** since cheaper units can substitute their production. The

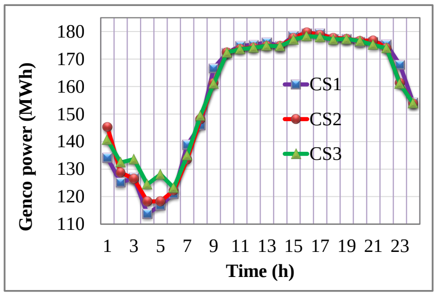

Figure 10: Power generation of Genco1

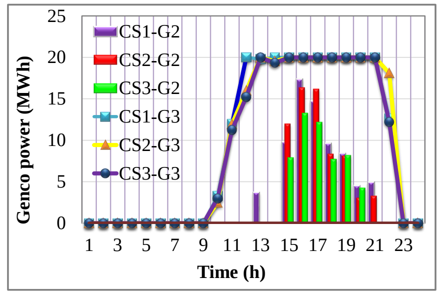

Figure 11: Power generation of Genco2-3

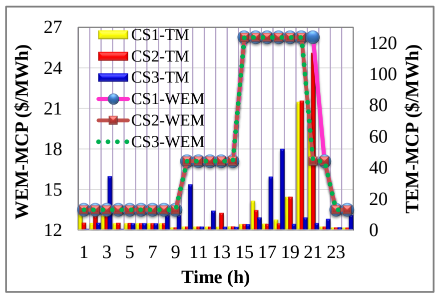

Figure 12: The MCP of WEM and TEM.

most important implication is how the three-level approach can benefit both AEVHs and IESP operators. The reason is that when EVs are charged smartly, there is a significant operational cost reduction for both operators. Despite the higher battery degradation in **CS3**, it is compensated by a greater reduction in overall AEVHs' cost. In order to provide a deeper insight about the cost values of Table 2, the hourly cost value is comparatively illustrated with total generation of each case study in Fig. 14, while Fig. 15 shows the hourly total generation and MCP in each case. As can be observed, **CS1** results in the highest operational cost value since in this case the EVFs are charged without a smart strategy, and it leads to highest total Genco production since peak demand is imported from the WEM. Thanks to the smart charging strategy of **CS2**, the demand is shifted from peak hours (15-19) to valley hour (1-7), while this shift is even more apparent in **CS3** as the thermal flexibilities open the electrical capacity of the CHP units. Overall, **CS2** provides 9.19% lower cost compared to CS1, and **CS3** provides 9.42% lower cost compared **CS1**. Based on the MCP outcomes of Fig. 15, it is noted that smart charging strategy and thermal

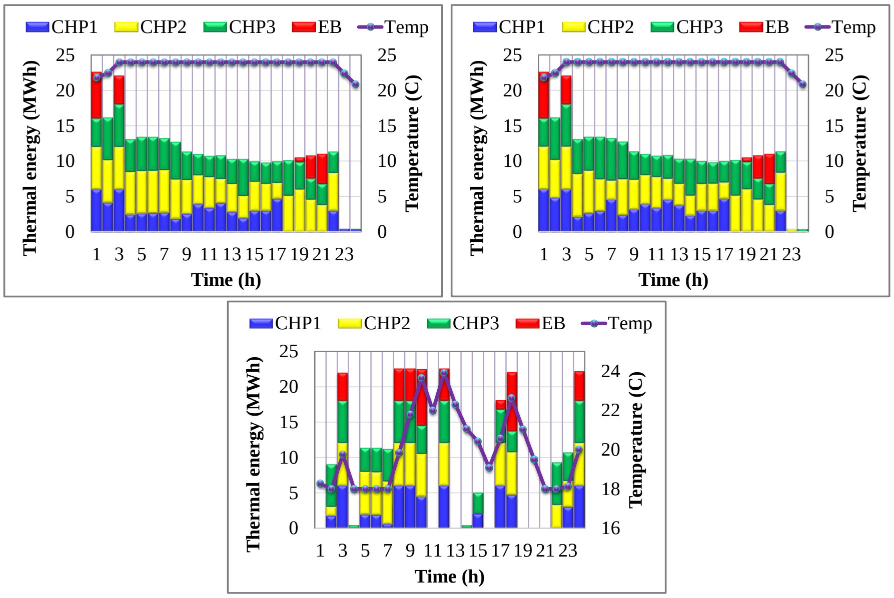

Figure 13: The thermal energy dispatch of the units in ADS and AEVHs' temperature: a) **CS1** b) **CS2** c) **CS3**

load flexibilities in **CS2** and **CS3** can lead to 2.10 % lower WEM price in regard to **CS1**.

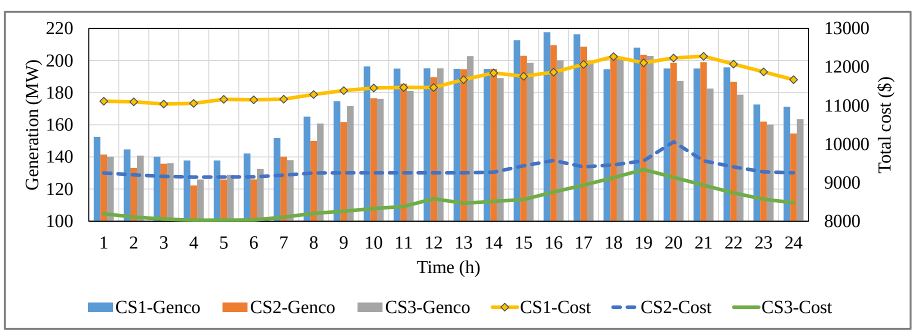

Figure 14: The MCP of the local electricity market (IEEE-33 bus)

The sensitivity analysis on the risk-aversion parameter of IGDT in **CS4** is summarized in Table 3. According to the results, a robust risk-averse strategy comes with a higher cost for IESP since operator self-schedules for the lower end of the

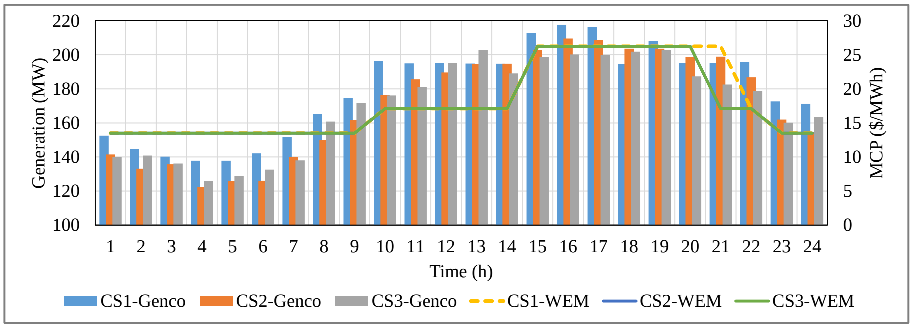

Figure 15: The MCP of the local electricity market (IEEE-33 bus)

predicted renewable energy spectrum. Therefore, the RES account for a lower share of the power, which is compensated by WEM and expensive NGU. In particular, the risk-averse IESP strategy benefits AEVHs operator. The reason is that risk-averse strategy increases the MCP of LEM at peak hours and EVs gain greater benefit by discharging at these periods.

Table 2: Operational costs through different cases

	CS1	**CS2**	**CS3**
NGUs ($)	3883.277	2886.737	2676.345
Gas producers ($)	6454.259	6448.75	6506.975
RES ($)	205.2701	205.2701	205.2701
Interruptible load ($)	31.27779	0	0
Purchased from WEM ($)	9266.553	8475.055	8582.386
Total IESP cost ($)	19840.64	18015.81	17970.98
AEVHs' cost ($)	5015.187	3796.107	1897.31
EV degradation cost ($)	0	642.64	864.24

The voltage level in all ADS buses at hour 21 is illustrated in Fig. 16. As can be seen, the uncoordinated charging scheduling in **CS1** leads to the worst voltage profile, which is also the reason for high power losses. In this regard, smart EV scheduling in **CS2** has 3.63% higher overall voltage. Moreover, including thermal flexibility in **CS3** improves voltage level by 0.39% compared to **CS2** and by 4.04% compared to **CS1**. The improvement in the voltage profile is particularly substan-

Table 3: Sensitivity analysis on risk aversion parameter of IGDT framework in **CS4**.

	$\sigma = 0$	$\sigma = 0.002$	$\sigma = 0.03$	$\sigma = 0.05$
$\sum_t P_t^{IESP}$	209.39	220.36	228.15	235.65
$\sum_t \sum_{k \in NGU} P_{k,t}^{DG}$	28.03	28.38	31.84	35.81
$\sum_t P_t^{RES}$	136.84	125.90	114.97	103.69
$\sum_{q \in \{CHP,EB\}} H_{t,\vartheta,q}^{sor}$	723.24	722.74	720.18	717.97
$\sum_{j \in DS} P_{ij,t}^{Loss}$	11.86	12.23	12.55	12.74
$\sum_t \sum_{k \in CHP} P_{k,t}^{DG}$	193.49	193.49	194.06	194.39
OF^{IP} (\$)	17970.98	18002.75	18486.17	18948.15
OF^{AH}(\$)	1897.31	1761.19	1499.67	1125.97
$\sum_s \sum_f {}^1/_{\pi_s} dg_{f,s,t}$ (\$)	564.24	623.03	689.09	730.68

tial at the end nodes of the ADS. The reason is that these nodes are far from the substation and higher voltage drop is required to transmit the electrical energy to these nodes. However, the smart charging strategy improves the voltage profile by shifting the demand to off-peak time periods.

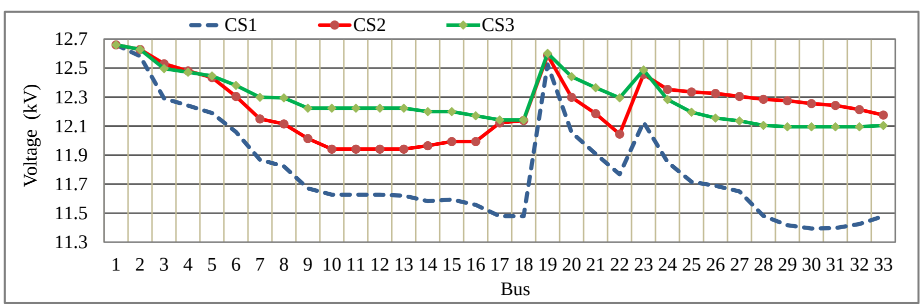

Figure 16: The voltage magnitude in ADS (IEEE-33 bus)

5. Conclusion

This study proposed a novel three-level optimization framework for AEVHs to participate in local electricity and thermal energy markets as a price-maker. In the proposed model, IESP (second level) was modelled as an intermediary entity between AEVHs (fist level) and WEM (third level). The impact of thermal flexibilities of households and smart charging capability of EV fleets on different markets was evaluated through different cases. The EV parameters such as their daily travelled miles and arrival/departure times were established through stochastic scenarios, while output energy of RES in the middle level was handled by the IGDT approach. The study illustrates that EVs can have a great influence on integrated energy networks, and their charging strategy can even influence the thermal energy market through CHP units. Overall conclusions were drawn as follows:

1. The three-level optimization framework shows that EVs can not only be price-influencers at local electricity and thermal energy markets, they can also manipulate price at the wholesale market level, as AEVHs can diminish the MCP of WEM, LEM and TEM by 18.85%, 2.1% and 5.82%, respectively.

2. AEVHs can utilize their thermal flexibilities to influence local electricity and thermal energy markets through CHP units.

3. Smart charging of EV fleets and thermal flexibility of the AEVH reduce the overall costs for both IESP and AEVH while improving overall voltage profile.

4. Using a three-level optimization framework, ensures the profits of AEVHs, IESP and WEM operators by reaching the market equilibrium for all players.

5. When the IGDT framework was integrated in IESP's problem, the risk-aversion increased the costs for IESP. However, the cost of AEVH was reduced. The reason is that the MCP of LEM was higher in this case, and it was more profitable for EVs to discharge at peak hours.

Ultimately, as a prospect for future studies, integrating traffic network models, and routing of electric vehicles offers a significant potential for novel research grounds.

Appendix A. Karush–Kuhn–Tucker (KKT) conditions

There are numerous methods to solve bi-level optimization problems. However, when the lower level is presented as a convex problem, KKT conditions are effective and practical in converting the bi-level problem into a single optimization problem with mathematical equilibrium constraints. In this study, the wholesale electricity market is the third level problem and IESP forms the second level. These two optimization problems of the bi-level framework are merged using the following quadruple KKT conditions [30].

Appendix A.1. Stationary conditions

In order to develop the stationary constraints, the lagrangian function is established by Eq. (a.1), where x represents the vector of decision variables at the third level of the problem. In this context, $f(x)$, $h(x)$ and $g(x)$ define the objective function, equality constraints and inequality constraints, respectively. The stationary constraints in Eqs. (a.1)-(refEq.a4) state that the derivatives of the lagrangian function over each variable must be equal to zero.

$$L^{EN} = f(x) + \lambda^T h(x) + \mu^T g(x) \tag{a.1}$$

$$\begin{aligned} \frac{\partial L^{EN}}{\partial P^{G}_{g,t}} &= C^G_g - \lambda^{WEM}_{b,t} + \overline{\mu^G_{g,t}} - \underline{\mu^G_{g,t}} + \mu^1_{g,t}|_{t>1} - \mu^1_{g,t+1}|_{t>1} \\ &+ \mu^2_{g,t}|_{t=1} - \mu^3_{g,t}|_{t>1} + \mu^3_{g,t+1}|_{t>1} + \mu^4_{g,t}|_{t=1} = 0, \forall g \in A^g_n, \forall b, \forall t \end{aligned} \tag{a.2}$$

$$\frac{\partial L^{EN}}{\partial P^{IESP}_t} = -C^{IESP}_t + \lambda^{WEM}_{b,t} + \overline{\mu^{IESP}_t} - \underline{\mu^{IESP}_t} = 0, \forall b, \forall t \tag{a.3}$$

$$\begin{aligned} \frac{\partial L^{EN}}{\partial \delta_{b,t}} &= \sum_{b' \in \theta_b} B_{b,b'}(\lambda^{WEM}_{b,t} - \lambda^{WEM}_{b',t}) + \sum_{b' \in \theta_b} B_{b,b'}(\overline{\nu_{b,b',t}} - \overline{\nu_{b',b,t}}) \\ &+ \sum_{b' \in \theta_b} B_{b,b'}(\underline{\nu_{b',b,t}} - \underline{\nu_{b,b',t}}) + \overline{\xi_{b,t}} - \underline{\xi_{b,t}} + \xi^1_{b=1,t} = 0, \forall b, \forall t \end{aligned} \tag{a.4}$$

Appendix A.2. Dual, primal, and complementary conditions

The dual, primal and complementary constraints of the WEM are defined by Eqs. (a.5)-(a.15).

$$0 \leqslant P^G_{g,t} \perp \underline{\mu^G_{g,t}} \geqslant 0, \forall g, \forall t \tag{a.5}$$

$$0 \leqslant (\overline{P^G_{g,t}} - P^G_{g,t}) \perp \overline{\mu^G_{g,t}} \geqslant 0, \forall g, \forall t \tag{a.6}$$

$$0 \leqslant (P^{IESP}_t - \underline{P^{IESP}_t}) \perp \underline{\mu^{IESP}_t} \geqslant 0 \tag{a.7}$$

$$0 \leqslant (\bar{P}^{in}_t - P^{IESP}_t) \perp \overline{\mu^{IESP}_t} \geqslant 0, \forall t \tag{a.8}$$

$$0 \leqslant (\overline{C_{b,b'}} + B_{b,b'}(\delta_{b,t} - \delta_{b',t})) \perp \underline{\nu_{b,b',t}} \geqslant 0, \forall b, \forall b', \forall t \tag{a.9}$$

$$0 \leqslant (\overline{C_{b,b'}} - B_{b,b'}(\delta_{b,t} - \delta_{b',t})) \perp \overline{\nu_{b,b',t}} \geqslant 0, \forall b, \forall b', \forall t \tag{a.10}$$

$$0 \leqslant (\pi - \delta_{b,t}) \perp \overline{\xi_{b,t}} \geqslant 0, \forall b, \forall t \tag{a.12}$$

$$0 \leqslant (\pi + \delta_{b,t}) \perp \underline{\xi_{b,t}} \geqslant 0, \forall b, \forall t \tag{a.12}$$

The dual variable concerning the equality terms must be free in sign, which is satisfied by Eq. (a.13)

$$\lambda^{WEM}_{b,t} \forall b, t \xi^{l}_{b=ref,t} \forall b, t \tag{a.13}$$

As can be observed, Eqs. (a.5)-(a.12) are nonlinear, which can be handled by big-M method and binary auxiliary variables [31], as follows:

$$0 \leqslant g_x \perp \mu \geqslant 0 \rightarrow g_x \geqslant 0, \mu \geqslant 0 \tag{a.14}$$

$$g_x \leqslant M_1 u, \mu \leqslant M_2(1-u) \tag{a.15}$$

Appendix B. The theory of strong duality

The theory of strong duality states that in the optimal solution point of the convex optimization problem, the primal and dual optimization functions have equal values [32]. In this study, this basic concept is deployed to develop a linear statement for the nonlinear term $\lambda^{WEM}_{b,t} P^{IESP}_t$ in Eq. (1). In this approach, the dual and primal objectives of the WEM are equated by Eq. (b.1).

$$\begin{aligned}
&Max \sum_t \left[\begin{array}{l}
-\sum_{g,b} \overline{P^{G}_{g,t}\mu^{G}_{g,t}} + \underline{P^{IESP}_t \mu^{IESP}_t} - \overline{P^{IESP}_t \mu^{IESP}_t} \\
+\sum_b P^{D}_{b,t}\lambda^{WEM}_{b,t} - \sum_{b,b' \in Tr} \underline{\nu_{b,b',t}}\,\overline{C_{b,b',t}} \\
-\sum_{b,b' \in Tr} \overline{\nu_{b,b',t}}\,\overline{C_{b,b',t}} - \sum_b \pi(\overline{\xi_{b,t}} + \underline{\xi_{b,t}}) \\
-\sum_g RU_g \mu^{1}_{g,t}|_{t>1} - \sum_g (RU_g + P^{G}_{g,ini})\mu^{2}_{g,t}|_{t=1} \\
-\sum_g RD_g \mu^{3}_{g,t}|_{t>1} - \sum_g (RD_g - P^{G}_{g,ini})\mu^{4}_{g,t}|_{t=1}
\end{array} \right] \\
&= Min \sum_g \sum_t C^{G}_g P^{G}_{g,t} - \sum_t C^{IESP}_t P^{IESP}_t
\end{aligned} \tag{b.1}$$

Based on Eqs. (a.7)-(a.8), following conclusions can be reached.

$$0 \leqslant (P^{IESP}_t - \underline{P^{IESP}_t}) \perp \underline{\mu^{IESP}_t} \geqslant 0 \rightarrow P^{IESP}_t \underline{\mu^{IESP}_t} = \underline{P^{IESP}_t \mu^{IESP}_t} \tag{b.2}$$

$$0 \leqslant (\overline{P^{IESP}_t} - P^{IESP}_t) \perp \overline{\mu^{IESP}_t} \geqslant 0 \rightarrow P^{IESP}_t \overline{\mu^{IESP}_t} = \overline{P^{IESP}_t \mu^{IESP}_t} \tag{b.3}$$

At this stage, Eq. (a.3) is multiplied by P^{IESP}_t to obtain a linear equivalent for $\lambda^{WEM}_{b,t} P^{IESP}_t$ as follows:

$$-P^{IESP}_t C^{IESP}_t + P^{IESP}_t \lambda^{WEM}_{b,t} + P^{IESP}_t \overline{\mu^{WEM}_t} - P^{IESP}_t \underline{\mu^{IESP}_t} = 0 \tag{b.4}$$

$$P^{IESP}_t C^{IESP}_t = P^{IESP}_t \lambda^{WEM}_{b,t} + P^{IESP}_t \overline{\mu^{WEM}_t} - P^{IESP}_t \underline{\mu^{IESP}_t} = 0 \tag{b.5}$$

Now the term $\lambda_{b,t}^{WEM} P_t^{IESP}$ can be replaced by X_1 as folows:

$$\begin{aligned}
&\sum_t C_t^{IESP} P_t^{IESP} = \sum_g \sum_t C_g^G P_{g,t}^G - \\
&\sum_t \left[\begin{array}{l}
-\sum_{g,b} \overline{P_{g,t}^G \mu_{g,t}^G} + \underline{P_t^{IESP} \mu_t^{IESP}} - \overline{P_t^{IESP} \mu_t^{IESP}} \\
+\sum_b P_{b,t}^D \lambda_{b,t}^{WEM} - \sum_{b,b' \in Tr} \underline{\nu_{b,b',t}}\, \overline{C_{b,b',t}} - \\
\sum_{b,b' \in Tr} \overline{\nu_{b,b',t}}\, \overline{C_{b,b',t}} - \sum_b \pi(\overline{\xi_{b,t}} + \underline{\xi_{b,t}}) - \\
\sum_g RU_g \mu_{g,t}^1|_{t>1} - \sum_g (RU_g + P_{g,ini}^G) \mu_{g,t}^2|_{t=1} \\
-\sum_g RD_g \mu_{g,t}^3|_{t>1} - \sum_g (RD_g - P_{g,ini}^G) \mu_{g,t}^4|_{t=1}
\end{array}\right]
\end{aligned} \tag{b.6}$$

$$\begin{aligned}
&X_1 = \sum_t C_t^{IESP} P_t^{IESP} = \sum_g \sum_t C_g^G P_{g,t}^G - \\
&\sum_t \left[\begin{array}{l}
-\sum_{b,b' \in Tr} \underline{\nu_{b,b',t}}\, \overline{C_{b,b',t}} - \sum_{b,b' \in Tr} \overline{\nu_{b,b',t}}\, \overline{C_{b,b',t}} \\
-\sum_b \pi(\overline{\xi_{b,t}} + \underline{\xi_{b,t}}) - \sum_g RU_g \mu_{g,t}^1|_{t>1} - \\
\sum_g (RU_g + P_{g,ini}^G) \mu_{g,t}^2|_{t=1} - \sum_g RD_g \mu_{g,t}^3|_{t>1} \\
-\sum_g (RD_g - P_{g,ini}^G) \mu_{g,t}^4|_{t=1} - \sum_{g,b} \overline{P_{g,t}^G \mu_{g,t}^G} \\
+\sum_b P_{b,t}^D \lambda_{b,t}^{WEM}
\end{array}\right]
\end{aligned} \tag{b.7}$$

Appendix C. Structural data of the utilized systems

In this study, the IESP consists of an IEEE-33 bus ADS, a 20-node NGN, and an 8-node DHS that is supplied by 3 CHPs, 2 NGUs, 3 PVAs and 3 WTs. The data on these networks can be observed in [11, 33, 34]. Furthermore, the WEM is made up of a standard 6-node TN and its structural data is available in[11]. Overall, the summery of the main parameters are included in Table C.4 to Table C.7.

References

[1] X. Li, M. Mulder, Value of power-to-gas as a flexibility option in integrated electricity and hydrogen markets, Applied Energy 304 (2021) 117863.

[2] M. Hofmeister, S. Mosbach, J. Hammacher, M. Blum, G. Röhrig, C. Dörr, V. Flegel, A. Bhave, M. Kraft, Resource-optimised generation dispatch strategy

Table C.4: Data and information on DGs

	$\overline{P}_k^{DG}$	$\underline{P}_k^{DG}$	R_k^{up}	R_k^{DN}	T_k^U	T_k^D	C_k^{DG}
CHP1	—	—	4.5	4.5	2	2	—
CHP2	—	—	4.5	4.5	1	1	—
CHP3	—	—	0.8	0.8	1	1	—
NGU1	7	0.75	1.8	1.8	1	1	87
NGU2	7	0.75	0.5	0.5	1	1	92

Table C.5: Data and information on EVFs

BC_f	$ECPM_f$	η_f	EB_f	Cr_f	a_0
400 ($/KWh)	0.3 (m/KWh)	0.95	30 (KWh)	10 (KW/h)	0.000524

Table C.6: Data and information on district heating network

C_p	R	$Cair_{\vartheta,e}$	$n_{\vartheta,e}^{ho}$
1(MWh/kg.○C)	18 (○C/MWh)	1.1578e-6 (MWhkg.c))	6000

Table C.7: Data and information on active distribution system

$\overline{V}_i^{DS}$	$\underline{V}_i^{DS}$	$\overline{I}_{i,j}^{DS}$	$\overline{P}_l^{IL}$	η_{EB}	$\overline{P}_{t,\vartheta,q}^{EB}$
1.1 (P.U)	0.9 (P.U)	1.2 (A)	3 (MW)	1	10 (MW)

for district heating systems using dynamic hierarchical optimisation, Applied Energy 305 (2022) 117877.

[3] Y. Yao, C. Gao, K. Lai, T. Chen, J. Yang, An incentive-compatible distributed integrated energy market mechanism design with adaptive robust approach, Applied Energy 282 (2021) 116155.

[4] T. Simolin, K. Rauma, R. Viri, J. Mäkinen, A. Rautiainen, P. Järventausta, Charging powers of the electric vehicle fleet: Evolution and implications at commercial charging sites, Applied Energy 303 (2021) 117651.

[5] P. Sheikhahmadi, S. Bahramara, J. Moshtagh, M. Y. Damavandi, A risk-based approach for modeling the strategic behavior of a distribution company in wholesale energy market, Applied energy 214 (2018) 24–38.

[6] A. Thingvad, L. Calearo, P. B. Andersen, M. Marinelli, Empirical capacity measurements of electric vehicles subject to battery degradation from v2g services, IEEE Transactions on Vehicular Technology 70 (8) (2021) 7547–7557.

[7] M. Mohiti, H. Monsef, H. Lesani, A decentralized robust model for coordinated operation of smart distribution network and electric vehicle aggregators, International Journal of Electrical Power and Energy Systems 104 (June 2018) (2019) 853–867. doi:10.1016/j.ijepes.2018.07.054.

[8] A. Asrari, M. Ansari, J. Khazaei, P. Fajri, A market framework for decentralized congestion management in smart distribution grids considering collaboration among electric vehicle aggregators, IEEE Transactions on Smart Grid 11 (2) (2020) 1147–1158. doi:10.1109/TSG.2019.2932695.

[9] Z. Liu, Q. Wu, S. S. Oren, S. Huang, R. Li, L. Cheng, Distribution locational marginal pricing for optimal electric vehicle charging through chance constrained mixed-integer programming, IEEE Transactions on Smart Grid 9 (2) (2018) 644–654. doi:10.1109/TSG.2016.2559579.

[10] B. S. K. Patnam, N. M. Pindoriya, Dlmp calculation and congestion minimization with ev aggregator loading in a distribution network using bilevel program, IEEE Systems Journal (2020) 1–12doi:10.1109/jsyst.2020.2997189.

[11] S. Bahramara, M. Yazdani-Damavandi, J. Contreras, M. Shafie-Khah, J. P. Catalão, Modeling the strategic behavior of a distribution company in wholesale energy and reserve markets, IEEE Transactions on Smart Grid 9 (4) (2018) 3857–3870. doi:10.1109/TSG.2017.2768486.

[12] P. Sheikhahmadi, S. Bahramara, A. Mazza, G. Chicco, J. P. Catalão, Bi-level optimization model for the coordination between transmission and distribution systems interacting with local energy markets, International

Journal of Electrical Power and Energy Systems 124 (2021) 106392. doi:10.1016/j.ijepes.2020.106392.

[13] S. Bahramara, P. Sheikhahmadi, A. Mazza, G. Chicco, M. Shafie-Khah, J. P. Catalão, A risk-based decision framework for the distribution company in mutual interaction with the wholesale day-ahead market and microgrids, IEEE Transactions on Industrial Informatics 16 (2) (2020) 764–778. doi:10.1109/TII.2019.2921790.

[14] T. Zhao, X. Pan, S. Yao, C. Ju, L. Li, Strategic bidding of hybrid ac/dc microgrid embedded energy hubs: A two-stage chance constrained stochastic programming approach, IEEE Transactions on Sustainable Energy 11 (1) (2020) 116–125. doi:10.1109/TSTE.2018.2884997.

[15] Y. Li, B. Wang, Z. Yang, J. Li, C. Chen, Hierarchical stochastic scheduling of multi-community integrated energy systems in uncertain environments via stackelberg game, Applied Energy 308 (2022) 118392.

[16] L. Liu, G.-H. Yang, Distributed optimal energy management for integrated energy systems, IEEE Transactions on Industrial Informatics (2022).

[17] F. Zhou, Y. Li, W. Wang, C. Pan, Integrated energy management of a smart community with electric vehicle charging using scenario based stochastic model predictive control, Energy and Buildings 260 (2022) 111916.

[18] W. Yang, J. Guo, A. Vartosh, Optimal economic-emission planning of multi-energy systems integrated electric vehicles with modified group search optimization, Applied Energy 311 (2022) 118634.

[19] S. Guo, G. Song, M. Li, X. Zhao, Y. He, A. Kurban, W. Ji, J. Wang, Multi-objective bi-level quantity regulation scheduling method for electric-thermal integrated energy system considering thermal and hydraulic transient characteristics, Energy Conversion and Management 253 (2022) 115147.

[20] A. Najafi, H. Falaghi, J. Contreras, M. Ramezani, A stochastic bilevel model for the energy hub manager problem, IEEE Transactions on Smart Grid 8 (5) (2017) 2394–2404. doi:10.1109/TSG.2016.2618845.

[21] S. Zeynali, N. Nasiri, M. Marzband, S. N. Ravadanegh, A hybrid robust-stochastic framework for strategic scheduling of integrated wind farm and plug-in hybrid electric vehicle fleets, Applied Energy 300 (2021) 117432.

[22] B. Xu, J. Zhao, T. Zheng, E. Litvinov, D. S. Kirschen, Factoring the cycle aging cost of batteries participating in electricity markets, IEEE Transactions on Power Systems 33 (2) (2018) 2248–2259. doi:10.1109/TPWRS.2017.2733339.

[23] M. F. Anjos, A. J. Conejo, et al., Unit commitment in electric energy systems, Foundations and Trends® in Electric Energy Systems 1 (4) (2017) 220–310.

[24] W. Gu, J. Wang, S. Lu, Z. Luo, C. Wu, Optimal operation for integrated energy system considering thermal inertia of district heating network and buildings, Applied Energy 199 (2017) 234–246. doi:10.1016/j.apenergy.2017.05.004.

[25] E. Mahboubi-Moghaddam, M. Nayeripour, J. Aghaei, A. Khodaei, E. Waffenschmidt, Interactive robust model for energy service providers integrating demand response programs in wholesale markets, IEEE Transactions on Smart Grid (2018). doi:10.1109/TSG.2016.2615639.

[26] M. Rezaeimozafar, M. Eskandari, V. A. Savkin, A self-optimizing scheduling model for large-scale ev fleets in microgrids, IEEE Transactions on Industrial Informatics (2021). doi:10.1109/TII.2021.3064368.

[27] M. Tasdighi, H. Ghasemi, A. Rahimi-Kian, Residential microgrid scheduling based on smart meters data and temperature dependent thermal load modeling, IEEE Transactions on Smart Grid 5 (1) (2014) 349–357. doi:10.1109/TSG.2013.2261829.

[28] A. Ahmadian, M. Sedghi, M. Aliakbar-Golkar, Stochastic modeling of plug-in electric vehicles load demand in residential grids considering nonlinear bat-

tery charge characteristic, Institute of Electrical and Electronics Engineers Inc., 2015, pp. 22–26. doi:10.1109/EPDC.2015.7330467.

[29] National household travel survey.
URL https://nhts.ornl.gov/

[30] N. Nasiri, S. Zeynali, S. N. Ravadanegh, M. Marzband, A hybrid robust-stochastic approach for strategic scheduling of a multi-energy system as a price-maker player in day-ahead wholesale market, Energy 235 (2021) 121398.

[31] N. Nasiri, S. Zeynali, S. N. Ravadanegh, N. Rostami, A robust decision framework for strategic behaviour of integrated energy service provider with embedded natural gas and power systems in day-ahead wholesale market, IET Generation, Transmission & Distribution (2022).

[32] A. J. Conejo, E. Castillo, R. Minguez, R. Garcia-Bertrand, Decomposition techniques in mathematical programming: engineering and science applications, Springer Science & Business Media, 2006.

[33] Y. Li, Z. Li, F. Wen, M. Shahidehpour, Privacy-preserving optimal dispatch for an integrated power distribution and natural gas system in networked energy hubs, IEEE Transactions on Sustainable Energy 10 (4) (2018) 2028–2038.

[34] Y. Jiang, C. Wan, A. Botterud, Y. Song, S. Xia, Exploiting flexibility of district heating networks in combined heat and power dispatch, IEEE Transactions on Sustainable Energy 11 (4) (2019) 2174–2188.

Acknowledgements

Funding: This research did not receive any specific grant from funding agencies in the public, commercial, or not-for-profit sectors.

A Three-level Framework for Strategic Participation of Aggregated Electric Vehicle-owning Households in Local Electricity and Thermal Energy Markets

Saeed Zeynali[a], Nima Nasiri[a], Sajad Najafi Ravadanegh[a], Mousa Marzband[b,c]

[a]*Resilient Smart Grids Research Lab, Electrical Engineering Department, Azarbaijan Shahid Madani University, Tabriz, Iran*
[b]*Northumbria University, Electrical Power and Control Systems Research Group, Ellison Place NE1 8ST, Newcastle upon Tyne, United Kingdom*
[c]*Center of Research Excellence in Renewable Energy and Power Systems, King Abdulaziz University, Jeddah 21589 Saudi Arabia*

Abstract

The impact of electric vehicles (EV) charging strategy will not be limited to power systems as integrated electricity, natural gas and thermal energy systems have become increasingly interconnected. We introduce a three-level framework for the aggregated electric vehicle-owning households (AEVH) to strategically participate in local electricity and thermal energy markets as a price-maker, while considering the strategic behavior of the integrated energy service provider (IESP) in thw wholesale electricity market (WEM) also as a price-maker. The AEVH operator forms the first level, while IESP and WEM operators are integrated at the second and third levels, respectively. To solve the three-level problem, the second and third levels are modified as a single-level problem through the Karush-Kuhn-Tucker (KKT) conditions, then the equilibrium point of the resulting single-level problem and the first level is achieved through two-step iterative method. At the first level, the arrival/departure time and daily travelled miles of EV fleets are modelled via stochastic scenarios, while renewable energy production at the second level is dealt with by information gap decision theory (IGDT). Ultimately, different case studies verify that AEVHs can deploy their thermal flexibility together with the smart charging strategy of the EVs

Email address: `s.najafi@azaruniv.ac.ir Corresponding author` (Sajad Najafi Ravadanegh)

to influence the local electricity, thermal energy and even WEM prices. Using the proposed three-level optimization framework reaches the best point of equilibrium between different market players. The outcomes prove the effectiveness of the proposed model. Based on the results, the AEVH can deploy the proposed model to diminish the WEM price by 2.1%, while the local electricity price was dropped by 18.85%. Furthermore, the thermal energy price was reduced by 5.82%, which illustrates that EVs can influence the thermal energy market through the combined heat and power units.

Keywords: Electric vehicles; Thermal energy market; Strategic scheduling; Three-level optimization; Wholesale electricity market; Local electricity market

---

Nomenclature

Indices

s, t, k, r	Indices of scenario, time, DGs, wind turbine
l, ϑ, e	Indices of pipeline, node, demand in DHS
q, f	Indices of DHS source and EV fleets
pv, c, R	Indices of PVA, ILs and FOR in CHP units
n, w, lg, c	Indices of NGN nods, NGN producer, active pipeline, non-active pipeline
d, dg	Indices of ADS and, NGN loads
g, b, b', i	Indices of Genco, TN bus's, ADS buses
A_n^m, CHP	Set of m equipment's located at ADS and TN bus's or NGN nodes n and CHP
Tr	Set of interconnected buses in the TN.
A_i^f	Set of EV parking lots at node i of ADS
NGU	Set of non-gas fired units
TA_f,TD_f	Set of arrival/departure times

Parameters

$SOC_{f,s}^{end}$	Highest possible SOC at departure time
SOC_f^{des}	Desired SOC at departure time

$\overline{SOC}_f$, $\underline{SOC}_f$	max/min SOC of EV fleets (%)
$ms_{t,l}$,$mr_{t,l}$	Water mass flow of supply/return DHS pipeline (kg/h)
$m^{de}_{t,\vartheta,e}$,$m^{sr}_{t,\vartheta,q}$	Water mass flow of demand/source at DHS nodes (kg/h)
$n^{ho}_{\vartheta,e}$	Number of households at DHS nodes
$Cair_{\vartheta,e}$	Average thermal capacity of AEVHs (MWh/°C)
π_s	Probability of scenario s
EB_f,η_f	EV fleets' battery capacity/efficiency (MWh)
$SOC^{In}_{f,s}$	SOC at arrival time (%)
$DT_{f,s}$	Travelled miles by EV fleets (mile)
EM_f	Energy consumption per mile (MWh/mile)
Cr_f	EV feets' nominal charge rate (MW)
C_p	Thermal capacity of water (MWh/kg.°C)
R	Thermal resistance of households (°C/MWh)
T^{out}_t	Outdoor temperature (°C)
$\underline{T}^{in}_{\vartheta,e}$,$\overline{T}^{in}_{\vartheta,e}$	Min/Max indoor temperature (°C)
$\underline{P}^{DG}_k$,$\overline{P}^{GD}_k$	Min/Max DG output (MWh)
P^R,ϕ^R	Thermal/electrical FOR of CHPs (MW)
η_{EB},$\overline{P}^{EB}_{t,\vartheta,q}$	Efficiency & max power of EB
γ_p,γ_H	Electrical/Thermal fuel ratio of CHP (%)
T^{Ue}_k,T^{De}_k	Min on, off time of DGs (h).
C^{SU}_k,C^{SD}_k	Start-up/shutdown cost of NGU ($/MWh)
R^{UP}_k	DGs' ramp rate (MWh)
$\overline{P}^{WT}_{r,t}$,$\overline{P}^{PV}_{pv,t}$	Maximum wind/solar production (MW)
Z^{DS}_{ij},R^{DS}_{ij}	Impedance/resistance of ADS feeders (ohm).
$\overline{I}^{DS}_{ij}$	Maximum current of ADS feeders (A).
$\underline{V}^{DS}_i$,$\overline{V}^{DS}_i$	Min/Max ADS node voltage (Kv)
$\underline{\nu_w}$,$\overline{\nu_w}$	Min/Max gas well production (kcf)
$\underline{Pr_n}$,$\overline{Pr_n}$	Min/Max NGN nodal pressure (bar)
$\overline{T}^{DHS}_l$,$\underline{T}^{DHS}_l$	Max/Min DHS pipe temp (°C)

$\overline{T_{\vartheta}^{DHS}}$,$\underline{T_{\vartheta}^{DHS}}$	Max/Min DHS node temperature (°C)
λ_l,L_l	Thermal conductivity & length of DHS pipeline (m)
$P_{f,s,t}^{L}$	Electrical AEVH demand (MW)
$K_{n,m}^{f}$	NGN pipeline coefficient
C^{PV},C^{WT}	Cost of PV/WT production ($/MWh)
C_{w}^{gas},C_{u}^{IL}	Gas well cost ($/kcf)/interruptible loads ($/MWh)
$\bar{P}_{t}^{RES}$	Expected RES production in IGDT (MW)
σ	Risk aversion controller in IGDT.
OF_{b}^{IP}	Optimal value of IESP objective ($)
C_{g}^{G},$B_{b,b'}$	Genco cost ($/MWh)/ TN suseptance (1/ohm)
$P_{g,t}^{GMax}$	Maximum Genco production (MW)

Variables

OF^{AH}	AEVHs' objective function
$dg_{f,s,t}$	Battery erosion of EV fleets ($)
$\lambda_{t,i}^{LM}$,$\lambda_{t,\vartheta}^{TM}$	MCP of LEM & TEM ($/MWh)
$P_{t,i}^{EH}$	AEVHs' Electrical energy purchase (MW)
$H_{t,\vartheta,e}^{ho}$	Thermal energy delivered to AEVHs (MWh)
$SOC_{f,s,t}$	State of charge of EV fleets (%)
$\sigma_{f,s,t}$	EV fleets' cycle depth (%)
$\psi_{f,s,t}$	Cycle depth degradation function
$MD_{f,s,t}$	Marginal battery degradation ($/MWh)
$P_{f,s,t}^{+}$,$P_{f,s,t}^{-}$	EV fleets' charge/discharge rate (MW)
$T_{t,\vartheta,e}^{in}$	Indoor temperature of AEVHs (°C)
$P_{k,t}^{DG}$,$H_{k,t}^{DG}$	DGs' electrical/thermal output (MW)
α_{t}^{R}	FOR coefficient of CHP (%)
$SU_{k,t}$,$SD_{k,t}$	Start-up/Shutdown cost of NGU ($)
$SU_{k,t}^{CHP}$, $SD_{k,t}^{CHP}$	Start-up/Shutdown fuel for CHP (kcf)
$G_{k,t}^{CHP}$	CHPs' natural gas consumption (kcf)
$I_{ij,t}^{DS}$,$V_{i,t}^{DS}$	Current/voltage of ADS (A), (kV)
$P_{ij,t}^{Loss}$	Power loss in ADS (MW)

$\nu_{w,t}$ $Pr_{n,t}$	Gas well production (kcf)/ node pressure (bar)
$f^{in}_{n,m,t}$, $f^{out}_{m,n,t}$	Inlet/Outlet flow of NGN pipe (KCF)
$f_{n,m,t}$	Average pipe flow of NGN (KCF)
$T^{ps,out}_{t.l}$, $T^{pr,out}_{t,l}$	End temp of supply/ return DHS pipe (°C)
$T^{ps,in}_{t.l}$,$T^{pr,in}_{t,l}$	Beginning temp of supply/return DHS pipe (°C)
$T^{ms}_{t,\vartheta}$,$T^{mr}_{t,\vartheta}$	Nodal temp of supply/return pipes in DHS (°C)
$H^{loss}_{t,l}$	Thermal energy loss in DHS (MWh)
$H^{sor}_{t,\vartheta,q}$	Thermal energy production in DHS (MWh)
$\lambda^{WEM}_{b,t}$	MCP of WEM ($/MWh)
P^{IESP}_{t}	Power purchased from WEM by IESP (MW)
$P^{IL}_{u,t}$	Interruptible loads (MW)
$P^{EB}_{t,\vartheta,q}$	EB power consumption
P^{RES}_{t},α	RES production (MW)/IGDT radios
$P^{G}_{g,t}$,$P^{D}_{b,t}$	Genco generation & TN demand (MWh)
$\delta_{b,t}$	TN bus voltage angle (°)
μ, ν, ζ	Inequality dual variables in the TN
λ	Equality dual variables in the TN
	Binary variables
$u^{+}_{f,s,t}$,$u^{-}_{f,s,t}$	EV fleets' charge/discharge state
$I_{k,t}$	Commitment state of DGs
$y_{k,t}$,$z_{k,t}$	Start-up / Shutdown state of DGs
	Abbreviations
AEVH	Aggregated electric vehicle-owning households
IESP	Integrated energy service provider
WEM	Wholesale electricity market
LEM,TEM	Local electricity market, Thermal energy market
ADS,DHS	Active distribution system,District heating system
NGN,MCP	Natural gas network, Market clearing price
RES,NGU	Renewable energy source, Non-gas-fired unit

Genco	Generation company
PHA	Photovoltaic array
IL,EB	Interruptible load, Electrical boiler

1. Introduction

The unprecedented boom in the electric vehicle (EV) sales testifies their economic viability and sustainability. For instance, the UK has pledged to enact legislation to prohibit the sales of fossil fuel-based vehicles by 2030 and only permit EVs by 2035. The co-occurrence of this trend with the proliferation of the high-efficiency combined heat and power units (CHP) is going to introduce new challenges since they entangle the thermal and electrical energy production [1], as well as influencing the natural gas demand [2]. Therefore, the CHPs create an interdependent energy market consisting of the active distribution system (ADS), natural gas network (NGN) and district heating systems (DHS), which is operated under the command of the integrated energy service provider (IESP) [3]. Considering the high penetration of EVs, their charging patterns will have a substantial impact on these markets. The reason is that smart charging strategies of the electric vehicles can increase the thermal and electrical flexibility of the CHP units, which will improve the thermal demand satisfaction in DHS, and reduce the pipeline congestion in NGN. The EVs can participate in energy markets individually as price-takers. However, it is known that a price-maker framework can induce greater profit by influencing market price [4]. Therefore, it is highly probable that EV-owning households would form a coalition to utilize their charging/discharging flexibilities together with their thermal demand flexibility to participate in local electricity and thermal energy markets as the price-makers. In other words, the aggregated EV-owning households (AEVHs) can influence the market-clearing price (MCP) in the thermal energy market (TEM) and local electricity market (LEM) to enhance their collective benefit. The IESP, as the local market operator, procures part of this energy from local distributed generation (DG) units and gas wells. At the same time, it also participates in the wholesale electricity market (WEM) as a price-maker that can submit offers/bids to purchase/sell electrical energy [5]. Accordingly, IESP is a price-maker in WEM, while AEVH operator is a price-maker in LEM and TEM (operated by the IESP), which makes the IESP an intermediary retailer between the WEM and AEVHs.

All these market formations have their individual objectives. For instance, the wholesale electricity market operator (WEMO) clears the WEM to maximize the public welfare, while the IESP's prime objective is to minimize the operational costs of ADS, DHS and NGN as well as the cost of participating in WEM. On the other hand, the AEVHs' objective is to minimize the cost of participating in LEM and TEM, using their flexibilities in thermal demand and EV-scheduling. To solve such a problem, a three-level framework should be devised that considers the AEVHs at the first level, the IESP at the second level and WEMO at the third level. Such a tool would be essential for market players to evaluate AEVHs as a thermal and electrical price-maker that can also pose a significant impact on WEM price through IESP.

Most of the small-scale consumers do not have enough power to participate in energy markets as a price-influencer. In this concern, some of the recent studies have unraveled the importance of demand response aggregators. Particularly, the EV-aggregators [6] have gained a great deal of attention on account of their flexibilities and green features. The altering direction method of multipliers (ADMM) has been proposed in [7] to investigate robust interaction between the EV-aggregator and the distribution company (Disco). Asrari *et al.* [8] evaluated the possibility of using the aggregated EVs to reduce distributed locational marginal price (DLMP), which showed that it is possible with proper congestion management. The authors in [9] inspected EVs as price-takers in LEM intending to diminish DLMP. In a more sophisticated study [10], the DLMP of the LEM was reduced through a bi-level optimization framework that considered EV-aggregators and Disco at upper and lower levels, respectively. These studies illustrate the impact that EVs can impose on Discos at the local level, while Disco's behavior at the wholesale market is also essential. In this regard, [11] proposed a bi-level framework to investigates Disco's strategic behavior at day-head and reserve markets, while information gap decision theory (IGDT) is adopted by [12] to investigate a similar problem. A risk-based Disco optimization has been investigated in [13], wherein the presence of microgirds was addressed at the lower level of the bi-level problem.

As can be observed, all of these studies have focused on a single type of energy, i.e., electricity. Nevertheless, co-generation technologies, such as CHP units, have created an interconnected energy market. Therefore, there has been increasing interest in this area. The authors in [14] proposed a stochastic bi-level approach to investigate strategic participation of a multi-energy system in WEM and real-time integrated markets. The authors in [15] proposed a hierarchical energy scheduling approach for the integrated energy systems, using Stackelberg game approach. The study modelled the energy service provider as a leader, while the households were defined as followers to minimize their cost. A decentralized optimization framework was proposed by [16] to minimize the cost and emissions of an integrated energy system via the multi-objective optimization framework. In [17], a model predictive energy management strategy was proposed for EV-charging stations and thermal energy supply of community buildings. The study used a moving-horizon stochastic programming approach to deal with the RES production uncertainties. The economic-environmental operation of a multi-energy system was addressed in [18], wherein the study aimed to maximize the benefits of the multi-energy operator and minimize the operational emissions at the same time. A non-dominated sorting genetic algorithm was investigated in [19] for the optimal emission-constrained operation of multi-energy systems. The main contribution of this study was to include thermo-hydraulic characteristic of the integrated electrical and thermal energy systems. The bi-level scheduling of multi-energy systems is scrutinized in [20], considering pool market, forward contracts and rival players.

Despite all the authentic novelties, the following shortcomings (**SH**) can be identified in these studies:

SH 1: In some studies [10–14, 17, 18, 20], the impacts of integrating EVs have been evaluated at local energy systems. However, EVs can also have a significant influence at WEM level.

SH 2: The current literature have not investigated the EVs as thermal price-makers that can be feasible through CHP units.

<u>SH</u> 3: The studies [11–13] have focused on a single type of energy (electricity)

<u>SH</u> 4: The IESP has not been studied as a price-maker in WEM.

To address the existing gaps, this study puts forward a three-level framework to model AEVHs as price-makers in LEM and TEM that is operated by IESP, which in turn is also a price-maker in WEM. At the first level, the AEVHs' objective is to minimize the cost of participating in TEM and LEM, using their thermal flexibility and smartly schedulable EVs. The IESP (second level) intends to minimize the operational cost and the cost of participating in WEM by submitting the best offer/bid. Eventually, at the third level, the WEMO clears the market to maximize public welfare. A hybridized KKT conditions and two-step iterative method is used to solve the three-level problem. Moreover, EVs' arrival/departure times are modelled through stochastic scenarios, while the IGDT framework is used to address the uncertainties of renewable energy sources (RES) at the second level. Table 1 provides the main traits of the previous publications and this study. Overall, the major contributions of this study can be summarized as follows:

i A three-level hybrid SP-IGDT framework is proposed to model AEVHs as price-makers in LEM and TEM, while considering IESP as a price-maker at WEM. (Addresses **<u>SH1</u>** and **<u>SH2</u>**)

ii The influence of strategic EV scheduling at local electricity, thermal markets as well as WEM is scrutinized. (Addresses **<u>SH2</u>** and **<u>SH3</u>**)

iii A novel method of integrating KKT conditions with the two-step iterative approach is proposed to solve the three-level optimization problem. (Addresses **<u>SH3</u>** and **<u>SH4</u>**)

2. problem description

In this study, the AEVHs partake in LEM and TEM as price-setter players, while considering that IESP is also a price-setter in WEM. For this purpose, a three-level optimization framework is established, where the AEVHs form the first level of the problem, while IESP and WEM are second and third level problems, respectively.

Table 1: Comparative evaluations between this study and previous publications

Ref	Uncertainty	Markets			Multi-level	Flexible technologies	
		WEM	LEM	TEM	solving method	EV	Thermal demand
[6]	SP	✓	×	×	WoLF	✓	×
[7]	RO	✓	✓	×	Two-step	✓	×
[8]	-	×	✓	×	-	✓	×
[9]	SP	×	✓	×	-	✓	×
[10]	RO	×	✓	×	KKT	✓	×
[11]	SP	✓	✓	×	KKT	×	×
[12]	IGDT	✓	✓	×	KKT	×	×
[13]	SP	✓	✓	×	KKT	×	×
[14]	SP	✓	×	✓	KKT	×	✓
[15]	SP	×	✓	✓	Stackelberg	×	×
[16]	-	×	✓	✓	-	×	✓
[17]	SP	×	×	✓	-	✓	✓
[18]	-	×	×	×	-	✓	✓
[19]	-	×	✓	✓	-	×	✓
[20]	SP	✓	×	✓	KKT	×	✓
This study	**SP-IGDT**	✔	✔	✔	**Hybrid KKT & Two-step**	✔	✔

In other words, IESP is a follower to AEVHs, and WEM is a follower to IESP. The AEVHs operator sends its energy requirements to IESP operator. Subsequently, the IESP self-schedules the DGs, NGN, ADS and DHS. Afterwards, partakes in WEM and clears TEM and LEM to announce MCP of retail electrical and thermal energy. Simultaneously, the WEM operator receives the offers/bids from IESP, and clears the WEM to announce the MCP of the WEM. The IESP is an intermediary retailer that links AEVHS to WEM. The EV-related uncertain data, such as vehicles arrival/departure time and daily travelled miles are handled by stochastic scenarios, while uncertain climatic data such as solar and wind power is dealt with via risk-averse IGDT framework. The solving procedure, which is established in the next sections, ensures the best equilibrium for these various levels. The overall interactive relationship between these three levels, their corresponding objectives and decision variables, can be observed in Fig. 1.

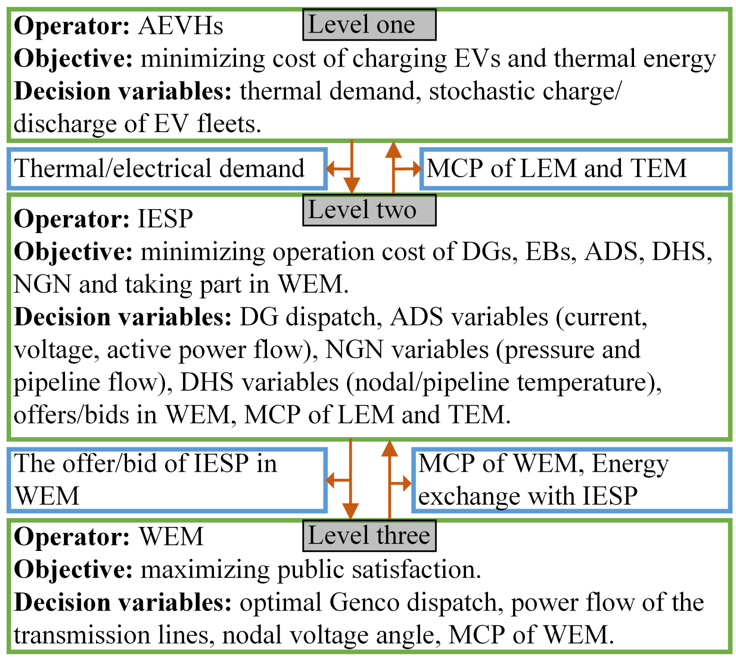

Figure 1: The interactive relationship of various levels of the problem

3. Formulation & Algorithm

3.1. Aggregated electric-vehicle-owning households (First level)

In this study, the EVs are clustered into fleets with distinct behavioral patterns via K-means clustering as presented in [21], and they are assumed to be present at the residential parking lots (equipped with level II chargers) from arrival to departure intervals. The objective function of the AEVHs (first level) is defined by Eq. (1), wherein the first term is the battery degradation cost of the EV fleets, while the second and the last terms represent the cost of participating in the local electricity and thermal energy markets. The decision variables of this level include thermal energy demand and stochastic charge/discharge of EV fleets. The SOC for each fleet is computed via Eqs. (2)-(3), while initial and final (at departure) SOC are declared in Eqs. (4)-(5). Eqs. (6)-(8) are conventional storage equations, and cycle depth is calculated by Eq. (9). Furthermore, the battery degradation cost is imposed in Eqs. (10)-(12), which is linearized and proved in [22]. Eventually, the flexible thermal demand of the households is established in Eq. (13), while Eq. (14) defines the expected electrical demand of the AEVHs.

$$\min OF^{AH} = \sum_{t} \begin{pmatrix} \sum_{s} \sum_{f} \pi_s . dg_{f,s,t} + \\ \sum_{i \in A_i^{EH}} \lambda_{t,i}^{LM} P_{t,i}^{EH} + \\ \sum_{\vartheta} \lambda_{t,\vartheta}^{TM} H_{t,\vartheta,e}^{ho} \end{pmatrix} \tag{1}$$

$$\begin{aligned} SOC_{f,s,t} &= SOC_{f,s,t-1} + \left(\eta_f . P_{f,s,t}^{+} / EB_f\right) \\ &- \left(P_{f,s,t}^{-} / EB_f . \eta_f\right) \forall f, s, t \neq TA_f \end{aligned} \tag{2}$$

$$\begin{aligned} SOC_{f,s,t} &= SOC_{f,s}^{In} + \left(\eta_f . P_{f,s,t}^{+} / EB_f\right) \\ &- \left(P_{f,s,t}^{-} / EB_f . \eta_f\right) \forall f, s, t = TA_f \end{aligned} \tag{3}$$

$$\begin{aligned} SOC_{f,s}^{In} = \max \begin{pmatrix} \underline{SOC_f}, 1- \\ (DT_{f,s} \times EM_f / EB_f) \end{pmatrix} \\ \forall f, s \end{aligned} \tag{4}$$

$$SOC_{f,s,t} = \min \left(SOC_{f,s}^{end}, SOC_{f}^{des}\right) \forall f, s, t = TD_f \tag{5}$$

$$\underline{SOC_f} \leqslant SOC_{f,s,t} \leqslant \overline{SOC_f} \forall f, s, t \tag{6}$$

$$P_{f,s,t}^{+} \leqslant Cr_f . uc_{f,s,t}, P_{f,s,t}^{-} \leqslant Cr_f . u_{f,s,t}^{-} \forall f, s, t \tag{7}$$

$$u_{f,s,t}^{+} + u_{f,s,t}^{-} = 1 \forall f, s, t \tag{8}$$

$$\sigma_{f,s,t} = \sigma_{f,s,t-1} - (P_{f,s,t}^{-} / EB_f . \eta_f) \forall f, s, t \tag{9}$$

$$\psi_{f,s,t} \left(\sigma_{f,s,t}\right) = a_0 . (\sigma_{f,s,t})^{2.03} \forall f, s, t \tag{10}$$

$$MD_{f,s,t} = 2.03 a_0 (BC_f / EB_f . \eta_f) {\sigma_{f,s,t}}^{1.03} \forall f, s, t \tag{11}$$

$$dg_{f,s,t} = P_{f,s,t}^{-} . MD_{f,s,t} \forall f, s, t \tag{12}$$

$$\begin{aligned} & T_{t,\vartheta,e}^{in} = T_{t-1,\vartheta,e}^{in} e^{-1/((R/n_{\vartheta,e}^{ho}).Cair_{\vartheta,e})} \\ & +(H_{t,\vartheta,e}^{ho} . R / n_{\vartheta,e}^{ho} + T_t^{out}).(1 - e^{-1/((R/n_{\vartheta,e}^{ho}).Cair_{\vartheta,e})}) \\ & , \underline{T_{\vartheta,e}^{in}} \leqslant T_{t,\vartheta,e}^{in} \leqslant \overline{T_{\vartheta,e}^{in}} \forall t, \forall \vartheta, \forall e \end{aligned} \tag{13}$$

$$P_{t,i}^{EH} = \sum_{s} \pi_s (P_{f,s,t}^{+} - PD_{f,s,t}^{-} + P_{f,s,t}^{L}) \forall s, t, f \in A_i^f \tag{14}$$

3.2. Integrated energy service provider (second level)

3.2.1. Units' commitment

The commitment status of units is imposed by Eq. (15), while Eqs. (16)-(18) restrict CHPs' thermal/electrical generation within feasible operation region. The NGUs' start-up/shutdown cost is declared in Eq. (19), while Eq. (20) defines the CHPs' gas consumption at start-up/shutdown, and Eq. (21) is the CHPs' overall gas consumption. The ramp rate restrictions are enforced in Eqs. (22)-(23), and minimum on/off time limits are defined in Eqs. (24)-(30). Eventually, solar/wind generation bounds are imposed by Eq. (31) [23].

$$\underline{P_k^{DG}} I_{k,t} \leqslant P_{k,t}^{DG} \leqslant \overline{P_k^{GD}} I_{k,t} \forall t, k \in \{NGU\} \tag{15}$$

$$P_{k,t}^{DG} = \sum_{R=1} \alpha_t^R P^R, H_{k,t}^{DG} = \sum_{R=1} \alpha_t^R \phi^R \forall t, k \in CHP \tag{16}$$

$$\sum_{R=1} \alpha_t^R = I_{k,t}, 0 \leqslant \alpha_t^R \leqslant 1 \forall t, k \in CHP \tag{17}$$

$$Q_{k,t}^{CHP} = \gamma_p P_{k,t}^{DG} + \gamma_H H_{k,t}^{DG} \forall t, k \in CHP \tag{18}$$

$$SU_{k,t} \geqslant C_k^{SU} y_{k,t}, SD_{k,t} \geqslant C_k^{SD} z_{k,t} \forall t, k \in NGU \tag{19}$$

$$\begin{aligned} &SU_{k,t}^{CHP} \geqslant C_k^{CHP} y_{k,t}, SD_{k,t}^{CHP} \geqslant C_k^{CHP} z_{k,t} \\ &\forall t, k \in CHP \end{aligned} \tag{20}$$

$$G_{k,t}^{CHP} = Q_{k,t}^{CHP} + SU_{k,t}^{CHP} + SD_{k,t}^{CHP} \forall k \in \{CHP\}, \forall t \tag{21}$$

$$P_{k,t}^{DG} - P_{k,t-1}^{DG} \leqslant (1 - y_{k,t}) R_k^{UP} + y_{i,t} \underline{P_k^{DG}} \forall t, k \tag{22}$$

$$P_{k,t-1}^{DG} - P_{k,t}^{DG} \leqslant (1 - z_{k,t}) R_k^{UP} + z_{i,t} \underline{P_k^{DG}} \forall t, k \tag{23}$$

$$T_k^{Ue} = \min\left\{T, T_k^{U0}\right\}, T_k^{De} = \min\left\{T, T_k^{D0}\right\} \forall k \tag{24}$$

$$\sum_{t=1}^{T_k^{Ue}} I_{k,t} = T_k^{Ue}, \sum_{t=1}^{T_k^{De}} I_{k,t} = 0 \forall k \tag{25}$$

$$\sum_{t=r}^{t+T_k^{Ue}-1} I_{k,r} \geqslant T_k^U y_{k,t} \forall k, \forall t = \begin{bmatrix} T_k^{Ue} + 1, \cdots, \\ T - T_k^U + 1 \end{bmatrix} \tag{26}$$

$$\sum_{t=r}^{T} (I_{k,r} - y_{k,t}) \geqslant 0 \forall k, \forall t = \left[T - T_k^U + 2, \cdots, T\right] \tag{27}$$

$$\sum_{t=r}^{t+T_k^D-1} (1 - I_{k,r}) \geqslant T_k^D z_{k,t} \forall k, \forall t = \begin{bmatrix} T_k^{De} + 1, \cdots, \\ T - T_k^D + 1 \end{bmatrix} \tag{28}$$

$$\sum_{t=r}^{T}(1-I_{k,r}-z_{k,t}) \geqslant 0 \forall k, \forall t = \begin{bmatrix} T-T_k^D \\ +2,\cdots,T \end{bmatrix} \quad (29)$$

$$y_{k,t}-z_{k,t}=I_{k,t-1}-I_{k,t}, y_{k,t}+z_{k,t} \leqslant 1 \forall t, k \quad (30)$$

$$0 \leqslant P_{r,t}^{Wind} \leqslant \overline{P_{r,t}^{WT}}, 0 \leqslant P_{pv,t}^{PV} \leqslant \overline{P_{pv,t}^{PV}} \forall t, w, v \quad (31)$$

3.2.2. Active distribution system

Here, the power flow equations are solved by the linearized framework presented in [13]. The feeders' power flow is defined in Eq. (32), and Eq. (33) is the power loss equation. The current value is computed by Eq. (34), and current/voltage bounds are enforced in Eq. (35). Finally, the nodal power equilibrium is established in Eq. (36) for the slack bus and in Eq. (37) for other buses. The MCP of the LEM is obtained from the dual value of Eq. (37), and it is specified by $\lambda_{t,i}^{LM}$.

$$P_{ij,t}^{flow} = \left(R_{ij}^{DS}/(Z_{ij}^{DS})^2\right).(V_{i,t}^{DS\_sqr} - V_{j,t}^{DS\_sqr}) \forall ij, \forall t \quad (32)$$

$$P_{ij,t}^{Loss} = R_{ij}^{DS} I_{ij}^{DS\_sqr} \forall ij, \forall t \quad (33)$$

$$I_{ij,t}^{DS} = (V_{i,t}^{DS} - V_{j,t}^{DS})/Z_{ij}^{DS} \forall ij, \forall t \quad (34)$$

$$-\overline{I_{ij}^{DS}} \leqslant I_{ij,t}^{DS} \leqslant \overline{I_{ij}^{DS}}, \underline{V_i^{DS}} \leqslant V_{i,t}^{DS} \leqslant \overline{V_i^{DS}} \forall ij, \forall t \quad (35)$$

$$\begin{aligned} &P_t^{IESP} + \sum_{r\in A_i^r} P_{r,t}^{Wind} + \sum_{v\in A_i^v} P_{v,t}^{PV} + \sum_{k\in A_i^k} P_{k,t}^{DG} \\ &+ \sum_{l\in A_i^l} P_{l,t}^{IL} = \sum_{l\in A_i^l} P_{l,t}^{DSRL} + \sum_{d\in A_i^d} P_{d,t}^{DSNRL} \\ &+0.5(\sum_{j\in DS} P_{ij,t}^{Loss} + \sum_{j\in DS} P_{ij,t}^{flow}) \forall i = 1, \forall t \end{aligned} \quad (36)$$

$$\begin{aligned} &\sum_{r\in A_i^r} P_{r,t}^{Wind} + \sum_{v\in A_i^v} P_{v,t}^{PV} + \sum_{k\in A_i^k} P_{k,t}^{DG} \forall i \neq 1, \forall t \\ &+ \sum_{l\in A_i^l} P_{l,t}^{IL} = \sum_{l\in A_i^l} P_{l,t}^{DSRL} + P_{t,i}^{EH} + \sum_{\vartheta\in B_i^\vartheta} P_{t,\vartheta,q}^{EB} : \lambda_{t,i}^{LM} \\ &+ \sum_{d\in A_i^d} P_{d,t}^{DSNRL} + 0.5(\sum_{j\in DS} P_{ij,t}^{Loss} + \sum_{j\in DS} P_{ij,t}^{flow}) \end{aligned} \quad (37)$$

3.2.3. Natural gas network

The natural gas wells' production and nodal pressure of the NGN are restricted in Eq. (38). Eqs. (39)-(40) describe the Weymouth natural gas flow equation in non-active and active (with compressor) pipelines. The method presented in [24] is deployed to address the nonlinearities of Weymouth equations. Eventually, the natural gas equilibrium is defined by Eq. (42).

$$\underline{v_w} \leqslant v_{w,t} \leqslant \overline{v_w}, \underline{Pr_n} \leqslant Pr_{n,t} \leqslant \overline{Pr_n} \forall n, w, t \tag{38}$$

$$f_{n,m,t}^2 = K_{n,m}^f (Pr_{n,t}^2 - Pr_{m,t}^2) \forall (n,m) \notin z, \forall t \tag{39}$$

$$f_{n,m,t}^2 \geqslant K_{n,m}^f (Pr_{n,t}^2 - Pr_{m,t}^2) \forall t \forall (n,m) \in z, \forall t \tag{40}$$

$$f_{n,m,t} = (f_{n,m,t}^{in} - f_{m,n,t}^{out})/2 \tag{41}$$

$$\sum_{sp \in A_n^{sp}} v_{sp,t} - \sum_{k \in A_n^k} G_{k,t}^{CHP} = \sum_{m \in z} (f_{n,m,t}^{in} - f_{m,n,t}^{out}) \quad \forall n, \forall t \tag{42}$$

3.2.4. District heating system

In this study, the hot water DHS model is deployed as presented in [25]. The thermal equilibrium of the nodes is established through the pipelines entering that node in Eqs. (43)-(44) for the supply/return pipe networks. The temperature at the beginning of the pipelines is defined by Eq. (45) as equal to the nodal temperature of the node that pipeline exists. The thermal demands are satisfied via Eq. (46), and Eq. (47) expresses the temperature at the end of pipelines. The thermal energy loss along the pipes is established in Eq. (48), while Eqs. (49)-(50) declare the EB constraints. Eq. (51) denotes the thermal energy dispatched from CHPs and electrical boilers (EB). Overall thermal energy equilibrium is satisfied by Eq. (52). Eventually, the temperature bounds of DHS are declared in Eq. (53). The MCP of TEM is obtained from the dual value of Eq. (46), and it is specified by $\lambda_{t,\vartheta}^{TM}$.

$$\sum_{l \in s_\vartheta^-} (T_{t,l}^{ps,out} . ms_{t,l}) = T_{t,\vartheta}^{ms} \sum_{l \in s_\vartheta^-} ms_l \forall t, \vartheta \tag{43}$$

$$\sum_{l \in s_\vartheta^+} (T_{t,l}^{pr,out} . mr_{t,l}) = T_{t,\vartheta}^{mr} \sum_{l \in s_\vartheta^+} mr_l \forall t, \vartheta \tag{44}$$

$$\begin{cases} T_{t,\vartheta}^{ps,in} = T_{t,l}^{ms}, & l \in S_\vartheta^+ \\ T_{t,\vartheta}^{pr,in} = T_{t,l}^{mr}, & l \in S_\vartheta^- \end{cases} \quad \forall t, l \tag{45}$$

$$H_{t,\vartheta,e}^{ho} = C_p m_{t,\vartheta,e}^{de} (T_{t,\vartheta,e}^{ms} - T_{t,\vartheta,e}^{mr}) \forall t, \vartheta, e{:}\lambda_{t,\vartheta}^{TM} \tag{46}$$

$$\begin{aligned} T_{t.l}^{ps,out} &= (T_{t,l}^{ps,in} - T_t^{out}) e^{-(\lambda_l L_l / C_p ms_l)} + T_t^{out} \\ T_{t,l}^{pr,out} &= (T_{t,l}^{pr,in} - T_t^{out}) e^{-(\lambda_l L_l / C_p ms_l)} + T_t^{out} \end{aligned} \quad \forall t, l \tag{47}$$

$$H_{t,l}^{loss} = C_p m_{t,l}^{de} (T_{t,l}^{in} - T_{t,l}^{out}) \forall t, l \tag{48}$$

$$H_{t,\vartheta,q}^{sor} = \eta_{EB} P_{t,\vartheta,q}^{EB} q \in \{EB\} \tag{49}$$

$$0 \leqslant P_{t,\vartheta,q}^{EB} \leqslant \overline{P_{t,\vartheta,q}^{EB}} \tag{50}$$

$$H^{sor}_{t,\vartheta,q} = C_p m^{sr}_{t,\vartheta,q}(T^{in}_{t,\vartheta,q} - T^{out}_{t,\vartheta,q}) \forall t, \vartheta, q_{\in\{CHP,EB\}} \tag{51}$$

$$\sum_{\vartheta} \sum_{q\in\{CHP,EB\}} H^{sor}_{t,\vartheta,q} - \sum_{l\in S^{+}_{\vartheta},S^{-}_{\vartheta}} H^{loss}_{t,l} - \sum_{\vartheta} \sum_{d} H^{ho}_{t,\vartheta,e} = 0 \tag{52}$$

$$\underline{T^{DHS}_{l}} \leqslant T^{ps,out}_{t.l}, T^{ps,in}_{t,l} \leqslant \overline{T^{DHS}_{l}}, \quad \underline{T^{DHS}_{\vartheta}} \leqslant T^{ms}_{t.\vartheta}, T^{mr}_{t,\vartheta} \leqslant \overline{T^{DHS}_{\vartheta}} \forall t, \forall l \tag{53}$$

3.2.5. IESP's Objective

The IESP's objective (second level) is established in Eq. (54), which consists of six terms, namely the cost of participating in WEM, wind turbine (WT) production, photovoltaic arrays (PHA) production, natural gas production, interruptible load (IL) shedding and non-gas-fired unit (NGU) operation. The decision variables of the IESP consist of DG dispatch power, ADS variables (current, voltage, active power flow), NGN variables (pressure and pipeline flow), DHS variables (nodal/pipeline temperature), offers/bids in WEM, MCP of LEM and MCP of TEM. Since IGDT framework is deployed to deal with uncertainties of renewable energy sources (RES), the main objective of the second level is redefined accordingly in Eq. (55), as the radius of uncertainty, while the accompanying constraints are expressed in Eqs. (56)-(59) [12].

$$OF^{IP} = \sum_{t} \left\{ \begin{array}{l} \lambda^{WEM}_{b,t} P^{IESP}_{t} + \sum_{r} C^{WT} P^{WT}_{r,t} \\ + \sum_{pv} C^{PV} P^{PV}_{pv,t} + \sum_{w} C^{gas}_{w} \nu_{w,t} \\ + \sum_{u} C^{IL}_{u} P^{IL}_{u,t} + \\ \sum_{k\in NGU} \left(\begin{array}{l} C^{DG}_{k} P^{DG}_{k,t} + \\ SU_{k,t} + SD_{k,t} \end{array} \right) \end{array} \right\} \tag{54}$$

$$\max\{\alpha\}, \alpha \geqslant 0 \tag{55}$$

$$u(\bar{P}^{RES}_{t}, \alpha) = \left\{ P^{RES}_{t} : \left| \frac{P^{RES}_{t} - \bar{P}^{RES}_{t}}{\bar{P}^{RES}_{t}} \right| \leqslant \alpha \right\} \tag{56}$$

$$OF^{IP}_{b} = \left\{ OF^{IP} : \min OF^{IP} \right\} \tag{57}$$

$$OF \leqslant OF_{b}(1+\sigma), 0 \leqslant \sigma \leqslant 1 \tag{58}$$

$$0 \leqslant P^{RES}_{t} \leqslant (1-\alpha)\bar{P}^{RES}_{t}, P^{RES}_{t} = P^{WT}_{r,t} + P^{PV}_{pv,t} \tag{59}$$

3.3. Wholesale electricity market (Third level)

The WEMO's objective (third level) is defined in Eq. (60). The terms of the equation include the production cost of Gencos and the profit/cost of selling/purchasing to/from IESP. The decision variable of the WEM are optimal Genco dispatch, power flow of the transmission lines, nodal voltage angle and MCP of WEM. Eq. (61) satisfies the energy equilibrium constraint of TN, while the capacity and ramp rate constraints are defined in Eqs. (62)-(66). The transaction with IESP is limited by Eq. (67). Ultimately, the power flow rate of the feeders and voltage angle limits of TN are restricted via Eqs. (68)-(69). The MCP of WEM is obtained from the dual value of the Eq. (61), it specified by $\lambda_{b,t}^{WEM}$.

$$\min\left\{\sum_t\sum_g C_g^G P_{g,t}^G - \sum_t\sum_g C_t^{IESP} P_t^{IESP}\right\} \tag{60}$$

$$\begin{aligned}&\sum_{g\in A_n^g} P_{g,t}^G - P_t^{IESP} - P_{b,t}^D = \sum_{b'\in Tr} B_{b,b'}(\delta_{b,t}-\delta_{b',t})\\ &:\lambda_{b,t}^{WEM}\forall b,t\end{aligned} \tag{61}$$

$$0\leqslant P_{g,t}^G\leqslant P_{g,t}^{GMax}:\underline{\mu_{g,t}^G},\overline{\mu_{g,t}^G}\forall g,\forall t \tag{62}$$

$$P_{g,t}^G - P_{g,t-1}^G\leqslant RU_g:\mu_{g,t}^1\forall g,t>1 \tag{63}$$

$$P_{g,t}^G - P_{g,ini}^G\leqslant RU_g:\mu_{g,t}^2\forall g,t=1 \tag{64}$$

$$P_{g,t-1}^G - P_{g,t}^G\leqslant RD_g:\mu_{g,t}^3\forall g,t>1 \tag{65}$$

$$P_{g,ini}^G - P_{g,t}^G\leqslant RD_g:\mu_{g,t}^4\forall g,t=1 \tag{66}$$

$$\underline{P_t^{IESP}}\leqslant P_t^{IESP}\leqslant\overline{P_t^{IESP}}:\underline{\mu_t^{IESP}},\overline{\mu_t^{IESP}}\forall t \tag{67}$$

$$\begin{aligned}&-\overline{C_{b,b'}}\leqslant B_{b,b'}(\delta_{b,t}-\delta_{b',t})\leqslant\overline{C_{b,b'}}\\ &:\underline{\nu_{b,b',t}},\overline{\nu_{b,b',t}}\forall b,b',t\end{aligned} \tag{68}$$

$$-\pi\leqslant\delta_{b,t}\leqslant\pi:\underline{\xi_{b,t}},\overline{\xi_{b,t}}\forall b,t \tag{69}$$

3.4. Proposed algorithm

In the proposed model, the IESP consists of an ADS, an NGN and a DHS. Furthermore, it is obliged to satisfy the energy demands of the customers in different markets. To this end, IESP incorporates WTs, gas wells, PVAs, NGUs, ILs, EBs and CHP units. That said, it also participates in WEM to procure/sell electrical energy. To solve this bi-level problem, IESP submits offers/bids in WEM; then the WEMO clears the market to announce the MCP. Afterwards, the IESP reschedules itself and resubmits offers/bids accordingly. This process is continued until reaching the equilibrium state for both IESP and WEM. In this study, KKT conditions are deployed to modify the WEM problem as constraints in IESPs' problem [13]. In other words, the second and third levels are merged into a single problem through KKT conditions, and the nonlinear production terms were addressed through the theory of strong duality. More information on the KKT conditions of the problem and the theory of strong duality is included in Appendix A and Appendix B. Henceforth, the equilibrium state of AEVHs and this merged problem is achieved. In this regard, the two-step method is used as it is elaborated in [25]. Accordingly, the IESP clears these markets (according to ADS and DHS limitations) and declares the thermal/electrical MCP. This process is the so-called first step. At the second step, the AEVHs' operator schedules the thermal demand of the households as well as smart charging of the EVs and submits thermal/electrical demand in LEM and TEM. These two steps are repeated until the criterion in Eq. (70) is satisfied. The overall algorithm is established as follows:

$$\left(\mathrm{OF}^{\mathrm{AH}^*}(\mathrm{Step1}) - \mathrm{OF}^{\mathrm{AH}^*}(\mathrm{Step2})\right) / \mathrm{OF}^{\mathrm{AH}^*}(\mathrm{Step1}) \leqslant \varepsilon \tag{70}$$

Algorithm: Hybrid KKT & two-step method.

Initialization: Get the input parameters of the first, second and third level problems.

1. Solve the second and third level problems based on KKT condition and theory of strong duality using Eqs. (15)-(69).

2. Receive $\lambda_{t,i}^{LM*}, \lambda_{t,\vartheta}^{TM*}$

3. Step1: Solve the first level problem using Eqs. (1)-(14) and calculate the optimal value of total cost.

4. Update values of $P_{t,i}^{EH*}, H_{t,\vartheta,e}^{ho\,*}$.

5. Step2: Solve the second and third level problems based on KKT condition and theory of strong duality using Eqs. (15)-(69).

6. Update values of $\lambda_{t,i}^{LM*}, \lambda_{t,\vartheta}^{TM*}$

7. Calculate the optimal value of OF^{AH} using Eq. (1).

8. If the stop criterion Eq. (70) is satisfied, terminate the algorithm, otherwise return to stage **3**

4. Case studies and results

In this study, AEVHs are modelled through 6000 aggregated households with 3000 EVs that are clustered into 5 fleets by K-means clustering [26]. The data on the thermal characteristics of the households is taken from [27], and EVs data is provided in [28] and national household travel survey (NHTS) [29]. The overall schematic of the systems, connections and locations is depicted in Fig. 2. Moreover, the structural data of the systems are summarized in Appendix C. The empirical probability distribution functions of NHTS data for EVs arrival/departure times are plotted in Fig. 3. The arrival/departure time data distribution of the clustered EV fleets is illustrated in Fig. 4 and the probability distribution of their daily travelled miles is depicted in Fig. 5. These empirical distributions are utilized to generate stochastic scenarios for EV fleets. Moreover, the mixed-integer linear problem

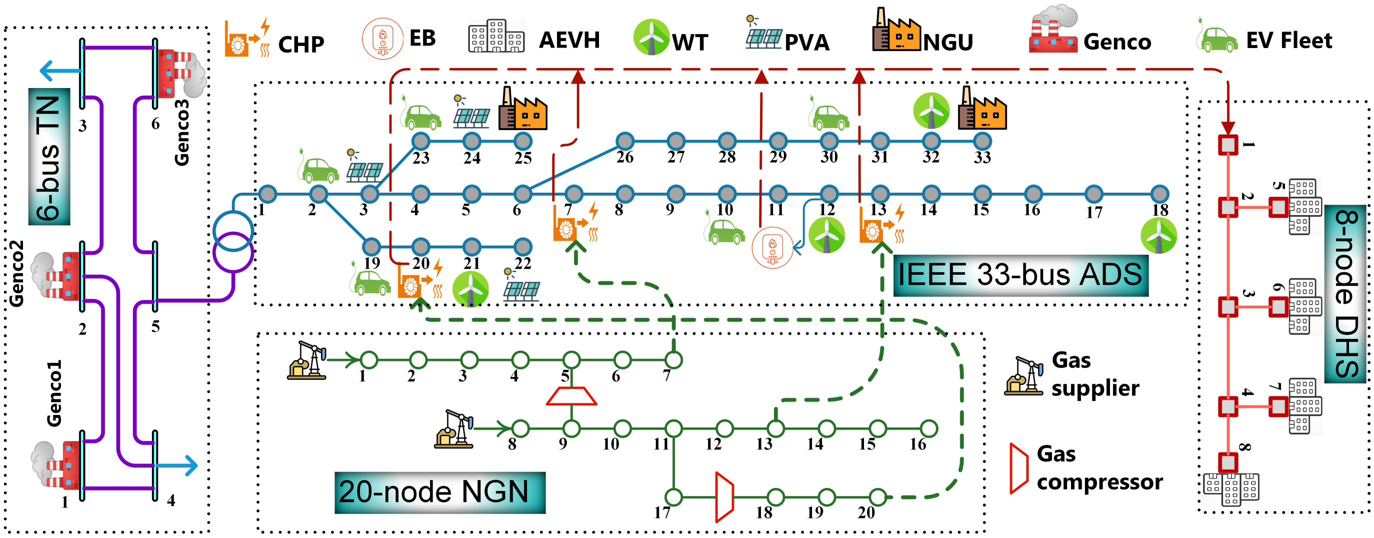

Figure 2: Overall schematic of the systems connections and locations

(MILP) was solved via the GUROBI solver. Eventually, the following case studies are designed to assess the proposed three-level framework.

- Case Study 1 (**CS1**): In this case, the thermal flexibility of the households is ignored (temperature fixed at 25°C), and EVs are charged uncoordinatedly as soon as they arrive.
- Case Study 2 (**CS2**): In this case, the thermal flexibility of the households is ignored (temperature fixed at 25°C), and EVs are charged smartly.
- Case Study 3 (**CS3**): In this case, the households are assumed to be thermally flexible (temperature interval of 18°C-25°C), and EVs are charged smartly.
- Case Study 4 (**CS4**): In this case, the IGDT approach is applied to RES in **CS3**.

It should be noted that in the smart charging method, the charge/discharge of the electric vehicles is a decision variable defined in the optimization process. Therefore, the electric vehicles charge/discharge schedule is obtained from solving the proposed formulation. However, when the charging scheduling is not smart (uncoordinated), the vehicles are charged without any control strategy.

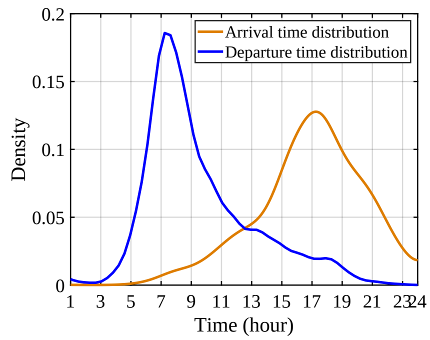

Figure 3: Arrival/departure time probability distribution of NHTS data

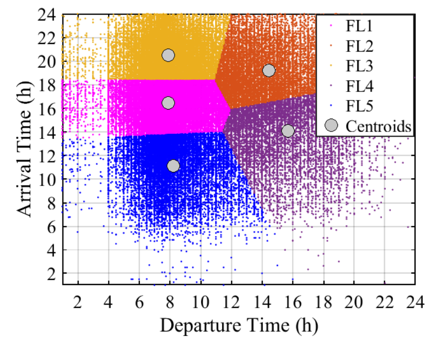

Figure 4: EV fleets' arrival/departure time distribution

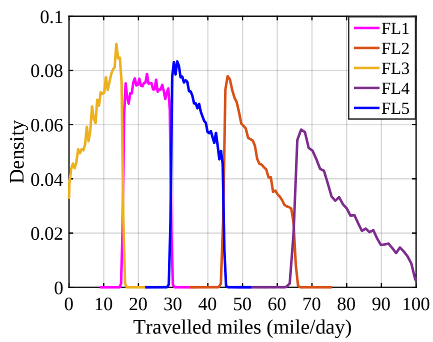

Figure 5: Probability distribution of EV fleets' daily travelled miles

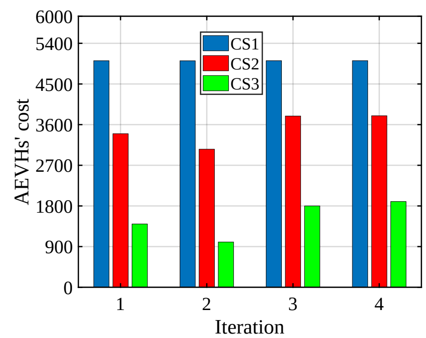

Figure 6: Convergence of the AEVHs' cost in two-step method.

The iterative convergence of the two-step method for different cases can be seen in Fig. 6. As can be seen, the AEVHs' cost is converged after three iterations in all cases. The expected SOC of EV fleets in different cases is demonstrated in Fig. 7. In **CS1**, the EV fleets are charged as soon as they arrive at the residential site. Therefore, EVs' SOC curve shows sharp slopes at hours 16-19. The reason is that according to Fig. 4, EV fleets' arrival time distribution is heavily concentrated around these times. However, hours 16-19 also coincide with the peak demand of IESP and WEM. In this regard, **CS2** enables the AEVHs' operator to shift demand to cheaper off-peak periods, which can be observed from the SOC of fleets in **CS2**, as EVs are mainly charged at hours 6-9, which is the departure time for most EVs. In **CS3**, this shift in demand is even more perceptible, as the thermal flexibility of

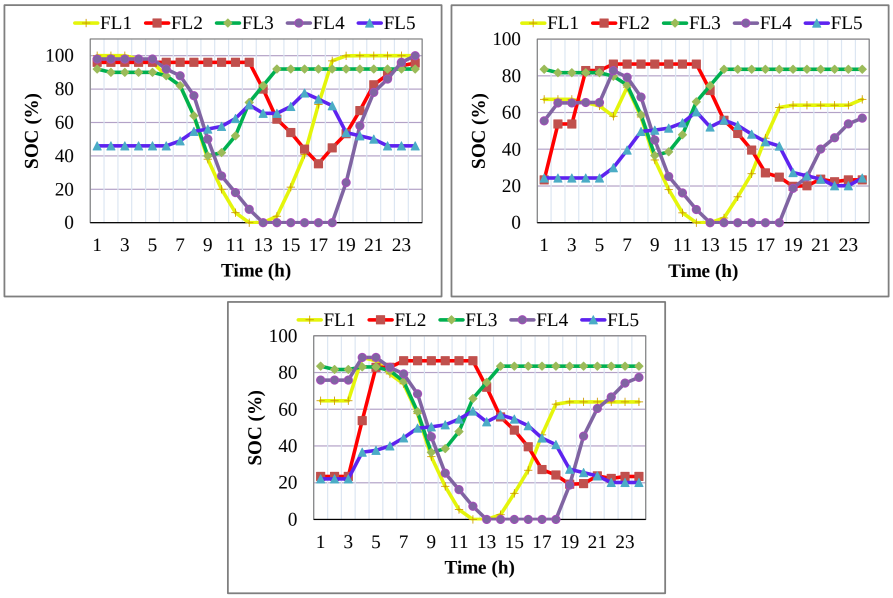

Figure 7: The SOC of EV fleets: a) **CS1** b) **CS2** c) **CS3**

AERHs improves the electrical capacity of the cheaper CHP units. The reason is that the electrical and thermal outputs of CHP units are inextricably interdependent.

The hourly dispatch scheduling of the IESP in three cases is illustrated by Fig. 8. Accordingly, in **CS1**, where there is no flexibility, the power imported from WEM is 0.45% less regarding **CS2** and 2.79% less regarding **CS3**. The reason is that in **CS2** and **CS3** more energy is imported during cheaper off-peak hours from WEM. As can be observed, **CS2** and **CS3** illustrate a sharp rise in the imported power from WEM during hours 1-5, which is the most inexpensive time interval for WEM price. Furthermore, the production of the expensive NGUs is declined by 25.40% and 32.25% in **CS2** and **CS3** compared to **CS1**. That said, the production of efficient CHP units is increased by 8.62% in **CS3** compared to **CS1**. Nevertheless, 0.06 MWh of the load is shed (with the cost of 500 $/MWh) in **CS1** to satisfy security bounds. Fig. 8 shows that there is a large demand profile for EVs at hours 15-18 in **CS1**, which is due to the uncontrolled charging strategy of the EVs in this case. Nonetheless, in **CS2**, this demand is spread over time periods 3-5 since the charging schedule is intelligent, and EVs are even discharged at time 21 to increase the profit.

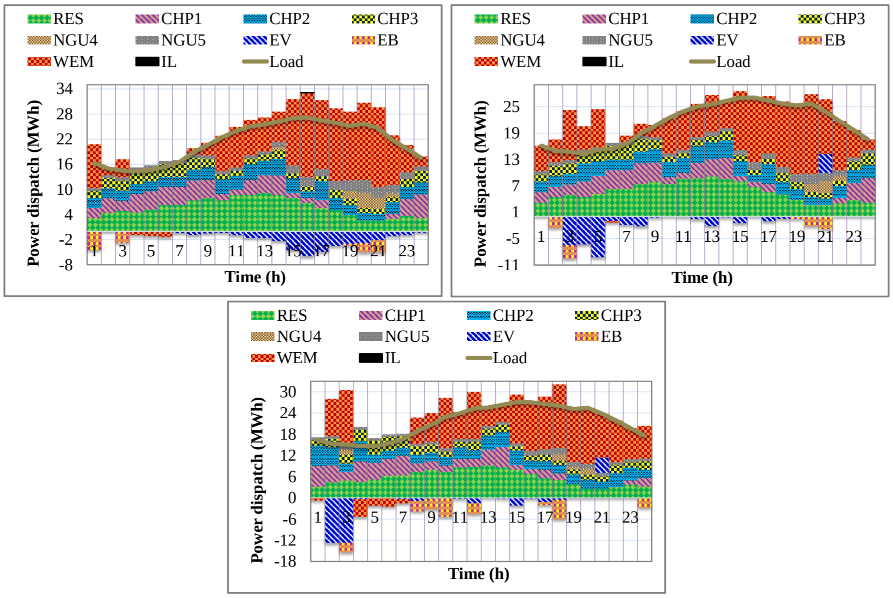

Figure 8: The power dispatch of units in ADS: a) **CS1** b) **CS2** c) **CS3**

These results also reflect on the MCP of the local electricity market. As it is illustrated in Fig. 9, **CS1** imposes the highest MCP cost. Overall, the MCP of the local electricity market in **CS2** is dropped by 2.42%, and in **CS3** by 11.87% in comparison to **CS1**. As can be seen, **CS2** and **CS3** have a slightly higher MCP at off-peak hours since they have shifted demand to these intervals.

Fig. 10 and Fig. 11 demonstrate the power dispatching of Genco1-3. In **CS1**, when EVs are charged uncoordinatedly, the IESP is forced to import energy at more expensive peak hours. Therefore, in **CS2**, the output power of the Genco1 (cheapest unit) has increased by 0.081%, and by 0.51% in **CS3**. Genco1 shows a slight rise in production during hours 1-6 for **CS2** and **CS3** since the smart charging improves the output of this cheap unit. On the other hand, Genco2 (the most expensive unit) shows a decline of 7.77% in **CS2** and 26.65% in **CS3** during peak hours of 16-19. The impact of this reduction can also be observed in the MCP of WEM in Fig. 12. For example, in **CS3** it is 2.10% less than that of the **CS1**. Furthermore, the thermal energy dispatch of IESP and the average temperature of the AEVHs are demonstrated by Fig. 13. Overall, in **CS3**, the thermal energy dispatch has decreased by 11.73%.

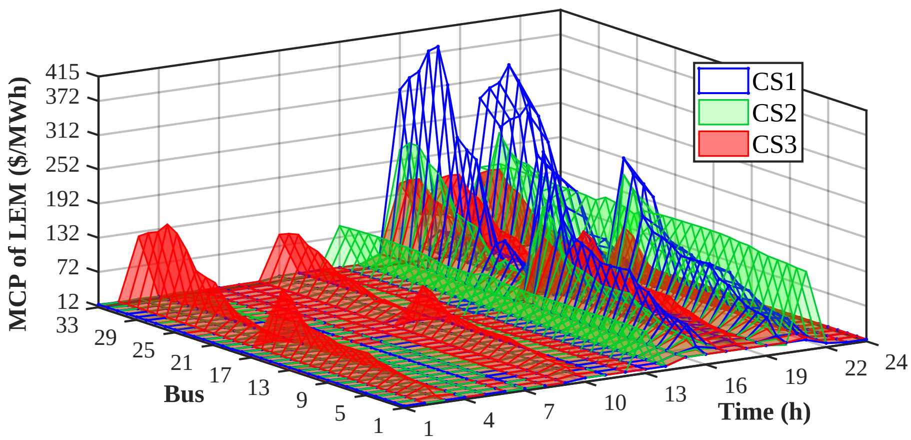

Figure 9: The MCP of the local electricity market (IEEE-33 bus)

However, the dispatch of EB in **CS3** has increased dramatically, as increased thermal flexibility enables the IESP to convert cheaper energy provided by RES to thermal energy. In this regard, the EB energy shows a significant rise during hours 8-10, where the electrical demand is low and RES production is not used. For the same reason, the temperature has risen at hours 8-10 to take maximum advantage of the available RES production. As can be seen from AEVHs' temperature curve in **CS3**, the temperature of the households is increased up to 24 C during off-peak periods to store energy in households, which is released back during peak hours, thereby enhancing thermal flexibility. The MCP of the TEM is illustrated in Fig. 12. Compared to **CS1**, the MCP of the TEM is 5.82% less in **CS3**, which illustrates how AEVHs can function as a thermal energy price-maker. Although the MCP of TEM is 16.01% more in **CS2**, this increment is compensated by a greater reduction in MCP of the LEM (in Fig. 9). The reason for this reduction is that the thermal and electrical outputs of the CHP units connect these two markets.

These findings can also be construed from cost values in different cases, as they are summarized in Table 2. As it was mentioned, in **CS3** and **CS2** higher quantity of electricity is procured at cheaper hours of WEM since EVs and thermal flexibilities shift the demand to cheaper periods. Moreover, the expensive NGUs show a great reduction in **CS3** and **CS2** since cheaper units can substitute their production. The

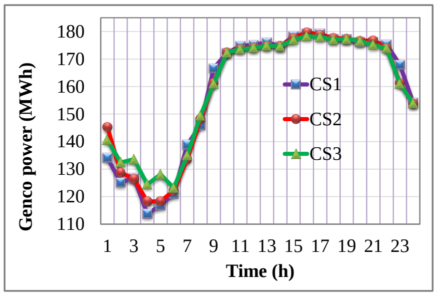

Figure 10: Power generation of Genco1

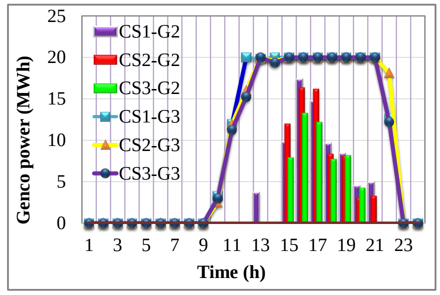

Figure 11: Power generation of Genco2-3

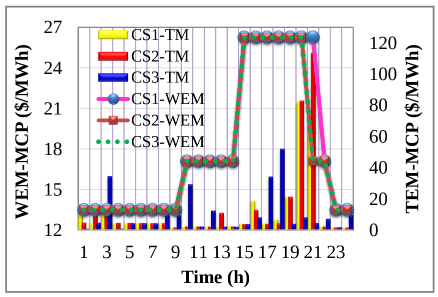

Figure 12: The MCP of WEM and TEM.

most important implication is how the three-level approach can benefit both AEVHs and IESP operators. The reason is that when EVs are charged smartly, there is a significant operational cost reduction for both operators. Despite the higher battery degradation in **CS3**, it is compensated by a greater reduction in overall AEVHs' cost. In order to provide a deeper insight about the cost values of Table 2, the hourly cost value is comparatively illustrated with total generation of each case study in Fig. 14, while Fig. 15 shows the hourly total generation and MCP in each case. As can be observed, **CS1** results in the highest operational cost value since in this case the EVFs are charged without a smart strategy, and it leads to highest total Genco production since peak demand is imported from the WEM. Thanks to the smart charging strategy of **CS2**, the demand is shifted from peak hours (15-19) to valley hour (1-7), while this shift is even more apparent in **CS3** as the thermal flexibilities open the electrical capacity of the CHP units. Overall, **CS2** provides 9.19% lower cost compared to CS1, and **CS3** provides 9.42% lower cost compared **CS1**. Based on the MCP outcomes of Fig. 15, it is noted that smart charging strategy and thermal

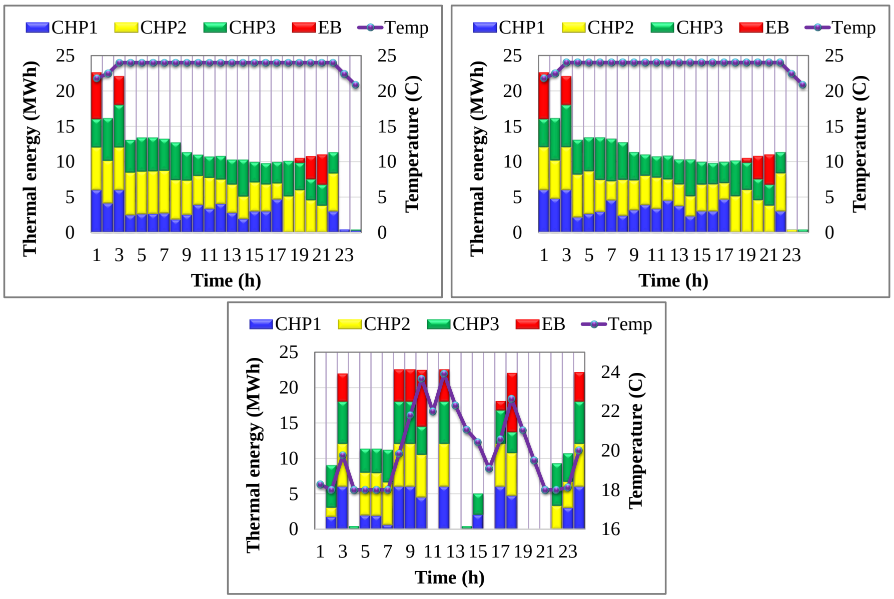

Figure 13: The thermal energy dispatch of the units in ADS and AEVHs' temperature: a) **CS1** b) **CS2** c) **CS3**

load flexibilities in **CS2** and **CS3** can lead to 2.10 % lower WEM price in regard to **CS1**.

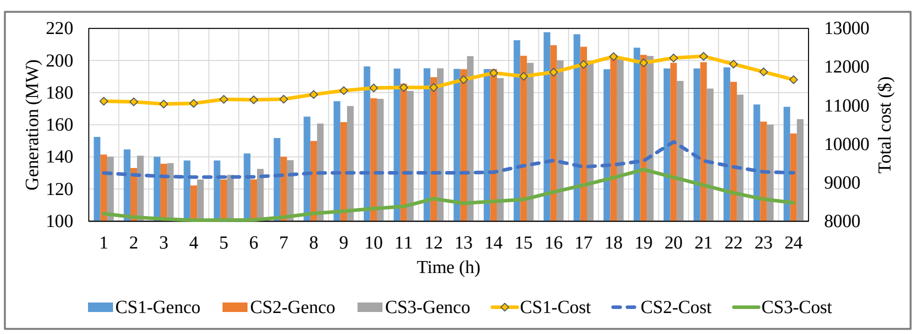

Figure 14: The MCP of the local electricity market (IEEE-33 bus)

The sensitivity analysis on the risk-aversion parameter of IGDT in **CS4** is summarized in Table 3. According to the results, a robust risk-averse strategy comes with a higher cost for IESP since operator self-schedules for the lower end of the

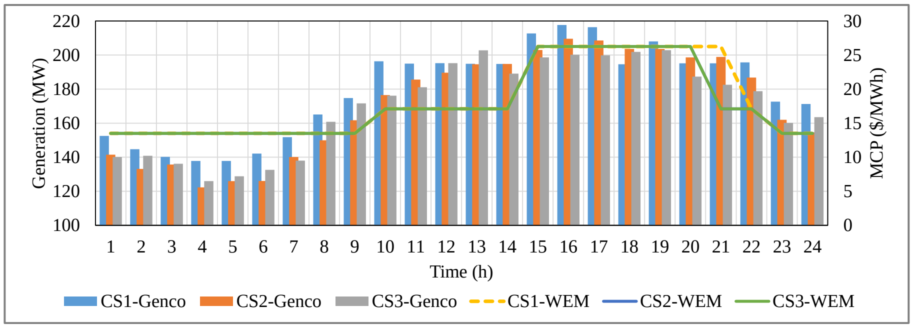

Figure 15: The MCP of the local electricity market (IEEE-33 bus)

predicted renewable energy spectrum. Therefore, the RES account for a lower share of the power, which is compensated by WEM and expensive NGU. In particular, the risk-averse IESP strategy benefits AEVHs operator. The reason is that risk-averse strategy increases the MCP of LEM at peak hours and EVs gain greater benefit by discharging at these periods.

Table 2: Operational costs through different cases

	CS1	**CS2**	**CS3**
NGUs ($)	3883.277	2886.737	2676.345
Gas producers ($)	6454.259	6448.75	6506.975
RES ($)	205.2701	205.2701	205.2701
Interruptible load ($)	31.27779	0	0
Purchased from WEM ($)	9266.553	8475.055	8582.386
Total IESP cost ($)	19840.64	18015.81	17970.98
AEVHs' cost ($)	5015.187	3796.107	1897.31
EV degradation cost ($)	0	642.64	864.24

The voltage level in all ADS buses at hour 21 is illustrated in Fig. 16. As can be seen, the uncoordinated charging scheduling in **CS1** leads to the worst voltage profile, which is also the reason for high power losses. In this regard, smart EV scheduling in **CS2** has 3.63% higher overall voltage. Moreover, including thermal flexibility in **CS3** improves voltage level by 0.39% compared to **CS2** and by 4.04% compared to **CS1**. The improvement in the voltage profile is particularly substan-

Table 3: Sensitivity analysis on risk aversion parameter of IGDT framework in **CS4**.

	$\sigma = 0$	$\sigma = 0.002$	$\sigma = 0.03$	$\sigma = 0.05$
$\sum_{t} P_{t}^{IESP}$	209.39	220.36	228.15	235.65
$\sum_{t} \sum_{k \in NGU} P_{k,t}^{DG}$	28.03	28.38	31.84	35.81
$\sum_{t} P_{t}^{RES}$	136.84	125.90	114.97	103.69
$\sum_{q \in \{CHP,EB\}} H_{t,\vartheta,q}^{sor}$	723.24	722.74	720.18	717.97
$\sum_{j \in DS} P_{ij,t}^{Loss}$	11.86	12.23	12.55	12.74
$\sum_{t} \sum_{k \in CHP} P_{k,t}^{DG}$	193.49	193.49	194.06	194.39
OF^{IP} ($)	17970.98	18002.75	18486.17	18948.15
OF^{AH}($)	1897.31	1761.19	1499.67	1125.97
$\sum_{s} \sum_{f} {}^{1}/_{\pi_s} dg_{f,s,t}$ ($)	564.24	623.03	689.09	730.68

tial at the end nodes of the ADS. The reason is that these nodes are far from the substation and higher voltage drop is required to transmit the electrical energy to these nodes. However, the smart charging strategy improves the voltage profile by shifting the demand to off-peak time periods.

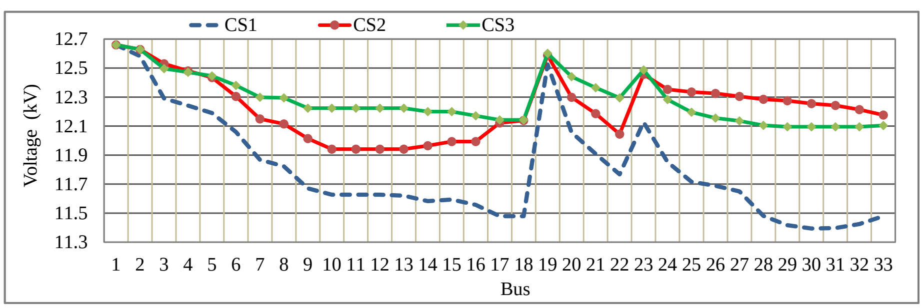

Figure 16: The voltage magnitude in ADS (IEEE-33 bus)

5. Conclusion

This study proposed a novel three-level optimization framework for AEVHs to participate in local electricity and thermal energy markets as a price-maker. In the proposed model, IESP (second level) was modelled as an intermediary entity between AEVHs (fist level) and WEM (third level). The impact of thermal flexibilities of households and smart charging capability of EV fleets on different markets was evaluated through different cases. The EV parameters such as their daily travelled miles and arrival/departure times were established through stochastic scenarios, while output energy of RES in the middle level was handled by the IGDT approach. The study illustrates that EVs can have a great influence on integrated energy networks, and their charging strategy can even influence the thermal energy market through CHP units. Overall conclusions were drawn as follows:

1. The three-level optimization framework shows that EVs can not only be price-influencers at local electricity and thermal energy markets, they can also manipulate price at the wholesale market level, as AEVHs can diminish the MCP of WEM, LEM and TEM by 18.85%, 2.1% and 5.82%, respectively.

2. AEVHs can utilize their thermal flexibilities to influence local electricity and thermal energy markets through CHP units.

3. Smart charging of EV fleets and thermal flexibility of the AEVH reduce the overall costs for both IESP and AEVH while improving overall voltage profile.

4. Using a three-level optimization framework, ensures the profits of AEVHs, IESP and WEM operators by reaching the market equilibrium for all players.

5. When the IGDT framework was integrated in IESP's problem, the risk-aversion increased the costs for IESP. However, the cost of AEVH was reduced. The reason is that the MCP of LEM was higher in this case, and it was more profitable for EVs to discharge at peak hours.

Ultimately, as a prospect for future studies, integrating traffic network models, and routing of electric vehicles offers a significant potential for novel research grounds.

Appendix A. Karush–Kuhn–Tucker (KKT) conditions

There are numerous methods to solve bi-level optimization problems. However, when the lower level is presented as a convex problem, KKT conditions are effective and practical in converting the bi-level problem into a single optimization problem with mathematical equilibrium constraints. In this study, the wholesale electricity market is the third level problem and IESP forms the second level. These two optimization problems of the bi-level framework are merged using the following quadruple KKT conditions [30].

Appendix A.1. Stationary conditions

In order to develop the stationary constraints, the lagrangian function is established by Eq. (a.1), where x represents the vector of decision variables at the third level of the problem. In this context, $f(x)$, $h(x)$ and $g(x)$ define the objective function, equality constraints and inequality constraints, respectively. The stationary constraints in Eqs. (a.1)-(refEq.a4) state that the derivatives of the lagrangian function over each variable must be equal to zero.

$$L^{EN} = f(x) + \lambda^T h(x) + \mu^T g(x) \tag{a.1}$$

$$\begin{aligned} \frac{\partial L^{EN}}{\partial P^{G}_{g,t}} &= C^G_g - \lambda^{WEM}_{b,t} + \overline{\mu^G_{g,t}} - \underline{\mu^G_{g,t}} + \mu^1_{g,t}|_{t>1} - \mu^1_{g,t+1}|_{t>1} \\ &+ \mu^2_{g,t}|_{t=1} - \mu^3_{g,t}|_{t>1} + \mu^3_{g,t+1}|_{t>1} + \mu^4_{g,t}|_{t=1} = 0, \forall g \in A^g_n, \forall b, \forall t \end{aligned} \tag{a.2}$$

$$\frac{\partial L^{EN}}{\partial P^{IESP}_t} = -C^{IESP}_t + \lambda^{WEM}_{b,t} + \overline{\mu^{IESP}_t} - \underline{\mu^{IESP}_t} = 0, \forall b, \forall t \tag{a.3}$$

$$\begin{aligned} \frac{\partial L^{EN}}{\partial \delta_{b,t}} &= \sum_{b' \in \theta_b} B_{b,b'}(\lambda^{WEM}_{b,t} - \lambda^{WEM}_{b',t}) + \sum_{b' \in \theta_b} B_{b,b'}(\overline{\nu_{b,b',t}} - \overline{\nu_{b',b,t}}) \\ &+ \sum_{b' \in \theta_b} B_{b,b'}(\underline{\nu_{b',b,t}} - \underline{\nu_{b,b',t}}) + \overline{\xi_{b,t}} - \underline{\xi_{b,t}} + \xi^1_{b=1,t} = 0, \forall b, \forall t \end{aligned} \tag{a.4}$$

Appendix A.2. Dual, primal, and complementary conditions

The dual, primal and complementary constraints of the WEM are defined by Eqs. (a.5)-(a.15).

$$0 \leqslant P^G_{g,t} \perp \underline{\mu^G_{g,t}} \geqslant 0, \forall g, \forall t \tag{a.5}$$

$$0 \leqslant (\overline{P^G_{g,t}} - P^G_{g,t}) \perp \overline{\mu^G_{g,t}} \geqslant 0, \forall g, \forall t \tag{a.6}$$

$$0 \leqslant (P^{IESP}_t - \underline{P^{IESP}_t}) \perp \underline{\mu^{IESP}_t} \geqslant 0 \tag{a.7}$$

$$0 \leqslant (\bar{P}^{in}_t - P^{IESP}_t) \perp \overline{\mu^{IESP}_t} \geqslant 0, \forall t \tag{a.8}$$

$$0 \leqslant (\overline{C_{b,b'}} + B_{b,b'}(\delta_{b,t} - \delta_{b',t})) \perp \underline{\nu_{b,b',t}} \geqslant 0, \forall b, \forall b', \forall t \tag{a.9}$$

$$0 \leqslant (\overline{C_{b,b'}} - B_{b,b'}(\delta_{b,t} - \delta_{b',t})) \perp \overline{\nu_{b,b',t}} \geqslant 0, \forall b, \forall b', \forall t \tag{a.10}$$

$$0 \leqslant (\pi - \delta_{b,t}) \perp \overline{\xi_{b,t}} \geqslant 0, \forall b, \forall t \tag{a.12}$$

$$0 \leqslant (\pi + \delta_{b,t}) \perp \underline{\xi_{b,t}} \geqslant 0, \forall b, \forall t \tag{a.12}$$

The dual variable concerning the equality terms must be free in sign, which is satisfied by Eq. (a.13)

$$\lambda_{b,t}^{WEM} \forall b, t \xi_{b=ref,t}^{l} \forall b, t \tag{a.13}$$

As can be observed, Eqs. (a.5)-(a.12) are nonlinear, which can be handled by big-M method and binary auxiliary variables [31], as follows:

$$0 \leqslant g_x \perp \mu \geqslant 0 \rightarrow g_x \geqslant 0, \mu \geqslant 0 \tag{a.14}$$

$$g_x \leqslant M_1 u, \mu \leqslant M_2(1-u) \tag{a.15}$$

Appendix B. The theory of strong duality

The theory of strong duality states that in the optimal solution point of the convex optimization problem, the primal and dual optimization functions have equal values [32]. In this study, this basic concept is deployed to develop a linear statement for the nonlinear term $\lambda_{b,t}^{WEM} P_t^{IESP}$ in Eq. (1). In this approach, the dual and primal objectives of the WEM are equated by Eq. (b.1).

$$\begin{aligned} &Max \sum_t \left[\begin{array}{l} -\sum_{g,b} \overline{P_{g,t}^{G} \mu_{g,t}^{G}} + \underline{P_t^{IESP} \mu_t^{IESP}} - \overline{P_t^{IESP} \mu_t^{IESP}} \\ + \sum_b P_{b,t}^{D} \lambda_{b,t}^{WEM} - \sum_{b,b' \in Tr} \underline{\nu_{b,b',t}} \overline{C_{b,b',t}} \\ - \sum_{b,b' \in Tr} \overline{\nu_{b,b',t}} \overline{C_{b,b',t}} - \sum_b \pi(\overline{\xi_{b,t}} + \underline{\xi_{b,t}}) \\ - \sum_g RU_g \mu_{g,t}^{1}|_{t>1} - \sum_g (RU_g + P_{g,ini}^{G}) \mu_{g,t}^{2}|_{t=1} \\ - \sum_g RD_g \mu_{g,t}^{3}|_{t>1} - \sum_g (RD_g - P_{g,ini}^{G}) \mu_{g,t}^{4}|_{t=1} \end{array} \right] \\ &= Min \sum_g \sum_t C_g^{G} P_{g,t}^{G} - \sum_t C_t^{IESP} P_t^{IESP} \end{aligned} \tag{b.1}$$

Based on Eqs. (a.7)-(a.8), following conclusions can be reached.

$$0 \leqslant (P_t^{IESP} - \underline{P_t^{IESP}}) \perp \underline{\mu_t^{IESP}} \geqslant 0 \rightarrow P_t^{IESP} \underline{\mu_t^{IESP}} = \underline{P_t^{IESP} \mu_t^{IESP}} \tag{b.2}$$

$$0 \leqslant (\overline{P_t^{IESP}} - P_t^{IESP}) \perp \overline{\mu_t^{IESP}} \geqslant 0 \rightarrow P_t^{IESP} \overline{\mu_t^{IESP}} = \overline{P_t^{IESP} \mu_t^{IESP}} \tag{b.3}$$

At this stage, Eq. (a.3) is multiplied by P_t^{IESP} to obtain a linear equivalent for $\lambda_{b,t}^{WEM} P_t^{IESP}$ as follows:

$$-P_t^{IESP} C_t^{IESP} + P_t^{IESP} \lambda_{b,t}^{WEM} + P_t^{IESP} \overline{\mu_t^{WEM}} - P_t^{IESP} \underline{\mu_t^{IESP}} = 0 \tag{b.4}$$

$$P_t^{IESP} C_t^{IESP} = P_t^{IESP} \lambda_{b,t}^{WEM} + P_t^{IESP} \overline{\mu_t^{WEM}} - P_t^{IESP} \underline{\mu_t^{IESP}} = 0 \tag{b.5}$$

Now the term $\lambda_{b,t}^{WEM} P_t^{IESP}$ can be replaced by X_1 as folows:

$$\begin{aligned}
&\sum_t C_t^{IESP} P_t^{IESP} = \sum_g \sum_t C_g^G P_{g,t}^G - \\
&\sum_t \left[\begin{aligned}
&-\sum_{g,b} \overline{P_{g,t}^G \mu_{g,t}^G} + \underline{P_t^{IESP} \mu_t^{IESP}} - \overline{P_t^{IESP} \mu_t^{IESP}} \\
&+\sum_b P_{b,t}^D \lambda_{b,t}^{WEM} - \sum_{b,b' \in Tr} \underline{\nu_{b,b',t}} \overline{C_{b,b',t}} - \\
&\sum_{b,b' \in Tr} \overline{\nu_{b,b',t}} \overline{C_{b,b',t}} - \sum_b \pi(\overline{\xi_{b,t}} + \underline{\xi_{b,t}}) - \\
&\sum_g RU_g \mu_{g,t}^1|_{t>1} - \sum_g (RU_g + P_{g,ini}^G) \mu_{g,t}^2|_{t=1} \\
&-\sum_g RD_g \mu_{g,t}^3|_{t>1} - \sum_g (RD_g - P_{g,ini}^G) \mu_{g,t}^4|_{t=1}
\end{aligned} \right]
\end{aligned} \tag{b.6}$$

$$\begin{aligned}
&X_1 = \sum_t C_t^{IESP} P_t^{IESP} = \sum_g \sum_t C_g^G P_{g,t}^G - \\
&\sum_t \left[\begin{aligned}
&-\sum_{b,b' \in Tr} \underline{\nu_{b,b',t}} \overline{C_{b,b',t}} - \sum_{b,b' \in Tr} \overline{\nu_{b,b',t}} \overline{C_{b,b',t}} \\
&-\sum_b \pi(\overline{\xi_{b,t}} + \underline{\xi_{b,t}}) - \sum_g RU_g \mu_{g,t}^1|_{t>1} - \\
&\sum_g (RU_g + P_{g,ini}^G) \mu_{g,t}^2|_{t=1} - \sum_g RD_g \mu_{g,t}^3|_{t>1} \\
&-\sum_g (RD_g - P_{g,ini}^G) \mu_{g,t}^4|_{t=1} - \sum_{g,b} \overline{P_{g,t}^G \mu_{g,t}^G} \\
&+\sum_b P_{b,t}^D \lambda_{b,t}^{WEM}
\end{aligned} \right]
\end{aligned} \tag{b.7}$$

Appendix C. Structural data of the utilized systems

In this study, the IESP consists of an IEEE-33 bus ADS, a 20-node NGN, and an 8-node DHS that is supplied by 3 CHPs, 2 NGUs, 3 PVAs and 3 WTs. The data on these networks can be observed in [11, 33, 34]. Furthermore, the WEM is made up of a standard 6-node TN and its structural data is available in[11]. Overall, the summery of the main parameters are included in Table C.4 to Table C.7.

References

[1] X. Li, M. Mulder, Value of power-to-gas as a flexibility option in integrated electricity and hydrogen markets, Applied Energy 304 (2021) 117863.

[2] M. Hofmeister, S. Mosbach, J. Hammacher, M. Blum, G. Röhrig, C. Dörr, V. Flegel, A. Bhave, M. Kraft, Resource-optimised generation dispatch strategy

Table C.4: Data and information on DGs

	$\overline{P_k^{DG}}$	$\underline{P_k^{DG}}$	R_k^{up}	R_k^{DN}	T_k^U	T_k^D	C_k^{DG}
CHP1	—	—	4.5	4.5	2	2	—
CHP2	—	—	4.5	4.5	1	1	—
CHP3	—	—	0.8	0.8	1	1	—
NGU1	7	0.75	1.8	1.8	1	1	87
NGU2	7	0.75	0.5	0.5	1	1	92

Table C.5: Data and information on EVFs

BC_f	$ECPM_f$	η_f	EB_f	Cr_f	a_0
400 ($/KWh)	0.3 (m/KWh)	0.95	30 (KWh)	10 (KW/h)	0.000524

Table C.6: Data and information on district heating network

C_p	R	$Cair_{\vartheta,e}$	$n^{ho}_{\vartheta,e}$
1(MWh/kg.$\circ$C)	18 ($\circ$C/MWh)	1.1578e-6 (MWhkg.c))	6000

Table C.7: Data and information on active distribution system

$\overline{V_i^{DS}}$	$\underline{V_i^{DS}}$	$\overline{I_{i,j}^{DS}}$	$\overline{P_l^{IL}}$	η_{EB}	$\overline{P^{EB}_{t,\vartheta,q}}$
1.1 (P.U)	0.9 (P.U)	1.2 (A)	3 (MW)	1	10 (MW)

for district heating systems using dynamic hierarchical optimisation, Applied Energy 305 (2022) 117877.

[3] Y. Yao, C. Gao, K. Lai, T. Chen, J. Yang, An incentive-compatible distributed integrated energy market mechanism design with adaptive robust approach, Applied Energy 282 (2021) 116155.

[4] T. Simolin, K. Rauma, R. Viri, J. Mäkinen, A. Rautiainen, P. Järventausta, Charging powers of the electric vehicle fleet: Evolution and implications at commercial charging sites, Applied Energy 303 (2021) 117651.

[5] P. Sheikhahmadi, S. Bahramara, J. Moshtagh, M. Y. Damavandi, A risk-based approach for modeling the strategic behavior of a distribution company in wholesale energy market, Applied energy 214 (2018) 24–38.

[6] A. Thingvad, L. Calearo, P. B. Andersen, M. Marinelli, Empirical capacity measurements of electric vehicles subject to battery degradation from v2g services, IEEE Transactions on Vehicular Technology 70 (8) (2021) 7547–7557.

[7] M. Mohiti, H. Monsef, H. Lesani, A decentralized robust model for coordinated operation of smart distribution network and electric vehicle aggregators, International Journal of Electrical Power and Energy Systems 104 (June 2018) (2019) 853–867. doi:10.1016/j.ijepes.2018.07.054.

[8] A. Asrari, M. Ansari, J. Khazaei, P. Fajri, A market framework for decentralized congestion management in smart distribution grids considering collaboration among electric vehicle aggregators, IEEE Transactions on Smart Grid 11 (2) (2020) 1147–1158. doi:10.1109/TSG.2019.2932695.

[9] Z. Liu, Q. Wu, S. S. Oren, S. Huang, R. Li, L. Cheng, Distribution locational marginal pricing for optimal electric vehicle charging through chance constrained mixed-integer programming, IEEE Transactions on Smart Grid 9 (2) (2018) 644–654. doi:10.1109/TSG.2016.2559579.

[10] B. S. K. Patnam, N. M. Pindoriya, Dlmp calculation and congestion minimization with ev aggregator loading in a distribution network using bilevel program, IEEE Systems Journal (2020) 1–12doi:10.1109/jsyst.2020.2997189.

[11] S. Bahramara, M. Yazdani-Damavandi, J. Contreras, M. Shafie-Khah, J. P. Catalão, Modeling the strategic behavior of a distribution company in wholesale energy and reserve markets, IEEE Transactions on Smart Grid 9 (4) (2018) 3857–3870. doi:10.1109/TSG.2017.2768486.

[12] P. Sheikhahmadi, S. Bahramara, A. Mazza, G. Chicco, J. P. Catalão, Bi-level optimization model for the coordination between transmission and distribution systems interacting with local energy markets, International

Journal of Electrical Power and Energy Systems 124 (2021) 106392. doi:10.1016/j.ijepes.2020.106392.

[13] S. Bahramara, P. Sheikhahmadi, A. Mazza, G. Chicco, M. Shafie-Khah, J. P. Catalão, A risk-based decision framework for the distribution company in mutual interaction with the wholesale day-ahead market and microgrids, IEEE Transactions on Industrial Informatics 16 (2) (2020) 764–778. doi:10.1109/TII.2019.2921790.

[14] T. Zhao, X. Pan, S. Yao, C. Ju, L. Li, Strategic bidding of hybrid ac/dc microgrid embedded energy hubs: A two-stage chance constrained stochastic programming approach, IEEE Transactions on Sustainable Energy 11 (1) (2020) 116–125. doi:10.1109/TSTE.2018.2884997.

[15] Y. Li, B. Wang, Z. Yang, J. Li, C. Chen, Hierarchical stochastic scheduling of multi-community integrated energy systems in uncertain environments via stackelberg game, Applied Energy 308 (2022) 118392.

[16] L. Liu, G.-H. Yang, Distributed optimal energy management for integrated energy systems, IEEE Transactions on Industrial Informatics (2022).

[17] F. Zhou, Y. Li, W. Wang, C. Pan, Integrated energy management of a smart community with electric vehicle charging using scenario based stochastic model predictive control, Energy and Buildings 260 (2022) 111916.

[18] W. Yang, J. Guo, A. Vartosh, Optimal economic-emission planning of multi-energy systems integrated electric vehicles with modified group search optimization, Applied Energy 311 (2022) 118634.

[19] S. Guo, G. Song, M. Li, X. Zhao, Y. He, A. Kurban, W. Ji, J. Wang, Multi-objective bi-level quantity regulation scheduling method for electric-thermal integrated energy system considering thermal and hydraulic transient characteristics, Energy Conversion and Management 253 (2022) 115147.

[20] A. Najafi, H. Falaghi, J. Contreras, M. Ramezani, A stochastic bilevel model for the energy hub manager problem, IEEE Transactions on Smart Grid 8 (5) (2017) 2394–2404. doi:10.1109/TSG.2016.2618845.

[21] S. Zeynali, N. Nasiri, M. Marzband, S. N. Ravadanegh, A hybrid robust-stochastic framework for strategic scheduling of integrated wind farm and plug-in hybrid electric vehicle fleets, Applied Energy 300 (2021) 117432.

[22] B. Xu, J. Zhao, T. Zheng, E. Litvinov, D. S. Kirschen, Factoring the cycle aging cost of batteries participating in electricity markets, IEEE Transactions on Power Systems 33 (2) (2018) 2248–2259. doi:10.1109/TPWRS.2017.2733339.

[23] M. F. Anjos, A. J. Conejo, et al., Unit commitment in electric energy systems, Foundations and Trends® in Electric Energy Systems 1 (4) (2017) 220–310.

[24] W. Gu, J. Wang, S. Lu, Z. Luo, C. Wu, Optimal operation for integrated energy system considering thermal inertia of district heating network and buildings, Applied Energy 199 (2017) 234–246. doi:10.1016/j.apenergy.2017.05.004.

[25] E. Mahboubi-Moghaddam, M. Nayeripour, J. Aghaei, A. Khodaei, E. Waffenschmidt, Interactive robust model for energy service providers integrating demand response programs in wholesale markets, IEEE Transactions on Smart Grid (2018). doi:10.1109/TSG.2016.2615639.

[26] M. Rezaeimozafar, M. Eskandari, V. A. Savkin, A self-optimizing scheduling model for large-scale ev fleets in microgrids, IEEE Transactions on Industrial Informatics (2021). doi:10.1109/TII.2021.3064368.

[27] M. Tasdighi, H. Ghasemi, A. Rahimi-Kian, Residential microgrid scheduling based on smart meters data and temperature dependent thermal load modeling, IEEE Transactions on Smart Grid 5 (1) (2014) 349–357. doi:10.1109/TSG.2013.2261829.

[28] A. Ahmadian, M. Sedghi, M. Aliakbar-Golkar, Stochastic modeling of plug-in electric vehicles load demand in residential grids considering nonlinear bat-

tery charge characteristic, Institute of Electrical and Electronics Engineers Inc., 2015, pp. 22–26. doi:10.1109/EPDC.2015.7330467.

[29] National household travel survey.
URL `https://nhts.ornl.gov/`

[30] N. Nasiri, S. Zeynali, S. N. Ravadanegh, M. Marzband, A hybrid robust-stochastic approach for strategic scheduling of a multi-energy system as a price-maker player in day-ahead wholesale market, Energy 235 (2021) 121398.

[31] N. Nasiri, S. Zeynali, S. N. Ravadanegh, N. Rostami, A robust decision framework for strategic behaviour of integrated energy service provider with embedded natural gas and power systems in day-ahead wholesale market, IET Generation, Transmission & Distribution (2022).

[32] A. J. Conejo, E. Castillo, R. Minguez, R. Garcia-Bertrand, Decomposition techniques in mathematical programming: engineering and science applications, Springer Science & Business Media, 2006.

[33] Y. Li, Z. Li, F. Wen, M. Shahidehpour, Privacy-preserving optimal dispatch for an integrated power distribution and natural gas system in networked energy hubs, IEEE Transactions on Sustainable Energy 10 (4) (2018) 2028–2038.

[34] Y. Jiang, C. Wan, A. Botterud, Y. Song, S. Xia, Exploiting flexibility of district heating networks in combined heat and power dispatch, IEEE Transactions on Sustainable Energy 11 (4) (2019) 2174–2188.

Credit Author Statement

Saeed Zeynali: Software, Methodology, Conceptualization, Writing - Original Draft, Visualization

Nima Nasiri: Conceptualization, Methodology, Software, Writing - Original Draft, Data Curation, Visualization

Sajad Najafi Ravadanegh: Formal analysis, Methodology, Supervision, Validation, Investigation, Project administration

Mousa Marzban: Supervision

Declaration of interests

☒ The authors declare that they have no known competing financial interests or personal relationships that could have appeared to influence the work reported in this paper.

☐The authors declare the following financial interests/personal relationships which may be considered as potential competing interests:

Fig_3

Click here to access/download
MATLAB File (.fig, .m)
Fig_3.fig

Fig_4

Fig_5

Click here to access/download

MATLAB File (.fig, .m)

Fig_5.fig

Fig_6

Click here to access/download
MATLAB File (.fig, .m)
Fig_6.fig

Fig_9

Click here to access/download
MATLAB File (.fig, .m)
Fig_9.fig

Editable figures: These figures are in editable format, and they are provided for the production office so that they customize the figure size in the final publication.

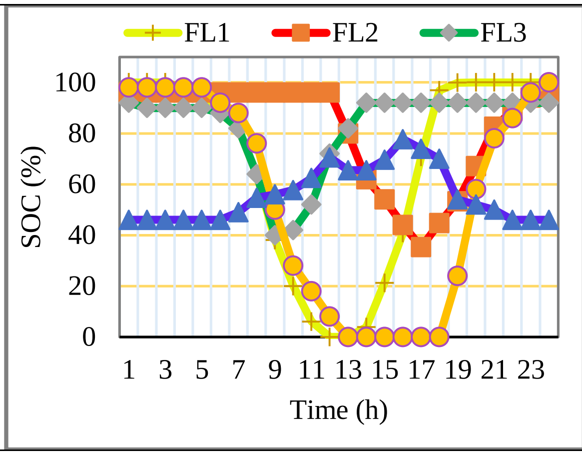

(a)

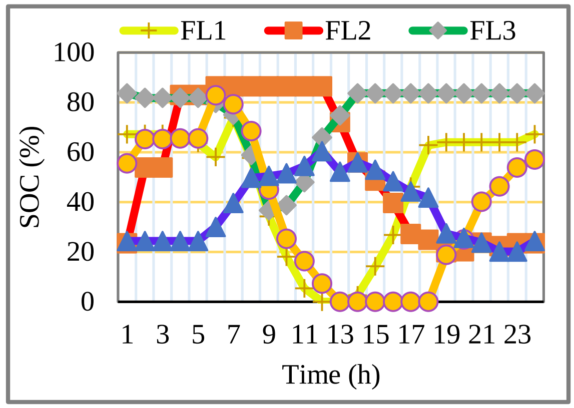

(b)

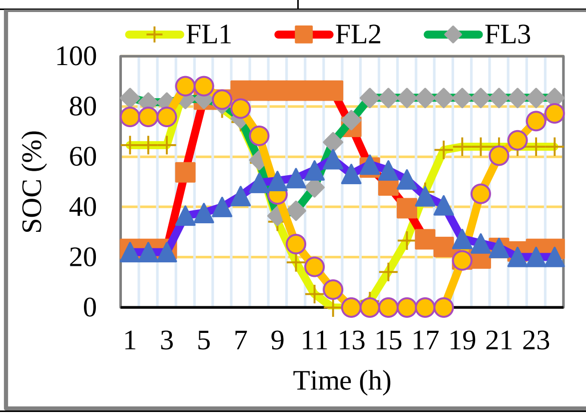

(c)

Figure 7: The SOC of EV fleets: a) **CS1** b) **CS2** c) **CS3**

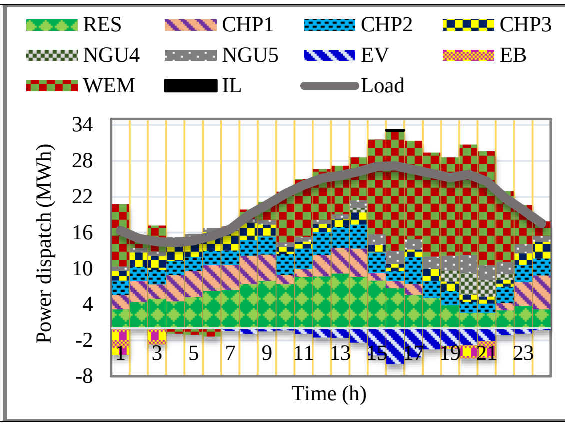

(a)

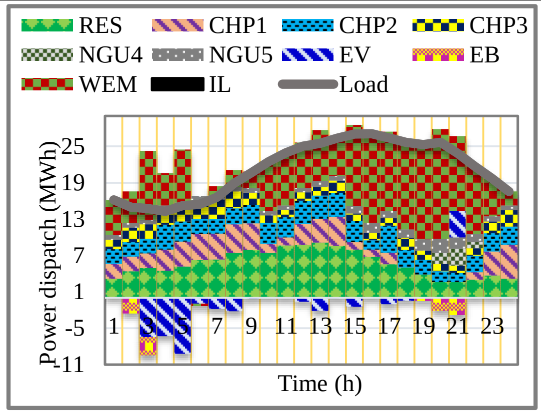

(b)

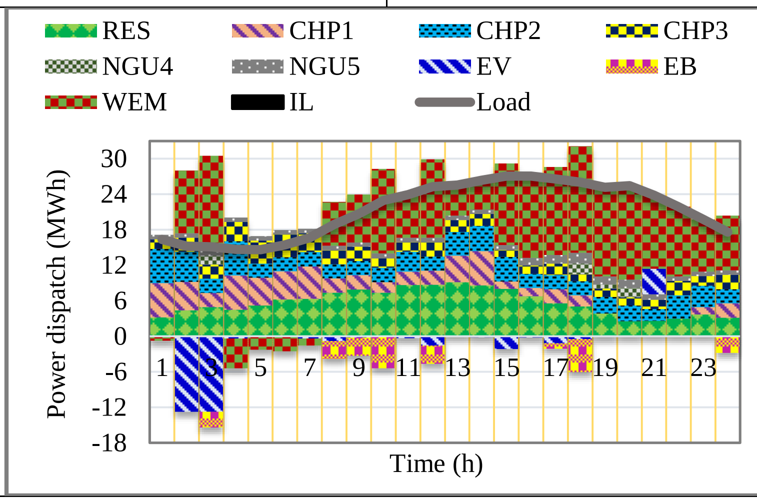

(c)

Figure 8: The power dispatch of units in ADS: a) **CS1** b) **CS2** c) **CS3**

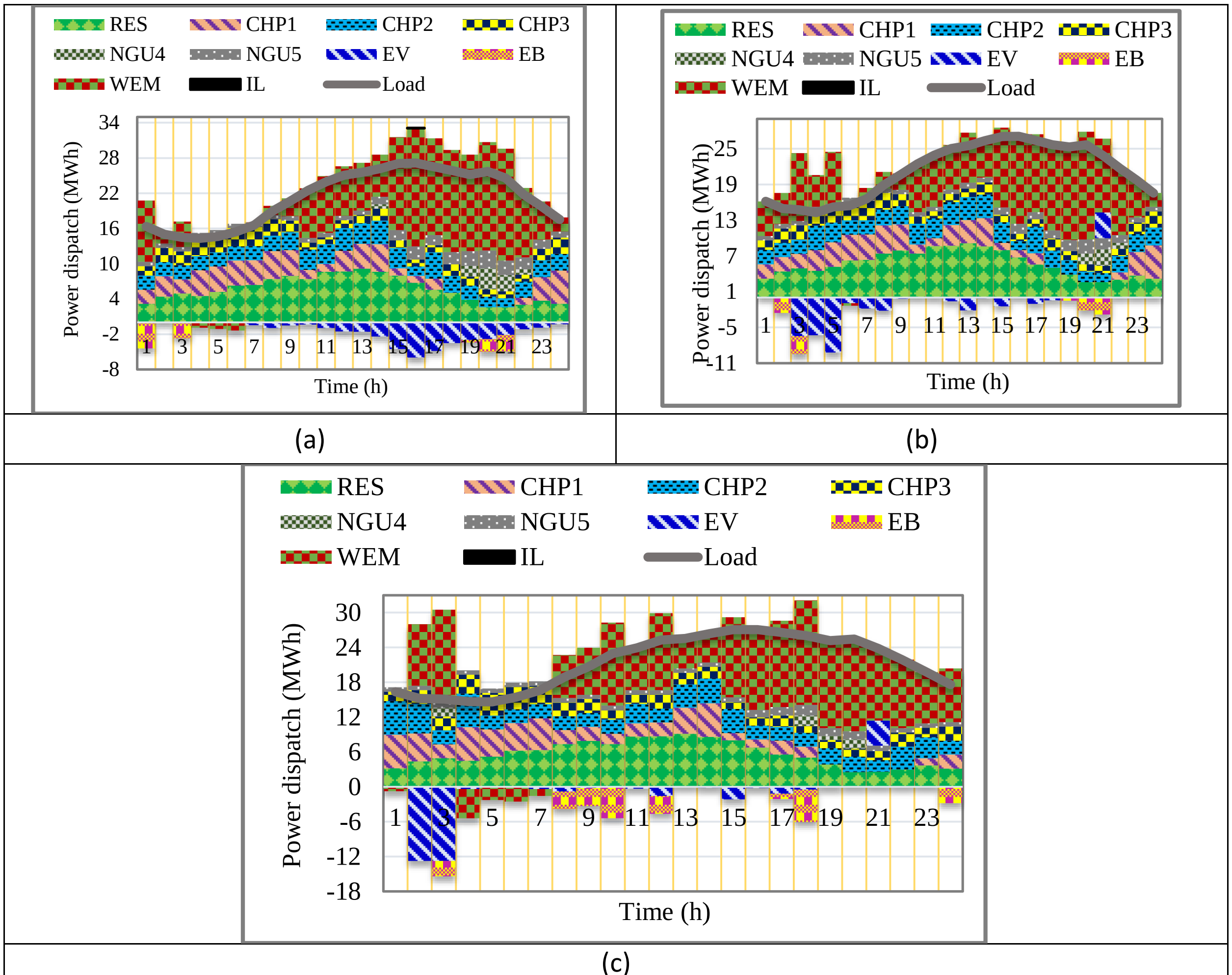

Figure 8: The power dispatch of units in ADS: a) **CS1** b) **CS2** c) **CS3**

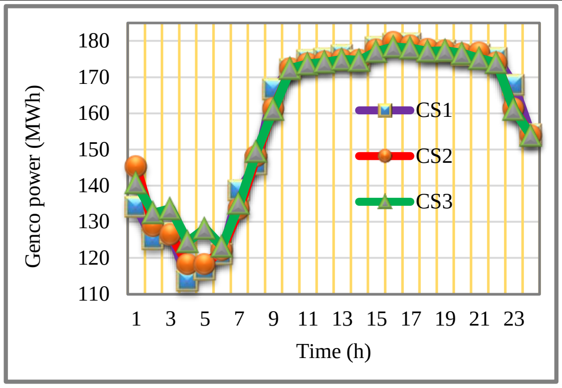	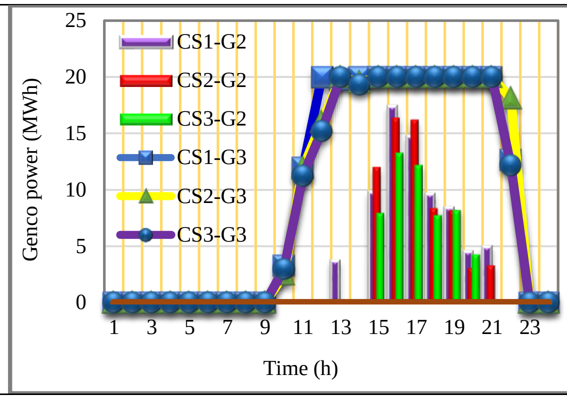
Figure 10: Power generation of Genco1	Figure 11: Power generation of Genco2-3

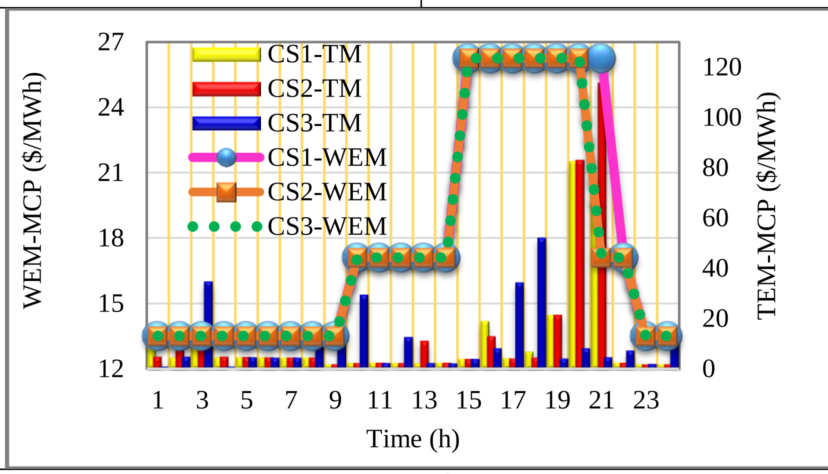

Figure 12: The MCP of WEM and TEM

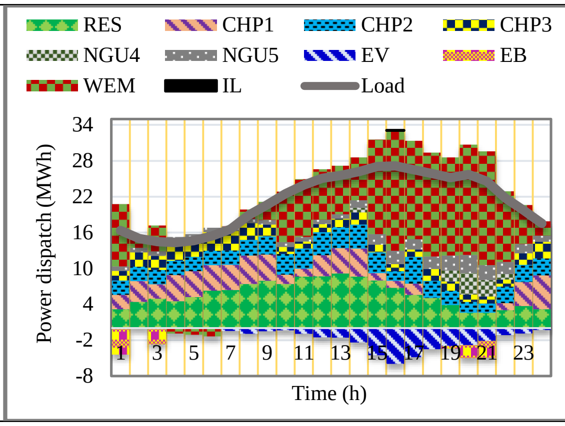

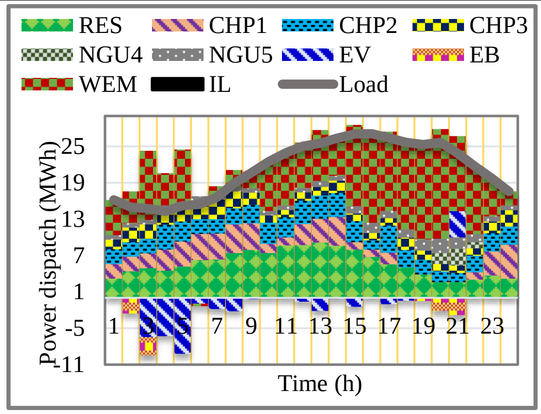

(a)

(b)

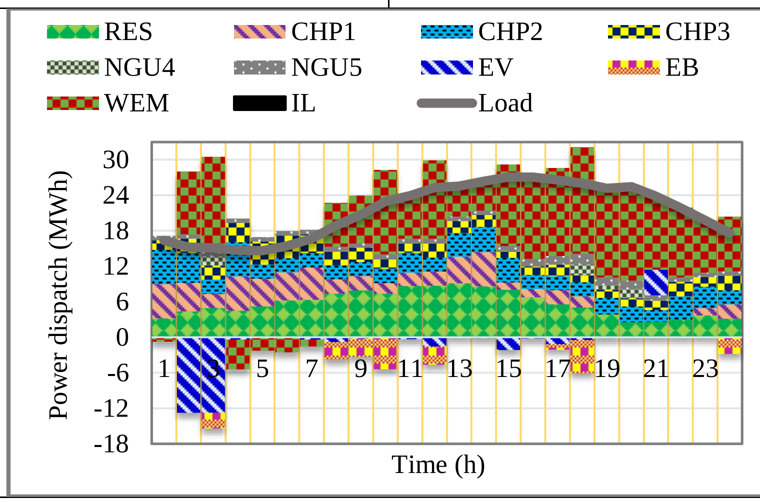

(c)

Figure 8: The power dispatch of units in ADS: a) **CS1** b) **CS2** c) **CS3**

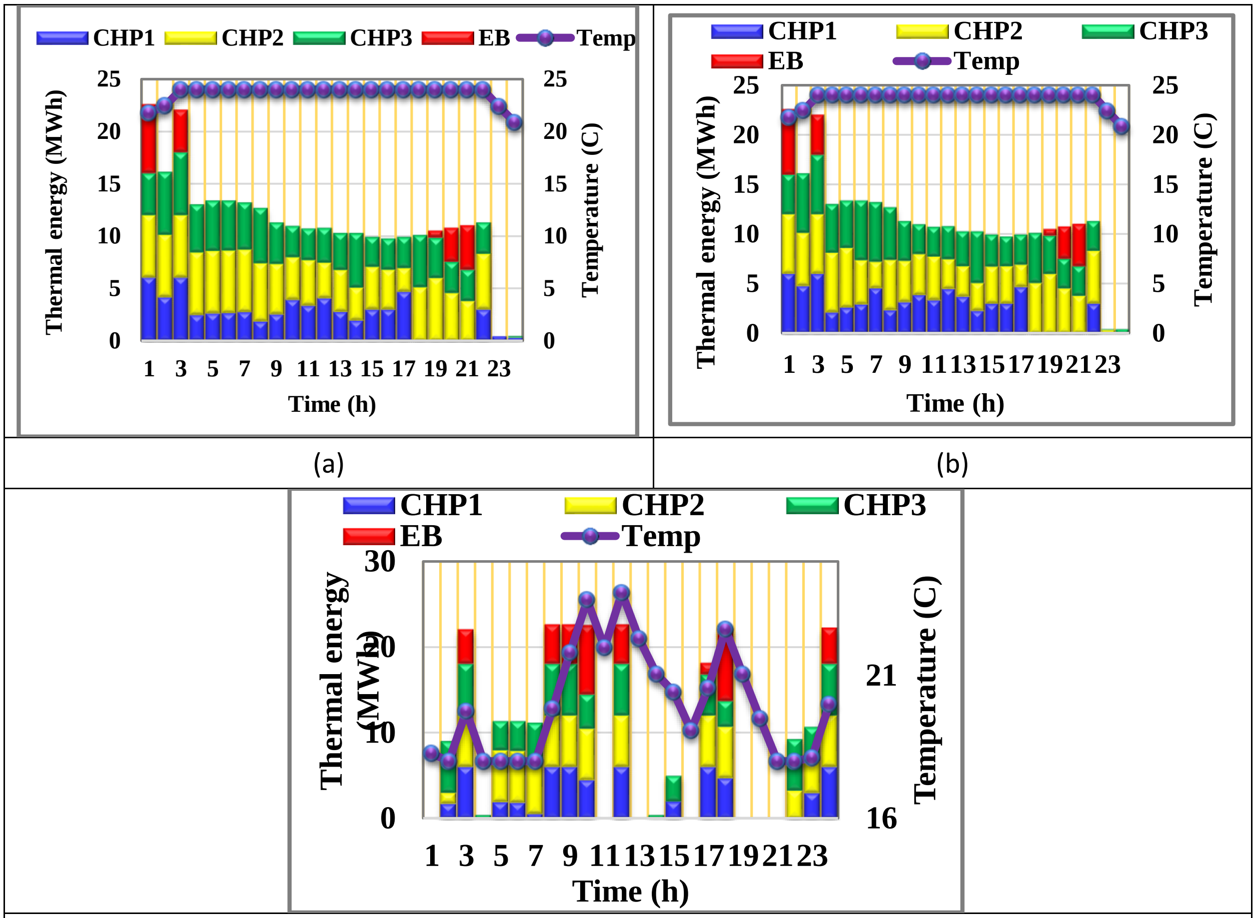

Figure 13: The thermal energy dispatch of the units in ADS and AEVHs' temperature: a) **CS1** b) **CS2** c) **CS3**

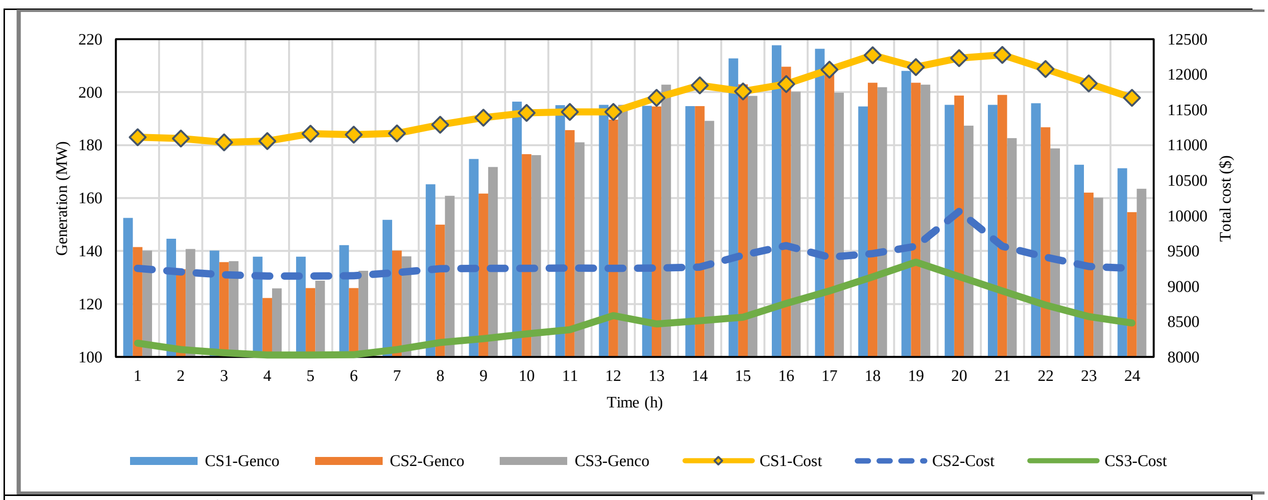

Figure 14: The MCP of the local electricity market (IEEE-33 bus)

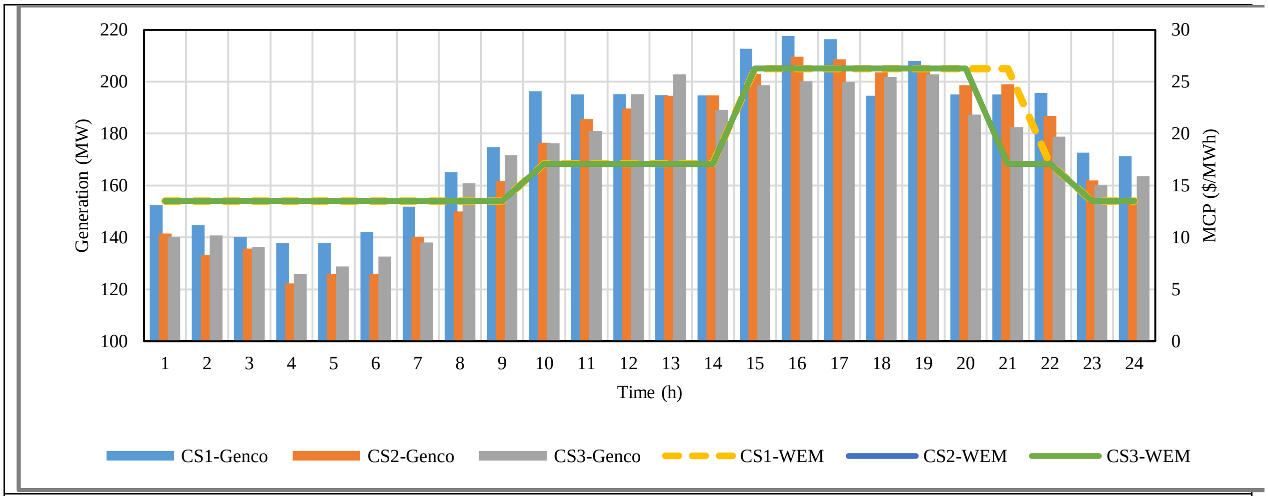

Figure 15: The MCP of the local electricity market (IEEE-33 bus)

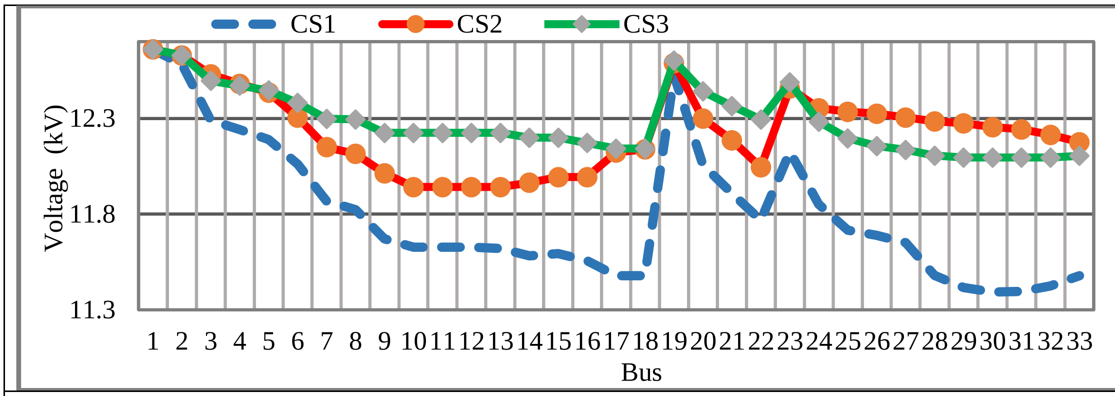

Figure 16: The voltage magnitude in ADS (IEEE-33 bus)